Control of flow networks with constraints and optimality conditions

Scholten, Tjeert Wobko

Control of Flow Networks with Constraints and Optimality Conditions

Tjardo Scholten

university of groningen

The research described in this dissertation has been carried out at the Faculty of Mathematics and Natural Sciences, University of Groningen, the Netherlands.

The research reported in this dissertation is part of the research program of the Dutch Institute of Systems and Control (DISC). The author has successfully completed the educational program of DISC.

This work was supported by Samenwerkingsverband Noord Nederland (SNN), Ministerie van Economische Zaken, Landbouw en Innovatie.

Cover by: Roderick Marsman

Printed by Michal Slawinsky, thesisprint.eu
Poland

ISBN 978-94-034-0060-0 (printed version)
ISBN 978-94-034-0059-4 (electronic version)

rijksuniversiteit
groningen

Control of Flow Networks with Constraints and Optimality Conditions

Proefschrift

ter verkrijging van de graad van doctor aan de
Rijksuniversiteit Groningen
op gezag van de
rector magnificus prof. dr. E. Sterken
en volgens besluit van het College voor Promoties.

De openbare verdediging zal plaatsvinden op

vrijdag 6 oktober 2017 om 14:30 uur

door

Tjeert Wobko Scholten

geboren op 12 januari 1987
te Assen

Promotor
Prof. dr. C. De Persis

Beoordelingscommissie
Prof. dr. A.J. van der Schaft
Prof. dr. G. Como
Prof. dr. D. Bauso

To Joke, Marijn and Freidl

Acknowledgments

Working as a PhD student has been an exciting journey in which I received much help, motivation and inspiration from many colleagues, friends and family. First of all, I would like to thank my promotor Claudio. When I first came to you I wasn't sure about pursuing a PhD, but this hesitation did not scare you and you were even able to convince me. Looking back I believe that this was a good decision and in the past five years I have learned a lot from you. I greatly admire the time you dedicate to your PhD students (and therefore also to me) despite your busy agenda. With everything you do you hold a high standard and it was impressive to witness how passionate and diligent you work. All this helped me significantly to improve my research and writing skills and therefore contributed greatly to the quality of this thesis. You have been an inspiration to me and a very good, friendly and wise supervisor. Pietro, I am very grateful for all the help you gave me. Not only for being a co-author in some of the studies but also for your positive and motivating attitude that helped me a lot during the difficult times.

My gratitude goes out to my paranymphs Erik and Tobias, both of you made going to work very enjoyable and I have great memories of our many coffee breaks, lunches and long discussions which were not necessarily always about research. I could always rely on your help regarding any issue. Also, I thoroughly enjoyed our board game sessions, festivals, (too long) sessions of factorio and countless many other great activities.

I can honestly say that I would never have obtained my PhD if it wasn't for Sebastian. Not only did you contact me in the first place about the position, you were able to convince me to take the position and encouraged me to continue during the times in which motivation was hard to find. I thoroughly enjoyed your company the past five years and will surely miss that in the future. I would like to thank my fellow SMS members Mark, Danial, Mingming, Tjerk, Henk, Shuai, Nima, Hongkeun and Matin. You all contributed to a very pleasant working environment and I have great memories of our group outings, coffee breaks, lunches, conferences and discussions. When something was required in the lab, Sietse, Pim and Martin were always a wonderful help. Also, Martin, Hector, Bao and Soheil, it was amazing to get together and make some music.

Filip, it was nice to explore New York together with you and always enjoyed your company at Zernike. Matthijs, we organized one of the group outings together which was an enjoyable and pleasant experience. Jesus, I've enjoyed your company a lot the past years. I still have great memories of our time in Linz during the ECC where you invited me to join your former colleagues to a beautiful restaurant on the top of the mountain. Anneroos and Hidde-Jan, I got to know you both during our mathematics study and I always enjoyed your company during the many homework sessions, conferences and social activities throughout the years. James, you were always available and enthusiastic to do various active and social activities such as ice skating, football, golf and drinks, thank you for that. I would also like to thank Mauricio, Robert, Gunn, Ewout and Pouria for the great moments that we have shared during our many coffee breaks, parties, lunches and conferences. It was great having you around.

Masahide, Monika, Jay, Rodolfo, Nelson, Hongyu, Pooya, Qingkyang, Xiaodong, Martijn, Shuai, Yuri, Chris, Hildeberto, Jie, Zaki, Hadi, Rully, xiaoshan, Yuzhen, Alain, Dong Xue, Laiz, Yu, Carlo, Desti, Hui, Ruiyue, Marko, Chen, Shuo, Fan, Liang, Shodhan, Anton, Weiguo, Jianlei and Noorma, you provided a stimulating and very enjoyable environment and I would like to thank you all for a great time.

Special thanks go out to our secretary Frederika, you were always on top of everything and wonderful to have around. I also have great memories of our group outings and movie nights. Also, I would like to thank Karin and Johanna for all their support and enthusiasm the past years. I would like to thank Jacquelien, Bayu, Ming, Arjan and Harry for creating an open and dynamic research environment which is very pleasant to work in. Also I would like to thank my master thesis supervisor Ernst for helping me pave the way towards this thesis and his positive recommendations for the PhD position. Beau-Anne, Bram and Koen, as my master students you all three provided great work and contributed to the quality of this thesis. I had very nice discussions and enjoyed working with you a lot. The supervision of the various Bachelor students throughout my PhD was very enjoyable as all of you provided great work. Thank you all for making this such a nice experience. I also had a lot of fun supervising the various bachelor students throughout my PhD, which all did great work. Thank you all for making this such a nice experience.

The Fexiheat project made my PhD possible and I would like to thank Paul, Arjen, Derk, Wim, Kees, Richard, Theo, Theo, Erika, Roel, Riksta, Paul, Arne, Erik, Pieter, Floris, Marco, Lies, Jacques and Wim along with all other management and the involved companies for their input, energy and trust is this project. Also, special thanks go out to my fellow Flexiheat researchers Alexandros, Kathelijne, Erika, Rien, Wenn, Juliana, Wouter and Marcel. Although the project could at some points be quite though, you all made it a very enjoyable experience. Also I would like to thank 'Samenwerkingsverband

Noord Nederland' (SNN) for the funding of this project.

I would also like to thank my new colleagues at the Hanze for making me feel very welcome in my new work environment and I look forward to a wonderful time together. All guys from Waterpolo, thanks for all the necessary distractions you provided me during training, matches and drinks. A significant number of ideas in this thesis came to me either right before or after playing this awesome game with you. A group of friends that are very close to me are Maaike, Charlotte, Rene, Wouter, Alex, Arnaud, Ruben, Marcella, Rianka, Charlotte, Sanne, Annika and Mark. I can't count the number of great moments we shared together and you all provided me with enough distractions, reflections and support required to finish my PhD. I look forward to creating many more memories together with all of you. Roderick, I would like to thank you both for the beautiful design of the cover of this thesis and for being a good friend.

I would like to thank my family Chris, Karla, Jeroen, Erik, Roberto, Arja and Gerda for their support and I hope we have many more Christmases and camping holidays together. I also would like to thank Mark, Jeanette, Roel, Petra, Jeroen, Linda, Arjan, Jan, Margot, Ilhan and Olias for their support throughout the years. Bert, my brother, thank you for always being there at the moments I was in need. Wulf, Gisela, Juli, Marcel und Herta, vielen Dank, dass ihr mich mit offenen Armen in eurer Familie aufgenommen habt.

Lastly I would like to thank the three most important people in my life to which I've dedicated this thesis. First, my dear Freidl, your passion, encouragement, spirit, support and love were endless and there are no words that describe how grateful I am for having you in my life and sharing our PhD endeavour together. Second my father Marijn, you have always been there for me and supported all the decisions I have made. You have learned me so many things and provided me unconditional love. Thank you for being a wonderful father and a big inspiration to me and everyone around you. And last my mother Joke, during my education I often struggled, but you always found a way to help me, which in the end brought me to writing this thesis. You've always been a wonderful mother and I've always cherished your support, love, wisdom and advise. I cannot put in to words how grateful I am for everything that you have done for me all these years.

Of course it is impossible to mention and recall all the people that contributed to this thesis directly or indirectly. I would like to thank all of them.

Tjardo Scholten
Groningen
September 3, 2017

Contents

Chapter 1

Introduction

Energy demand is rising and a considerable fraction of the energy is consumed in the form of heat. While high quality resources such as natural gas are used for heating, waste heat is left unutilized in many cases. Since this increase in energy consumption has a negative impact on the environment, there is a need for more energy efficient systems. One of the proposed solutions is the integration of heat networks into the existent infrastructure. Such heat networks are commonly referred to as district heating systems (DHS) when found in an urban area or heat exchanger networks (HEN) in industrial environments.

1.1 District heating and geothermal energy

A district heating system consists of pipes filled with heated water that is pumped from a producer to a consumer. The heat is injected or extracted via a heat exchanger in order to separate the water in the network from any possible contamination outside of it. Although DHS's have been around since the 14^{th} century (Lemale and Jaudin 1999), recent years have witnessed a renewed interest in heating systems for two reasons. The first reason is the change in governmental policies with the intention to reduce carbon dioxide emissions. Since adding a DHS to existing infrastructure often increases the energy efficiency of the overall system, the total carbon dioxide emissions drop. Two examples of higher energy efficiencies due to a DHS are utilizing waste heat and incorporating environmentally friendly sources such as biomass incinerators. Furthermore, combined heat power plants (CHP) can be integrated into a DHS which have a better energy efficiency compared to conventional power plants that produce only electricity. The second reason is the recent advances in geothermal energy production methods. In the past the use of waste heat and geothermal energy was challenged by the wide use of cheap fossil fuels, but with the revived focus on renewable energy sources, district heating and heat energy networks are gaining importance in the provision of renewable energy (Lund et al. 2014), (Rezaie and Rosen 2012) (Sayegh et al. 2016). The complexity and challenges related to geothermal heat distribution have been outlined (Gelegenis 2009) and the efficient

production and use of geothermal resources is identified as an important aspect of their sustainable development (Shortall et al. 2015).

Despite this renewed interest, the number of networks in which multiple heat producers and/or waste heat sources are connected is limited, especially if the producers are owned by different companies. The main reason for this, is that it is hard to coordinate supply and demand such that they are matched. Heat may be produced when it is not needed, and conversely, may not be available when needed. There are three solutions in order to balance a supply and demand, first a storage device can be included, second the production can be adjusted, and third, and incentive can be send to the consumers in order to adjust their demand. The latter is also referred to a demand side management and the incentive is often a dynamic price (Li et al. 2015). A combination of storage, dynamic production and demand side management provides the most flexibility to balance demand and supply.

The synthesis and control of DHS's and HENs has a long history. Until the 1980s the synthesis and control of DHS's and HENs were mostly focused on the steady state optimal design of heat exchangers, which resulted in simple engineering techniques such as the pinch method (Linnhoff and Hindmarsh 1983). With the introduction of linear optimization techniques such as model predictive control, the focus later shifted to the design of optimal controllers where optimal steady states were considered (Glemmestad et al. 1999). The same approach applied to cooling systems can be found in (Ma et al. 2009) and (Borghesan et al. 2013). Although cooling systems serve a different purpose, the principles and dynamics that describe heating systems also apply. Thus the control methodologies used in this thesis can easily be applied to cooling systems. In order to validate the controllers several models of district heating systems have been proposed. Two examples are flow networks and hydraulic networks. These models neglect the temperature dynamics which is a valid assumption as long as the operating temperature is approximately constant. We will introduce both these networks in the following sections.

1.2 Flow networks

Flow networks consist of nodes on which material can be stored and links that exchange this material (flow). Moreover, these networks can include inflows and outflows at the nodes. In the case of a district heating system the stored material is heated water, inflows are producers and outflows consumers. There flow networks are also referred to as distribution networks, transportation networks or compartmental systems. The design and regulation of these networks received significant attention due to its many applications, including supply chains (Alessandri et al. 2011), heating, ventilation and air conditioning (HVAC) systems (Gupta et al. 2015), data networks (Moss and Segall 1982), traffic net-

works (Iftar 1999) and compartmental systems (Blanchini et al. 2016). Depending on the specific application the associated control objective can vary. If the considered objective is static, the study of flow networks has a long history within the field of network optimization (Bertsekas 1998), (Rockafellar 1984). Many networks must on the other hand react dynamically on changes in the external conditions such as a change in the demand. In these cases continuous feedback controllers are required that dynamically adjust inputs at the nodes and the flows along the edges. Since flow networks are ubiquitous in engineering systems, many solutions have been proposed to coordinate them, exploiting methodologies from e.g. model predictive control (Danielson et al. 2013) and passivity (Arcak 2007).

In the context of district heating systems flow networks are used to model multiple storage tanks (located on the nodes) that can store heated water. A common objective in flow networks is to regulate the outputs of the nodes (e.g. storage or inventory levels) to their desired value or to achieve consensus in the presence of unknown and potentially time-varying demand (Bürger and De Persis 2015). The dynamics of the edges follow either from underlying physical principles (Blanchini et al. 2016) or from designed controllers adjusting the flow rates. Moreover, it is common that the capacity of the edges is constrained (Wei and van der Schaft 2013) and that flows have an associated cost depending on the rate (Bürger et al. 2015).

1.3 Hydraulic networks

In contrast to flow network models, which relate flows and volumes, a model of an hydraulic network relates flows and pressures using algebraic and dynamic expressions. These networks are a well studied class of systems where a fluid flows through a network containing many interconnected branches. Hydraulic networks have many applications and are generally categorized into one of two classes. The first class are open networks which contain inlets and outlets for fluids, while in the second class the hydraulic network is closed and the fluid is circulating. Examples of open large scale hydraulic networks are irrigation networks (Cantoni et al. 2007), water distribution networks (Wang et al. 2006), (Cantoni et al. 2007) and sewer networks (Wan and Lemmon 2007), (Marinaki 1999). Examples of closed networks are mine ventilation networks (Hu et al. 2003), cardiovascular systems and district heating networks (Scholten et al. 2016b), (Gambino et al. 2016). Moreover, the models used for electrical circuits share similarities with those of hydraulic networks (Jayawardhana et al. 2007). A common control objective is to regulate flow rates and pressure drops in the individual sections of the network. Various controllers have been proposed to guarantee that that control objective is satisfied, such as PI controllers (Sloth and Wisniewski 2015),

(De Persis et al. 2014) and nonlinear adaptive controllers (Hu et al. 2003), (Koroleva and Krstic 2005), (Koroleva et al. 2006).

1.4 Motivation

Around the world government regulations are changing in order to cut down CO_2 emissions due to global warming. As a consequence both government and industry are looking for new and more efficient ways to provide the energy demanded by consumers. A drastic reduction can be made by using a new generation of district heating systems. That is, space heating constitutes for 40% of the total energy demand and is currently mostly generated by fossil fuel while waste heat is left unutilized. Moreover, in these networks other heat sources can be included such as biomass and geothermal energy.

Although district heating systems have been around for a long time there are still several problems that need to be solved in order to increase the efficiency and versatility of these networks. The first problem is to coordinate the storage and production when multiple producers owned by different entities are connected. Second, in order to reduce heat dispersion in the pipes, smaller pipes have been suggested. However, the increased friction due to the smaller pipes require a new topology that includes multiple pumps. Lastly, in order to avoid wasting heat, the production and demand need to be better matched.

In this thesis we provide an answer to these problems by designing smart control systems for district heating systems. However, we also note that the results can be applied to many other applications that have similar dynamics. All the studies are carried out within the Flexiheat project for which the aim was to design an intelligent heat grid with a multidisciplinary approach.

1.5 Outline of the thesis and origin of the chapters

In this thesis we consider the control of large scale networked systems. Many of the results are motivated by control problems encountered in district heating systems. More specific, we aim to design controllers that regulate temperatures, storage levels and pressures in these networks in combination with the following conditions:

- capacity and directional flow constraints
- production capacity constraints
- multiple controllable and/or dynamic producers

- multiple consumers
- time varying demand
- multiple storage devices
- distributed control
- economic optimality

However, as it is difficult to include all these conditions at once, the approach used in this thesis is best described as divide and conquer. That is, each chapter addresses the regulation of a different state variable and a subset of the above conditions. Furthermore, each chapter considers a different model that captures the dynamics of interest for a particular control problem. Ultimately, the various models and control problems can be integrated in a single model and control design as discussed in the last part of Chapter 8.

In the remainder of this section we provide an outline of the thesis and the references to the original content of the chapters.

In Chapter 2 three different models are introduced that are used in the controller design in the remainder of the thesis. First the flow and temperature dynamics of a district heating system with a single producer, single storage device and multiple consumers are derived. Second a flow network is considered with multiple producers and consumers and lastly an hydraulic network is introduced. Additionally an optimization problem is introduced that is used in the control design of several controllers.

In Chapter 3 a district heating system with a single producer and storage tank is considered such as presented in the first model of Chapter 2. As the demand in these networks has often a highly repetitive pattern an internal model based controller is designed. The proposed controller is able to regulate the storage level and temperatures despite a possible time varying demand. The results are based on the following papers:

> **Scholten, T.W.**, De Persis, C. and Tesi, P.: 2016, Modeling and control of heat networks with storage: The single-producer multiple-consumer case, *Transactions on Control Systems Technology*, pp. 414–428.
>
> **Scholten, T.W.**, De Persis, C. and Tesi, P.: 2015, Modeling and control of heat networks with storage: The single-producer multiple-consumer case, *Proc. of the 2015 European Control Conference (ECC)*, pp. 2242–2247.

Chapter 4 shifts the focuss to a network in which multiple producers storages are connected. Motivated by slow temperature dynamics which are approximately constant we consider only the flow dynamics. In order to guarantee scalability we design distributed

controllers that regulate the flows and inputs in a flow network with multiple storages. The output of the controllers is saturated in order to satisfy transient constraints at all time. Moreover, a communication graph is introduced in order to guarantee an economic optimal production at steady state. Convergence is proven towards a point that, depending on the controller gains, lies arbitrary close to the desired optimal steady state. The results in this chapter were published in the following paper:

> **Scholten, T.W.**, De Persis, C. and Tesi, P.: 2016, Optimal steady state regulation of distribution networks with input and flow constraints, *Proc. of the 2016 American Control Conference (ACC)*, pp. 6953–6958.

In Chapter 5 the results of Chapter 4 are extended. In this extension the controllers are adapted to include an additional state which gives more flexibility in the design. Moreover, the saturation functions are changed to nonlinear strictly increasing functions with a possible bound on the range. These changes allow us to prove asymptotic stability of the optimal steady state. This chapter originates from the following papers:

> Trip, S., **Scholten, T.W.** and De Persis, C.: 2017, Optimal regulation of flow networks with input and flow constraints, *Proc. of the 2017 IFAC World Congress*, pp. 9854–9859.

> Trip, S., **Scholten, T.W.** and De Persis, C.: 2017, Optimal regulation of flow networks with transient constraints, *Automatica*, *Submitted*.

In Chapter 6 we return to a single producer without any storage capabilities. In order to decrease the size of the pipes we consider a topology with a multiple pump architecture. The goal is to regulate the centrifugal pumps in order to regulate the pressure at each consumer. As these pumps can often only provide positive pressures we constrain the control input to take on only non-negative values. We show local asymptotic stability of the desired pressure setpoints. This chapter stems from the following papers:

> **Scholten, T.W.**, Trip, S. and De Persis, C.: 2017, Pressure Regulation in Large Scale Hydraulic Networks with Input Constraints, *Proc. of the 2017 IFAC World Congress*, pp. 5534–5539.

> **Scholten, T.W.**, Trip, S. and De Persis, C., Pressure Regulation in Large Scale Hydraulic Networks with Positivity Constraints, *In preparation*.

In Chapter 7 we return to the setup as in Chapter 3 where the producer is taken to be a geothermal well. These wells are currently only used to provide a constant baseload while demand fluctuates throughout the year. For this reason we investigate if such a well of producing fluctuating patterns. In order to do this we design a model predictive

controller and perform a simulation to generate a realistic demand pattern. This demand pattern is used in a second simulation that simulates the two dimensional geochemistry of a reservoir located in Groningen, The Netherlands. The chapter originates from the following paper:

> Daniilidis, A., **Scholten, T.W.**, Hoogheim, J. De Persis, C., and Herber, R.: 2017, Geochemical implications of production and storage control by coupling a direct use geothermal system with heat networks, *Applied Energy*, pp. 254–270.

Finally, in the appendices model derivations, supporting lemmas and a case study can be found.

1.6 Preliminaries and notation

We denote by $\mathbb{R}^n$ and $\mathbb{R}^n_{>0}$ the set of n-dimensional vectors with real and strictly positive real entries respectively. Given a vector $x \in \mathbb{R}^n$, x^T is considered its transpose and we define $\|x\|$ to be its norm. The i-th element of vector x is denoted by $[x]_i$, where the brackets are omitted if it causes no ambiguity. For $a, b \in \mathbb{R}^n$ we define the inequalities (*e.g.* $a \leq b$) element-wise. Let the vector of all zeros be given by $\mathbf{0}_n$ and the vector of all ones by $\mathbb{1}_n$ where n is the length of the vector. The subscript is omitted in case the length of the vector is clear from the context. If the entries of x are functions of time then the time derivative of x is denoted as $\dot{x} := \frac{dx}{dt}$ unless stated otherwise. A steady state solution to system $\dot{x} = f(x)$, satisfying $\mathbf{0} = f(x)$, is denoted by $\overline{x}$, *i.e.* $\mathbf{0} = f(\overline{x})$. In many cases we drop the explicit dependency on t for time-dependent variables to simplify the notation. We define the operator $[x] := \text{diag}\begin{pmatrix} x_1 & x_2 & \dots & x_n \end{pmatrix}$ as the diagonal matrix of elements x_i, and block.diag$\begin{pmatrix} A_1 & A_2 & \dots & A_n \end{pmatrix}$ as the block-diagonal matrix for which the block diagonal matrices are A_i for $i = 1, ..., n$. The identity matrix of dimension n is given by I_n and a $n \times m$ matrix containing only zeros is denoted by $\mathbf{0}_{n\times m}$. For any matrix A we define Im(A) to be the image, ker(A) to be the kernel and $A^\dagger$ to be the Moore-Penrose pseudo-inverse of A. In case A is positive definite we denote it as $A \succ \mathbf{0}$. Moreover, the matrix norm is defined as

$$\|A\| = \max\{\|Ax\| : x \in \mathbb{R}^n \text{ with } \|x\| = 1\}.$$

For a vector space $\mathcal{S}$ we define $\mathcal{S}^\perp$ to be the orthogonal complement of $\mathcal{S}$, and for a set $\mathcal{W}$ of vectors let its span be defined as

$$\text{span}(\mathcal{W}) = \left\{ \sum_{i=1}^{k} \lambda_i x_i \middle| k \in \mathbb{N}, x_i \in \mathcal{W}, \lambda_i \in \mathbb{R} \right\}.$$

We denote the cardinality of a set $\mathcal{V}$ as $|\mathcal{V}|$. Let $C^1(\mathbb{R}; \mathbb{R})$ be the class of continuously differentiable functions with domain $\mathbb{R}$ and codomain $\mathbb{R}$. Occasionally write $f(x)$ as $f(\cdot)$ in case the argument x is clear from the context. We denote the range of $f(\cdot)$ as $\mathcal{R}(f(\cdot))$. Lastly we define the multidimensional saturation function $\text{sat}(x; x^-, x^+) : \mathbb{R}^n \to \mathbb{R}^n$ as

$$\text{sat}(x; x^-, x^+)_i := \begin{cases} x_i^- & : \text{if } x_i \leq x_i^- \\ x_i & : \text{if } x_i^- < x_i < x_i^+ \\ x_i^+ & : \text{if } x_i^+ \leq x_i, \end{cases}$$

where $x_i^-, x_i^+ \in \mathbb{R}$.

1.6.1 Graphs

Similar to (Bapat 2010) we define a graph as $\mathcal{G} = (\mathcal{V}, \mathcal{E})$, where $\mathcal{V} = \{1, ..., n\}$ is the set of nodes and $\mathcal{E} = \{1, ..., m\}$ is the set of edges connecting the nodes. We arbitrarily assign a $-$ and $+$ to the ends of each link, where it connects to a vertex. Using this we introduce the *incidence matrix* $B \in \mathbb{R}^{n\times m}$, whose elements are defined as

$$b_{ik} = \begin{cases} 1 & : \text{ if the } i\text{th node connects to the positive } (+) \text{ end of edge } k \\ -1 & : \text{ if the } i\text{th node connects to the negative } (-) \text{ end of edge } k \\ 0 & : \text{ otherwise,} \end{cases} \tag{1.1}$$

and the Laplacian matrix is defined as $L = BB^T$. Let $\mathcal{T}$ be a spanning tree of $\mathcal{G}$, i.e., a connected subgraph which does not contain any cycle and contains all the nodes of the graph. As a consequence any edge in $\mathcal{G}$ which is not in $\mathcal{T}$ is necessarily a chord. This implies that by including a chord i in $\mathcal{T}$, a cycle $\mathcal{L}_i$ is obtained. We will also assign a reference direction to each of the cycles and refer to them as *fundamental loops*. Let $|\mathcal{L}|$ be the number of cycles in $\mathcal{G}$, we finally define the entries of the *fundamental loop matrix* $D \in \mathbb{R}^{|\mathcal{L}|\times|\mathcal{E}|}$ as

$$d_{ij} = \begin{cases} 1 & \text{edge } j \text{ is in } \mathcal{L}_i \text{ and directions agree} \\ -1 & \text{edge } j \text{ is in } \mathcal{L}_i \text{ and directions don't agree} \\ 0 & \text{edge } j \text{ is not in } \mathcal{L}_i. \end{cases} \tag{1.2}$$

Chapter 2

Models and load sharing

A district heating system consists of many components of which the main ones are pipes, valves, pumps, storage tanks, heat exchanges, producers, consumers. Models of these components in district heating systems are widely available. Most of these models are based on general modeling principals of thermodynamic systems such as in (Skogestad 2009). The modeling of heat exchangers is discussed in *e.g.* (Hangos et al. 2004), where also the controllability and observability is investigated. Moreover, there is a wide variety of possibilities for thermal storage. A survey of different techniques can be found in (Dincer and Rosen 2002). The most common way is to use water tanks with a fixed volume that can be heated and cooled. In such tanks there are three layers, one with hot water, one with cold water and a separation layer called a thermocline, which has a steep thermal gradient. This type of storage is referred to as stratification and is studied in detail in both (Yoo and Pak 1993) and (Verda and Colella 2011). An alternative is to have an empty tank which can be filled/drained with hot water but has the disadvantages of lower efficiency and higher dissipation rates. Recent interest has shifted towards heat storage in phase-changing materials, which have some interesting properties such as low dissipation rates but are not considered in this thesis. Models of the pressure and flow dynamics in pipes, valves, pumps are discussed in (De Persis and Kallesoe 2011). Moreover, the open loop model of a network consisting of these components is also derived.

In this chapter we introduce three models that describe a district heating system by considering the relations between volumes, temperatures, flow rates and pressures. Since the modeling itself is not novel, this chapter is mainly intended to set the ground for the remaining chapters. In these remaining chapters controllers are designed and analysed that (optimally) regulate the distribution of energy in a district heating network. Since the considered dynamics in most of these models represent a broader class of systems the results of the modeling (and subsequent controller design) have many other applications. Examples of these applications are therefore discussed when these models are introduced. We conclude this chapter with an optimization problem which we refer to as the optimal economic dispatch problem of which the solution will be considered in the

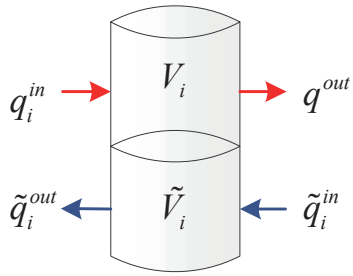

Figure 2.1: Stratified storage tank.

design of some of the controllers.

2.1 Flow networks

The first model that we consider relates volumes to flow rates and is in the literature referred to as a flow network or compartmental system. The design and regulation of these networks received significant attention due to its many applications, including supply chains (Alessandri et al. 2011), heating, ventilation and air conditioning (HVAC) systems (Gupta et al. 2015), data networks (Moss and Segall 1982), traffic networks (Iftar 1999) and compartmental systems (Blanchini et al. 2016). To motivate the relation to district heating system we first introduce a storage tank and its dynamics. By interconnecting multiple storage devices in a network and connecting each to a producer and consumer we obtain a model which is referred to as a flow network.

2.1.1 Storage model

The storage tank that we consider uses a stratification principle where hot water on the top is separated from cold water at the bottom by a thermocline. This device has four valves, two at the top and two at the bottom. These valves are used as in- and out-lets of the hot and cold part of the storage device such as depicted in Figure 2.1. The temperatures of the top and bottom layer are approximately constant with respect to the height of the tank. On the contrary, the thermocline is a thin layer with a steep temperature gradient (Verda and Colella 2011), (Ma et al. 2009). We neglect the thermocline which allows us to model the storage device as two separate storage tanks that are placed on top of each other[1]. This is motivated by a low heat exchange rate between the hot and the

[1]Under this assumption the model the exact same model can be used for a topology with separate hot and cold water storage tanks. The results presented in this work can therefore also be applied to such a network.

cold layer of the storage tank. Additionally it is possible to add an insulation layer that decreases the heat exchange even further. Such a layer can also prevent mixing during long discharging or charging periods which causes a more severe and undesirable heat exchange rate. Furthermore we assume that each layer is perfectly stirred. In Section 2.2 the temperature dynamics are introduced which are neglect in the remainder of this section.

First let us consider the volume dynamics for storage tank i, which are given by

$$\dot{V}_i = q_i^{in} - q_i^{out} \tag{2.1a}$$

$$\dot{\tilde{V}}_i = \tilde{q}_i^{in} - \tilde{q}_i^{out}, \tag{2.1b}$$

where (2.1a) models the hot layer and (2.1b) the cold one. Moreover, q_i^{in}, q_i^{out} and V_i are the inflow, outflow and volume of the hot layer, respectively and the variables with a tilde are their counterparts that correspond to the cold layer.

Remark 2.1 (Other applications)**.** *The single integrator dynamics in (2.1a) (and (2.1b)) model many other systems such as inventory systems (De Persis 2013) and multi-agent systems (Olfati-Saber et al. 2007).*

We denote the total capacity of the storage tank i by $V_i^{\max}$ and consider the storage device to be always completely filled with water. In order to guarantee that both the hot and the cold layer are strictly positive we require a proper initialization and restrictions on q_i^{in}, q_i^{out}, $\tilde{q}_i^{in}$ and $\tilde{q}_i^{out}$. The restrictions will be taken care of in the controller design in Chapter 3, but we make the following assumption with respect to the initialization of the storage tanks:

Assumption 2.2 (Volume constraints)**.** *Let $V_i(0), \tilde{V}_i(0) \in \mathcal{V}_i$ where*

$$\mathcal{V}_i := \left[V_i^{\min}, V_i^{\max} - V_i^{\min}\right], \tag{2.2}$$

with $0 < 2V_i^{\min} \leq V_i^{\max} < \infty$. Moreover $V_i(0)$ and $\tilde{V}_i(0)$ satisfy

$$V_i(0) + \tilde{V}_i(0) = V_i^{\max}. \tag{2.3}$$

Note that Assumption 2.2 implies that both $V_i(0)$ and $\tilde{V}_i(0)$ are bounded away from zero by $V_i^{\min}$ and it has the following implication:

Lemma 2.3 (Persistence of a completely filled storage)**.** *If Assumption 2.2 is satisfied and $\tilde{q}_i^{in}$ and $\tilde{q}_i^{out}$ are such that $q_i^{in} - q_i^{out} = \tilde{q}_i^{in} - \tilde{q}_i^{out}$ then*

$$V_i(t) + \tilde{V}_i(t) = V_i^{\max} \quad \textit{for all } t > 0. \tag{2.4}$$

Proof. From (2.1) it follows that $\dot{V}_i + \dot{\tilde{V}}_i = 0$ and together with (2.3) it follows that (2.4) is satisfied. ∎

We interconnect multiple storage devices through a network as presented in the next section.

2.1.2 Model flow networks

We consider a network of physically interconnected *undamped* dynamical systems. Each dynamical system is described by (2.1a) and the topology of the system is described by an undirected graph $\mathcal{G} = (\mathcal{V}, \mathcal{E})$, where $\mathcal{V} = \{1, ..., n\}$ is the set of nodes and $\mathcal{E} = \{1, ..., m\}$ is the set of edges connecting the nodes. We represent the topology by its corresponding incidence matrix $B \in \mathbb{R}^{n\times m}$ as defined in Section 1.6.1. Each node (storage) can have a disturbance (demand) and input (production). Let $\mathcal{V}_e \subset \mathcal{V}$ be the set of nodes that are controlled by an *external* input, with $|\mathcal{V}_e| = p$ and we define

$$e_i = \begin{cases} 1 & i \in \mathcal{V}_e \\ 0 & \text{otherwise.} \end{cases} \tag{2.5}$$

The dynamics of node i are given by

$$T_{x_i}\dot{x}_i(t) = -\sum_{k\in\mathcal{E}_i} B_{ik}\lambda_k(t) + e_i u_i(t) - d_i \tag{2.6a}$$

$$y_i(t) = h_i(x_i(t)), \tag{2.6b}$$

where $x_i(t)$ is the storage (inventory) level, $u_i(t)$ the control input, $T_{x_i} \in \mathbb{R}_{>0}$ a constant[2], d_i is a constant *unknown* disturbance and $y_i = h_i(x_i)$ the measured output with $h_i(\cdot)$ a continuously differentiable and strictly increasing function. Moreover, $\mathcal{E}_i$ is the set of edges connected to node i and $\lambda_k(t)$ is the flow on edge k. We can represent the complete network compactly as[3]

$$T_x\dot{x} = -B\lambda + Eu - d \tag{2.7a}$$

$$y = h(x), \tag{2.7b}$$

where $T_x \in \mathbb{R}^{n\times n}_{>0}$, $B \in \mathbb{R}^{n\times m}$, $\lambda \in \mathbb{R}^m$, $u \in \mathbb{R}^p$ and $d \in \mathbb{R}^n$. Without loss of generality we assume that only the first p nodes have a controllable input, i.e. $\{1, \ldots, p\} = \mathcal{V}_e$, and

[2]Usually we have $T_{x_i} = 1$ in the classical flow networks, where a material is transported.

[3]For the sake of simplicity, the dependence of the variables on time t is omitted in most of the remainder this thesis.

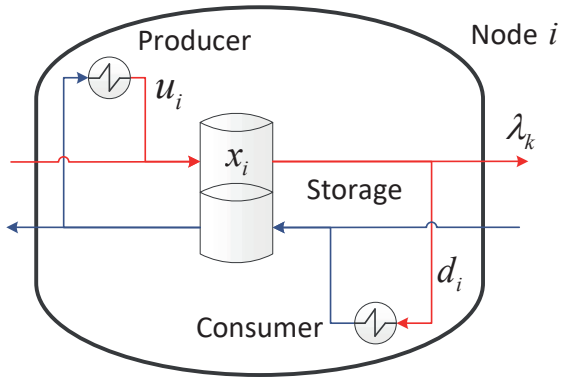

Figure 2.2: A node in the district heating network.

consequently $E \in \mathbb{R}^{n\times p}$ is of the form

$$E = \begin{pmatrix} I_{p\times p} \\ \mathbf{0}_{(n-p)\times p} \end{pmatrix}. \tag{2.8}$$

Furthermore, $y \in \mathbb{R}^n$ and $h(x) \in \mathbb{R}^n$ of which the i-th component is given by $h_i(x_i)$.

Remark 2.4 (Example of model (2.7))**.** *Consider a district heating network where each node has a producer, a consumer and a stratified storage tank interconnected as in Figure 2.2. Motivated by Lemma 2.3 we set the flows in the return pipes such that* $\tilde{q}_i^{in} = q_i^{in}$ *and* $\tilde{q}_i^{out} = q_i^{out}$*. For this reason we can neglect (2.1b) and consider that the storage device is only modeled by (2.1a). This implies that (2.7) can model a network of interconnected storage devices connected to heat exchangers that inject and extract their heat production and demand.*

We make two basic Assumptions on the network. First, in order to guarantee that each node can be reached from anywhere in the graph we make the following Assumptions on the topology:

Assumption 2.5 (Connectedness)**.** *The graph* $\mathcal{G}$ *is connected.*

We recall (see *e.g.* (Bapat 2010, Lemma 2.2)) the following useful lemma:

Lemma 2.6 (Rank of B)**.** *Let* $\mathcal{G}$ *be a graph with n nodes and let B be the incidence matrix of* $\mathcal{G}$*. Then the rank of B is* $n - 1$ *if and only if* $\mathcal{G}$ *is connected.*

Proof. For a general graph we have that $B^T x = 0$ implies that $x_i - x_j = 0$ for all nodes i and j which are connected. Therefore we have that Assumption 2.5 implies that

$\ker(B^T) = \mathrm{Im}(\mathbb{1})$. Since the kernel is one dimensional the row-rank of B^T is at least $n-1$ and since the rows of B^T are linearly dependent, the row-rank of B^T is at most rank $n-1$. This implies that the row-rank of B^T is $n-1$ and therefore $L = BB^T$ has rank $n-1$. ■

Second, to compensate for the disturbances to the network, the following assumption is required:

Assumption 2.7 (Controllable inputs)**.** *There is at least one node that has a controllable input, i.e.* $p \geq 1$.

An immediate consequence of Assumption 2.5 and its related Lemma 2.6 is the following result:

Lemma 2.8 (Rank of $\begin{pmatrix} B & E \end{pmatrix}$)**.** *If Assumption 2.5 is satisfied, then Assumption 2.7 is equivalent to* $\begin{pmatrix} B & E \end{pmatrix}$ *being full row rank, i.e.* $\mathrm{rank}\left(\begin{pmatrix} B & E \end{pmatrix}\right) = n$.

Particularly, in Chapter 5 we will use the fact that the pseudoinverse of $\begin{pmatrix} B & E \end{pmatrix}$ constitutes a right inverse, which has been exploited within a similar context in *e.g.* (Blanchini et al. 2016).

2.2 Temperature dynamics

Additionally to (2.7) we consider the temperature dynamics. Motivated by the predominant topology we restrict the topology to a single node (*i.e.* one storage device) to which a single producer and multiple consumers are connected. First we introduce the temperature dynamics of the storage tank after which we do the same for the producer and consumers which are modeled as a heat exchanger. Finally we interconnect the different components in order to derive a model that describes the volume, flow and temperature dynamics.

2.2.1 Storage tank

We consider a stratified storage tank as in Figure 2.1 and define the temperatures in the hot and cold layer of the storage tank as T and $\tilde{T}$, respectively. With the help of (A.4) in Appendix A we derive a model of a heat exchanger and storage device.

Since there is no heat generation and, since we assume that the heat losses are negligible, no heat absorption we have that $P = 0$. This implies that the temperature dynamics of the storage device are given by

$$V\dot{T} = q^{in}(T^{in} - T) \tag{2.9}$$

$$\tilde{V}\dot{\tilde{T}} = \tilde{q}^{in}(\tilde{T}^{in} - \tilde{T}), \tag{2.10}$$

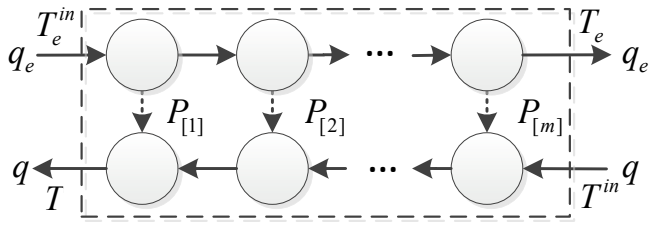

Figure 2.3: Model of a heat exchanger adopted from (Hangos et al. 2004) with m cells with power transfer in cell k given by $P_{[k]}$. Since the inflow equals the outflow, flow rates q_e and q are defined only once. T_e^{in} and T^{in} are the inflow and T_e and T the outflow temperatures.

where q^{in} and $\tilde{q}^{in}$ are the flowrates with temperatures T^{in} and $\tilde{T}^{in}$ entering the hot and cold layer respectively.

2.2.2 Heat exchanger

A heat exchanger exchanges energy between two streams of liquid (or gas) while they are physically separated. Each producer and consumer is modeled by a heat exchanger with a corresponding heat production and demand. A heat exchanger can be modeled as m cells connected in series such as depicted in Figure 2.3. In this figure each cell contains two volumes separated by a heat conducting element. We restrict ourselves to a model where $m = 1$, and assume that both volumes in the cell are perfectly stirred[4]. Moreover, we assume the following quantities to be constant in each cell: volume, mass, specific heat c_P, density ρ, heat transfer coefficient U and contact area of the heat conducting element A_h. Assuming that the used fluid is incompressible and since there is no storage nor loss of mass in a heat exchanger, the inflow rate equals the outflow rate. Hence, it is enough to associate to each heat exchanger a single flow variable. Using (A.4), we obtain that the dynamics for the temperatures of the two volumes are then given by

$$V_e^h \dot{T}_e = q_e^h \left(T_e^{h,in} - T_e^h \right) - P^h \tag{2.11}$$

$$V^h \dot{T}^h = q^h \left(T^{h,in} - T^h \right) + P^h, \tag{2.12}$$

where $V_e^h > 0$ and $V^h > 0$ are the volumes in the upper and lower cell, respectively. The superscripts h are used to denote the heat exchanger and the subscripts e denote the upper part of the cell, *i.e.* the compartments that connect to the producer or consumer. In case the heat exchanger is located at a producer and is considered to be the controllable input.

[4]Alternatively a logarithmic mean temperature difference (Thulukkanam 2013) can be used to approximate the heat exchange between the m cells which we leave for further research.

When it is located at a consumer P^h is the heat extraction considered to be an unknown disturbance.

Remark 2.9 (Controllability of the heat exchanger)**.** *Since V_e^h is relatively small compared to the storage volumes considered in (2.9), the dynamics (2.11) are relatively fast compared to (2.9). For this reason we are can neglect (2.11) and consider P^p as a control input. Moreover, the heat transfer rate P^h is given by*

$$P^h = \frac{UA_h}{c_p \rho} \left(T_e^h - T^h \right), \tag{2.13}$$

which implies that the temperature T^h can be regulated by q^h and q_e as long as $T_e^h \neq T_e^{h,in}$, $T^h \neq T^{h,in}$. Therefore a heat exchanger is controllable with the exception of this singular point (Hangos et al. 2004). In order to avoid this operation point a sufficiently high (or, in case of cooling, low) supply temperature $T_e^{h,in}$ should be applied.

Motivated by Remark 2.9 we neglect the dynamics (2.11) and model a heat exchanger solely by (2.12). Therefore the dynamics of the heat exchanger located at the producer and each consumer i is given by

$$V^p \dot{T}^p = q^p \left(T^{p,in} - T^p \right) + P^p \tag{2.14}$$

$$V_i^c \dot{T}_i^c = q_i^c \left(T_i^{c,in} - T_i^c \right) + P_i^c, \tag{2.15}$$

respectively.

Remark 2.10 (Bypass of a heat exchanger)**.** *Note that the heat exchangers separate the fluid in the network from both the fluids of the consumers and producer. This separation ensures that no contamination can enter the network and storage device. In certain cases it can however be beneficial to bypass the heat exchangers (and storage) by adding a direct connections between a producer and consumer. For example, when the producers generates steam, such a connection can be used to further heat up the hot water delivered to the consumer.*

2.2.3 Topology and compact form

Motivated by the predominant topology used for district heating system we consider a setup with a single producer of heat (*e.g.* a waste-to-energy plant (Bardi and Astolfi 2010) or a combined heat power plant) and n consumers (*e.g.* industrial or residential buildings). A storage tank is included in the topology to guarantee a heat supply while the heat demand is time dependent. The considered topology is depicted in Figure 2.4.

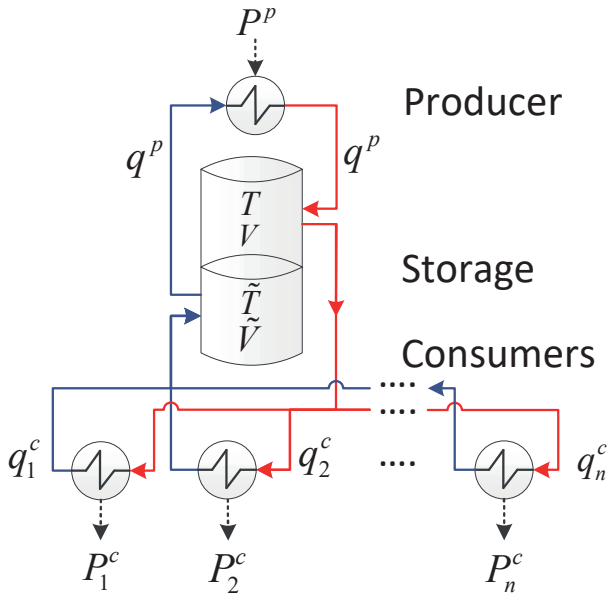

Figure 2.4: Topology of a district heating network.

The open loop temperature dynamics are obtained by interconnecting the storage and heat exchangers modeled by (2.12) and (2.14)–(2.15) as in the considered topology. Since in this topology multiple pipes with different flowrates and temperatures merge we require an expression of the resulting temperature after merging in order to obtain the model. Using the conservation of energy we obtain

$$T^{in} = \frac{\sum_{i=1}^{n} q_i^c T_i^c}{\sum_{i=1}^{n} q_i^c}, \tag{2.16}$$

where q_i^c is the flow rate and T_i^c the temperature of the fluid passing through pipe that originates from consumer i. By combining (2.14)-(2.16) and considering the topology of Figure 2.4 we obtain

$$\begin{aligned} V^p \dot{T}^p &= \left(\tilde{T} - T^p\right) q^p + P^p \\ V\dot{T} &= \left(T^p - T\right) q^p \\ \tilde{V}\dot{\tilde{T}} &= \sum_{i=1}^{n} \left(T_i^c - \tilde{T}\right) q_i^c \\ V_j^c \dot{T}_j^c &= \left(T - T_j^c\right) q_j^c - P_j^c, \;\; j = 1, 2, \ldots, n. \end{aligned} \tag{2.17}$$

Moreover, the volume dynamics of the storage device are obtained from (2.6a) by letting

$T_{x_1} = 1$, $x_1 = V$, $e_1 = 1$, $u_1 = q^p$ and $d_1 = \sum_{i=1}^{n} q_i^c$. Moreover $b_{1k} = 0$ since we only consider one node, and the resulting dynamics are given by

$$\dot{V} = q^p - \sum_{i=1}^{n} q_i^c \tag{2.18a}$$

$$\dot{\tilde{V}} = \sum_{i=1}^{n} q_i^c - q^p, \tag{2.18b}$$

where (2.18b) follows from the conservation of mass and (2.18a), *i.e.* there is no dissipation of mass in the pipes and heat exchangers. We therefore note that (2.4) is satisfied independent of q^p and q^c as a result of Lemma 2.3.

Remark 2.11 (Delay)**.** *Since the length of the pipes in district heating systems are often very large the temperature dynamics can be subject to a possibly large delay. The addition of such a delay can cause oscillation or even instability for otherwise asymptotical stable systems. However, as it is hard to include this delay in the stability analysis we do not include the pipe dynamics. Consequently, all the results based on this model do not take this delay into account and the inclusion is left for future research.*

We now write system (2.17)-(2.18) in a more compact form and define the inputs, states, outputs and disturbances of the system. Because we can control both the heat injection and the flow rates in the pipes, these are taken as inputs and are respectively given as $u = P^p$ and

$$\nu = \begin{pmatrix} \nu_p \\ \nu_c \end{pmatrix} = \begin{pmatrix} q^p \\ q^c \end{pmatrix},$$

where $q^c := \begin{pmatrix} q_1^c & q_2^c & \dots & q_n^c \end{pmatrix}^T$. The disturbances are given as $d = \begin{pmatrix} P_1^c & \dots & P_n \end{pmatrix}^T$, and we collect temperatures and volumes in the state vectors

$$z := \begin{pmatrix} z_p \\ z_s \\ z_{\tilde{s}} \\ z_c \end{pmatrix} = \begin{pmatrix} T^p \\ T^{s_h} \\ T^{s_c} \\ T^c \end{pmatrix}$$

$$x := \begin{pmatrix} x_s \\ x_{\tilde{s}} \end{pmatrix} = \begin{pmatrix} V^{s_h} \\ V^{s_c} \end{pmatrix},$$

where $T^c := \begin{pmatrix} T_1^c & T_2^c & \dots & T_n^c \end{pmatrix}^T$. It follows that (2.17)-(2.18) is equivalent to

$$M(x)\dot{z} = A(\nu)z + Uu - d \tag{2.19a}$$

$$\dot{x} = N\nu \tag{2.19b}$$

$$y = Cz, \tag{2.19c}$$

where

$$M(x) = \text{block.diag}\begin{pmatrix} V^p & [x] & [V^c] \end{pmatrix} \tag{2.20a}$$

$$A(\nu) = \begin{pmatrix} -\nu_p & 0 & \nu_p & \mathbf{0}_{1\times n} \\ \nu_p & -\nu_p & 0 & \mathbf{0}_{1\times n} \\ 0 & 0 & -\mathbb{1}_n^T \nu_d & \nu_d^T \\ \mathbf{0}_{n\times 1} & \nu_d & \mathbf{0}_{n\times 1} & -[\nu_d] \end{pmatrix} \tag{2.20b}$$

$$U = \begin{pmatrix} 1 \\ \mathbf{0}_{(n+2)\times 1} \end{pmatrix} \tag{2.20c}$$

$$N = \begin{pmatrix} 1 \\ -1 \end{pmatrix}\begin{pmatrix} 1 & -\mathbb{1}_n^T \end{pmatrix} \tag{2.20d}$$

$$C = \begin{pmatrix} 0 & 1 & 0 & \mathbf{0}_{1\times n} \end{pmatrix}, \tag{2.20e}$$

with $V^c := \begin{pmatrix} V_1^c & V_2^c & \dots & V_n^c \end{pmatrix}^T$. Observe that $A(\nu)$ is a time varying matrix due to the dynamics of $\nu(t)$.

2.3 Hydraulic networks

So far we have considered the flowrate as an input that we can control. However, pumps that regulate the flows generate a pressure and as a consequence produce a flow. Motivated by this observation we introduce a model of a hydraulic network that models the pressure and flow dynamics of a district heating system. We adopt this model from (De Persis and Kallesoe 2011) with a topology similar as in Figure 2.4 with the difference that no storage device is included. Moreover, in this model the heat dynamics are not considered, the heat exchangers are modeled as a valve and additionally models of pumps and pipes are introduced. We briefly state the models of these components along with assumptions after which we derive the model of the overall network by connecting the components.

2.3.1 Components

The hydraulic network consists of multiple components (pumps, pipes and valves) that are characterized by their dynamic and algebraic relationships between the flow $\tilde{q}_k$ through the component k and the pressure drop $h_i - h_j$ across that component, where subscripts i and j denote the two ends of component k. We summarize the relations for the considered components below.

1. *Pump:* A pump is a device that is able to deliver a desired pressure difference

$$h_i - h_j = -\Delta h_{pk}, \tag{2.21}$$

where Δh_{pk} is the pressure difference created by the pump and can be regarded as a *control input*. We consider pumps that can only apply positive pressures *i.e.* $\Delta h_{pk} \geq 0$.

2. *Pipe:* We assume that the fluid is incompressible and that the diameter of the pipe is constant. From this it follows that the model for the k-th pipe is given by

$$h_i - h_j = \mathcal{J}_k \frac{d\tilde{q}_k}{dt} + \lambda_k(K_{pk}, \tilde{q}_k), \tag{2.22}$$

where $\mathcal{J}_k$ is a constant that depends on the mass density of the fluid and pipe dimensions, $\tilde{q}_k$ is the flow through pipe k and $\lambda_k(K_{pk}, \tilde{q}_k) \in C^1(\mathbb{R}; \mathbb{R})$ is strictly increasing in $\tilde{q}_k$ and $K_{pk} \in \mathbb{R}$ is a constant that models the pipe characteristics[5].

3. *Valve:* The vales are modeled by a relationship between the pressure drop across the valve and the flow through it, *i.e.*

$$h_i - h_j = \mu_k(K_{vk}, \tilde{q}_k), \tag{2.23}$$

where $\mu_k(K_{vk}, \tilde{q}_k) \in C^1(\mathbb{R}; \mathbb{R})$ is increasing in $\tilde{q}_k$ and and $K_{vk} \in \mathbb{R}$ is a constant that models the valve opening.

Note that each of these components can be written as

$$\Delta h_k = \mathcal{J}_k \frac{d\tilde{q}_k}{dt} + \lambda_k(K_{pk}, \tilde{q}_k) + \mu_k(K_{vk}, \tilde{q}_k) - \Delta h_{pk}, \tag{2.24}$$

when we take for the different components

[5] λ is introduced with some abuse of notation since there is no relation with the nonlinear mapping in (2.7a).

1. *Pump:* $\mathcal{J}_k = 0$, $\lambda_k = 0$ and $\mu_k = 0$.

2. *Pipe:* $\mu_k = 0$ and $\Delta h_{pk} = 0$.

3. *Valve:* $\mathcal{J}_k = 0$, $\lambda_k = 0$ and $\Delta h_{pk} = 0$.

2.3.2 Topology and compact form

Motivated by the predominant topology for district heating networks, we consider a topology with a single producer and multiple end-users. In order to guarantee that each end-user is connected to the producer we make the following assumption:

Assumption 2.12 (Connected graph)**.** *The graph $\mathcal{G}$ is connected.*

We associate each end-user to a valve and make the following assumption on topology of the network:

Assumption 2.13 (End-user valves located on a chord)**.** *All end-user valves are located on a chord of $\mathcal{G}$ and are connected in series with a pump and a pipe.*

We also associate the producer to a valve and to guarantee that each end-user can be reached from the producer we make the assumption:

Assumption 2.14 (Location producer valve)**.** *The edge corresponding to the producer valve belongs to each fundamental loop as defined in (1.2).*

An example of a topology that satisfies Assumptions 2.12-2.14 is given in Figure 2.5.

We now collect all $\tilde{q}_k$ in a vector $\tilde{q} \in \mathbb{R}^m$, where m is the total number of components in the network and we let the first n entries correspond to the valves of the n end-users. It has been proven in (De Persis and Kallesoe 2011) that these assumptions imply that the fundamental loop matrix takes the form of

$$D = \begin{pmatrix} I_n & F \end{pmatrix}, \tag{2.25}$$

where F has entries $f_{ij} \in \{0, 1\}$. The measured output is the pressure drop across the end-user valves, that is

$$y_i = \mu_i(K_{vi}, \tilde{q}_i), \tag{2.26}$$

for $i \in \{1, \ldots, n\}$.

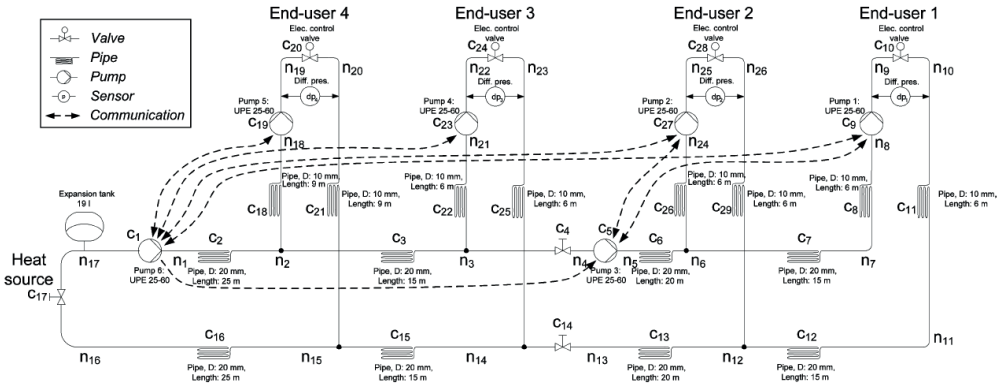

Figure 2.5: Example topology of a hydraulic network (De Persis and Kallesoe 2011).

In order to write the system in compact form we define

$$f(\tilde{q}) = \lambda(\tilde{q}) + \mu(\tilde{q}), \tag{2.27}$$

where

$$\lambda(\tilde{q}) = \begin{pmatrix} \lambda_1(K_{p1}, \tilde{q}_1) \\ \vdots \\ \lambda_m(K_{pm}, \tilde{q}_m) \end{pmatrix} \tag{2.28}$$

$$\mu(\tilde{q}) = \begin{pmatrix} \mu_1(K_{v1}, \tilde{q}_1) \\ \vdots \\ \mu_m(K_{vm}, \tilde{q}_m) \end{pmatrix}. \tag{2.29}$$

Moreover, let $\mu_c(\tilde{q})$ be the first n components of $\mu(\tilde{q})$, *i.e.*

$$\mu_c(\tilde{q}) = \begin{pmatrix} \mu_1(K_{v1}, \tilde{q}_1) \\ \vdots \\ \mu_n(K_{vn}, \tilde{q}_n) \end{pmatrix}. \tag{2.30}$$

We also introduce a new state vector $q \in \mathbb{R}^{|\mathcal{L}|}$ with $|\mathcal{L}|$ be the number of cycles in $\mathcal{G}$ which is more convenient for the analysis

$$\tilde{q} = D^T q. \tag{2.31}$$

The components of the vector $\tilde{q}$ denote the flow through their corresponding cycle while

the components of q denote the flow through a component. We are now ready to compactly write the overall network model.

Lemma 2.15 (Compact form hydraulic network)**.** *Under Assumptions 2.12–2.14 we can write the dynamics and output of a hydraulic network as*

$$\begin{aligned} J\dot{q} &= -Df(D^T q) + u \\ y &= \mu_c(q), \end{aligned} \tag{2.32}$$

where $J = D\mathcal{J}D^T$, $u = D\Delta h_p$, $f(\cdot)$ as in (2.27) and $\mu_c(\cdot)$ as in (2.30).

Proof. A detailed proof can be found in (De Persis and Kallesoe 2011). ∎

Remark 2.16 (Inputs in a fundamental loop)**.** *Note that the input to system (2.32) is given by $u = D\Delta h_p$ and therefore u_i consists of the sum of all the pump pressures delivered in the i-th fundamental loop. Since D has full row rank and consists of non-negative entries it is possible to find a (not necessarily unique) $\Delta h_p \geq 0$ for any given $u = D\Delta h_p \geq 0$.*

2.4 Optimal load sharing

In case multiple producers are connected to a district heating system it is desirable to coordinate the production optimally among the producers. To this end, we assign a strictly convex linear-quadratic cost function $C_i(u_{pi})$ to each producer of the form

$$C_i(u_i) = \frac{1}{2} q_i u_i^2 + r_i u_i + s_i, \tag{2.33}$$

with $q_i \in \mathbb{R}_{>0}$ and $s_i, r_i \in \mathbb{R}$. The total cost can be expressed as

$$C(u) = \sum_{i \in \mathcal{V}} C_i(u_i) = \frac{1}{2} u^T Q u + r^T u + s, \tag{2.34}$$

where $Q = \mathrm{diag}(q_1, \ldots, q_n)$, $r = (r_1, \ldots, r_n)^T$ and $s = \Sigma_{i=1}^n s_i$. Minimizing (2.34) while satisfying the equilibrium condition

$$\mathbf{0} = -B\lambda + Eu - d, \tag{2.35}$$

of system (2.7a) gives rise to the following optimization problem:

$$\begin{aligned} \underset{u,\lambda}{\text{minimize}} \quad & C(u) \\ \text{subject to} \quad & \mathbf{0} = -B\lambda + Eu - d. \end{aligned} \tag{2.36}$$

A solution to (2.36) is derived in (Trip et al. 2016, Lemma 4) and for completeness we provide a similar lemma.

Lemma 2.17 (Solution to optimization problem (2.36))**.** *The solution to (2.36) is given by*

$$\overline{u} = Q^{-1}(\kappa - r), \tag{2.37}$$

where

$$\kappa = E^T \frac{\mathbb{1}_n \mathbb{1}_n^T}{\mathbb{1}_p^T Q^{-1} \mathbb{1}_p}(d + EQ^{-1}r). \tag{2.38}$$

Proof. The proof follows standard arguments from convex optimization as discussed in (Boyd and Vandenberghe 2004). First we introduce the Lagrangian

$$L(u, \zeta) = C(u) + \zeta(-B\lambda + Eu - d), \tag{2.39}$$

where $\zeta \in \mathbb{R}$ is the Lagrange multiplier. Observe that $L(u, \zeta)$ as in (2.39) is strictly convex in u since $C(u)$ is strictly convex and concave in ζ. It follows that there exists a saddle point $(\overline{u}, \overline{\zeta})$ corresponding to $\max_\zeta \min_u L(u, \zeta)$, and it satisfies

$$\begin{aligned} \mathbf{0} &= \nabla C(\overline{u}) + \mathbb{1}_p \overline{\zeta} \\ \mathbf{0} &= -B\lambda + E\overline{u} - d. \end{aligned} \tag{2.40}$$

From (2.34) we obtain that $\nabla C(\overline{u}) = Q\overline{u} + r$ and together with (2.40) this implies that

$$\overline{u} = -Q^{-1}(\mathbb{1}_p \overline{\zeta} + r) \tag{2.41}$$

$$\mathbb{1}_p^T \overline{u} = \mathbb{1}_n^T d, \tag{2.42}$$

and solving for $\overline{\zeta}$ yields

$$\overline{\zeta} = -\frac{d + \mathbb{1}_n^T (EQ^{-1}r)}{\mathbb{1}_p^T Q^{-1} \mathbb{1}_p}. \tag{2.43}$$

By defining

$$\kappa = E^T \mathbb{1}_n \overline{\zeta}, \tag{2.44}$$

it follows that κ is as in (2.38) and we obtain from (2.41) that

$$\overline{u} = -Q^{-1}(\kappa + r). \tag{2.45}$$

For this reason the solution to (2.36) is given by (2.37), which proves the thesis. ∎

Remark 2.18 (Identical marginal costs)**.** *Note that we can rewrite (2.37) as*

$$\kappa = Q\overline{u} + r, \tag{2.46}$$

and that $\kappa \in \mathrm{Im}(\mathbb{1}_p)$*. It follows that, when evaluated at the solution to (2.36), the so-called marginal costs* $\frac{\partial C_i(u_i)}{\partial u_i} = q_i u_i + r_i$ *are identical for all* $i \in \mathcal{V}_e$ *(Hoy et al. 2011).*

Chapter 3

Temperature and volume regulation with a single producer

Abstract

In heat networks, energy storage in the form of hot water in a tank is a viable approach to balancing supply and demand. In order to store a desired amount of energy, we require that both the volume and temperature of the water in the tank converge to desired setpoints. Therefore we consider a volume and temperature regulation problem of a storage in a district heating system. The storage tank is fed by a single producer and provides multiple consumers in a district heating system. We design a proportional controller for the flows and an internal model based controller for the heat injection that guarantees the achievement of the desired goals despite a possibly time varying demand. In order to analyse the stability of the closed loop system we consider a nonlinear model that describes the temperature and volume dynamics. The controllers are designed such that only measurements of the volume and temperature in the storage device are required and we prove asymptotic stability towards the desired setpoints despite the time varying demand.

The proposed methods to (optimally) regulate a district heating system can be categorized into three approaches. The first approach is to control control the pumps and heat injection in a district heating network is by means of a PID controllers (Liu and Daley 2001). The second approach is to solve an optimization problem and implement the optimal control inputs such as in (Aringhieri and Malucelli 2003), where a linear programming model for optimal resource management of a combined heat power plant, in combination with a distribution network is presented. Another example of this approach is a model predictive control strategy such as in (Sandou et al. 2005). The last approach is to optimize the topology such as has been proposed in (Jäschke and Skogestad 2014) where an optimization problem is solved to maximize the heat transfer in heat exchanger networks with stream splits. Note that these approaches are not mutually exclusive and can therefore be combined. The stability analysis is of these systems is often simplified. In (Hangos et al. 2004) the stability of the individual components is analyzed instead of the whole closed loop system. Moreover, in many cases the dynamics of the

network are linearized such as in (Hao et al. 2014) and for model predictive controllers it is well known that it is difficult to prove any stability results. Another possibility to simplify the model is to neglect the temperature dynamics and consider only the dynamics of the mass flow rates. Examples of this approach can be found in (De Persis and Kallesoe 2011) and (De Persis et al. 2014) were a pressure regulation problem was solved for nonlinear hydraulic networks. In Chapters 4-6 we follow a similar approach by neglecting the temperature dynamics.

In this chapter we consider a district heating system with a topology that consists of a single producer, a storage device and multiple consumers. The non-linear model corresponding to this topology was derived in Section 2.2.3. Since the heat supply and demand has a fluctuating behaviour, storage tanks can guarantee a balance between demand and supply. For example an optimization problem can provide optimal storage levels in order to secure supply in the future. An example of this is discussed in Chapter 7. Within an interval that is defined between two times in which a setpoint is provided, the (optimal) storage levels are required to be reached and maintained. For this reason we consider a setpoint tracking problem. However, the demand is not necessarily constant during these intervals, but fortunately we can model the periodicity that occurs in these demand signals and we can use this in the design of the controllers that regulate the flowrates and heat injection in these networks.

We design two controllers, a proportional controller that regulates the flowrates and an internal model based controller that regulates the heat production. For the design of the latter controller the model of the heat demand is used such that we can guarantee that the stored volume and temperature converges asymptotically towards their desired reference values. The controllers are robust to parametric uncertainties in the model and only measurements in the storage tank are required. Finally we provide a stability analysis of the considered nonlinear model in closed loop with both controllers along with a case study to illustrate the performance of the controllers.

The chapter is organized as follows: In Section 3.1 we introduce the model and problem formulation, followed by the controller design in Section 3.2. The main result is stated in Section 3.3 and a case study with corresponding simulations is presented in Section 3.4.

3.1 Temperature and volume regulation

In this chapter we consider the model (2.19) that was derived in Section 2.2. For convenience we restate the model here

$$M(x)\dot{z} = A(\nu)z + Uu - d \tag{3.1a}$$

$$\dot{x} = N\nu \tag{3.1b}$$

$$y = Cz, \tag{3.1c}$$

with $M(x)$, $A(\nu)$, U, N and C as in (2.20a).

Optimization techniques aiming at maximizing profit, *e.g.* by shifting loads in time, can be commonly found in the power systems literature (Li et al. 2011). Motivated by these techniques, which provide optimal storage levels, we define a setpoint tracking problem with the objective to store a desired amount of energy. These setpoints are considered for both the temperature and volume of the hot layer in the storage device. The motivation for this approach is that a combination of a temperature and a volume defines the amount of energy that is stored, as shown in Appendix A.1. Hence the regulation problem is defined as follows:

Problem 3.1 (Output regulation problem)**.** *Design controllers that regulate the heat injection u and the flow rates ν such that the controllers in closed loop with system (3.1) satisfy*

$$\lim_{t\to\infty} (x_s - \overline{x}_s) = 0 \tag{3.2}$$

$$\lim_{t\to\infty} (z_s - \overline{z}_s) = 0, \tag{3.3}$$

for an unknown demand d, where $\overline{x}_s$ and $\overline{z}_s$ are desired setpoints for the storage volume and temperature, respectively. □

Since $\overline{x}_s$ cannot exceed the capacity of the storage tank we introduce the following standing assumption in this chapter:

Assumption 3.2 (Feasible setpoint)**.** *We assume that the setpoint $\overline{x}_s \in \mathcal{V}$ with $\mathcal{V}$ as in (2.2).*

Moreover, we restrict ourself to a setup which allows only for measurements that are located at storage device. We therefore introduce the following assumption:

Assumption 3.3 (Measurements)**.** *Only the storage volume x_s and temperature z_s are measured and available for the controllers.*

We will show that Assumption 3.3 together with the controller design implies that no communication between the controllers is required.

3.1.1 Modeling of the power demand

In order to solve Problem 3.1 the disturbance d (energy demand) needs to be rejected. Since we assume that d is unavailable to the controller we make the following assumption in order to guarantee that the problem is solvable:

Assumption 3.4 (Disturbance model)**.** *The disturbance d_i for all $i \in \{1, ..., n\}$ is generated by the exosystem*

$$\begin{aligned} \dot{w}_i &= S_i w_i \\ d_i &= \Gamma_i w_i, \end{aligned} \tag{3.4}$$

where $\omega_i \in \mathbb{R}^{\omega_i}$, $\Gamma_i \in \mathbb{R}^{1\times\omega_i}$ and $S_i \in \mathbb{R}^{\omega_i\times\omega_i}$ for some integer $\omega_i > 0$. Moreover, S_i and Γ_i are available to the controller for all $i \in \{1, ..., n\}$. Finally, all eigenvalues of $\tilde{S} := \text{block.diag}\begin{pmatrix} S_1 & \dots & S_n \end{pmatrix}$ have zero real part and multiplicity one in the minimal polynomial.

Remark 3.5 (Implication of Assumption 3.4)**.** *Assumption 3.4 implies that all trajectories of (3.4) are bounded and none of them decay to zero as $t \to \infty$. For this reason d_i consists of a linear combination of constants and sinusoidal signals of which the frequencies are known and the amplitudes and phase shifts are unknown to the controller. A large class of disturbance signals can be modelled by resorting to a sufficiently large number of frequencies (Isidori et al. 2003). Moreover, these frequencies can be obtained from historical data or heat demand predictions such as in (Dotzauer 2002). If these historical data are not available, adaptive and robust methods to deal with the case of unknown frequencies are available (Isidori et al. 2003). The investigation of these methods in the present context, however, goes beyond the scope of this thesis.*

In line with Problem 3.1 we define the tracking error of the system as

$$e = z_s - \bar{z}_s,$$

which is due to Assumption 3.3 available to the controller. We incorporate the reference signal $\bar{z}_s$ in the exosystem by defining

$$S := \text{block.diag}\begin{pmatrix} \tilde{S} & 0 \end{pmatrix} \tag{3.5}$$

$$\Gamma := \text{block.diag}\begin{pmatrix} \Gamma_1 & \dots & \Gamma_n & 1 \end{pmatrix} \tag{3.6}$$

$$w := \begin{pmatrix} w_1^T & \dots & w_n^T & w_{n+1}^T \end{pmatrix}^T, \tag{3.7}$$

with $w_{n+1}^T \in \mathbb{R}$. Moreover, we assume that w_{n+1} is initialized such that $w_{n+1}(0) = \bar{z}_s$ which implies that

$$\begin{aligned} \dot{w} &= Sw \\ d &= \Gamma w, \end{aligned} \tag{3.8}$$

satisfies $d_{n+1}(t) = \bar{z}_s$ for all $t \geq 0$. Using (3.1) and (3.4)-(3.8) we can write the dynamics as

$$M(x)\dot{z} = A(v)z + Uu + Pw \tag{3.9a}$$

$$\dot{x} = Nv \tag{3.9b}$$

$$\dot{w} = Sw \tag{3.9c}$$

$$e = Cz + Qw, \tag{3.9d}$$

where

$$\begin{aligned} P &= \begin{pmatrix} \mathbf{0}_{3\times(s-1)} & \mathbf{0}_{3\times 1} \\ -\Gamma & \mathbf{0}_{n\times 1} \end{pmatrix} \\ Q &= \begin{pmatrix} \mathbf{0}_{1\times n} & 1 \end{pmatrix}. \end{aligned} \tag{3.10}$$

We are now ready for the controller design.

3.2 Controller design

The design of the controller consists of two parts. In the first part we design a controller that regulates the flowrates in the pipes such that (3.2) is satisfied. The controller that regulates the flowrate at the consumers is implicitly set to a constant depending on their heat demand. We assume that this flowrate is not communicated to any other controller but instead the aggregated flow that returns to the cold layer in the storage device is measured. This measurement along with a measurement of the volume in the hot storage layer is communicated to the producer. In the second part we design a internal model based controller that regulates u such that (3.3) is satisfied. The motivation for the choice of these controllers follows from the stability analysis as presented in Section 3.3. In that section we show that the two controllers in closed loop with (3.9) asymptotically converges towards the desired setpoints and therefore solves Problem 3.1.

3.2.1 Proportional control of the flow rates

We first design a controller that regulates the flow ν such that (3.2) is satisfied. The proposed controller for the flowrates is given as

$$\begin{aligned} \nu_p &= \mathbf{1}_n^T \overline{\nu}_c - \upsilon(x_s - \overline{x}_s) \\ \nu_c &= \overline{\nu}_c, \end{aligned} \tag{3.11}$$

where $\upsilon \in \mathbb{R}_{>0}$ is the gain of the controller and $\overline{\nu}_c \in \mathbb{R}^n_{>0}$ is the vector of flowrates set by (a controller located at) the consumers.

Lemma 3.6 (Solution of the volume dynamics)**.** *System (3.9b) in closed loop with controller (3.11) has solution*

$$x_s(t) = e^{-\upsilon t}(x_s(0) - \overline{x}_s) + \overline{x}_s, \tag{3.12}$$

and

$$x_s(t) \in \mathcal{V} \times \mathcal{V}, \tag{3.13}$$

for all $t \geq 0$ where $\mathcal{V}$ is as in (2.2).

Proof. Evaluating (3.9b) with input (3.11) provides

$$\dot{x}_s = -\upsilon(x_s - \overline{x}_s), \tag{3.14}$$

which yields (3.12). Together with Assumption 3.2, it follows that (3.13) is satisfied. ■

From Lemma 3.6 we can conclude that (3.2) is satisfied. Moreover, observe that system (3.9b) in closed loop with controller (3.11) is independent from the temperature dynamics. This observation will be used in the design of the controller that regulates the heat injection and is presented in the next section.

3.2.2 Internal model based control of the heat injection

We design a controller that regulates the heat injection u, such that (3.3) is satisfied. The control design is motivated by the observation that (3.9b) in closed loop with controller (3.11) satisfy $\lim_{t\to\infty} x(t) = \overline{x}$ and $\lim_{t\to\infty} \nu(t) = \overline{\nu}$ where

$$\begin{aligned} \overline{x} &= \begin{pmatrix} \overline{x}_s \\ V^{max} - \overline{x}_s \end{pmatrix} \\ \overline{\nu} &= \begin{pmatrix} \mathbb{1}^T \overline{\nu}_c \\ \overline{\nu}_c \end{pmatrix}, \end{aligned} \tag{3.15}$$

with V^{max} as in Section 2.1.1. Similar as in (Isidori et al. 2003) we consider a controller of the form

$$\begin{aligned} \dot{\xi} &= F\xi + Ge \\ u &= H\xi + Ke, \end{aligned} \tag{3.16}$$

with $\xi \in \mathbb{R}^l$, $l = 1 + \sum_{i=1}^{n} \omega_i + r$ and where r the relative degree between the input u and the output e of system (3.9a) with (3.9d) with $x = \overline{x}$ and $\nu = \overline{\nu}$. Furthermore let F, G, H and K be matrices such that there exist matrices Π, Σ and R that solve

$$\begin{aligned} \Sigma S &= F\Sigma \\ R &= H\Sigma, \end{aligned} \tag{3.17}$$

and

$$\begin{aligned} \Pi S &= \overline{A}\Pi + \overline{U}R + \overline{P} \\ 0 &= C\Pi + Q, \end{aligned} \tag{3.18}$$

where

$$\begin{aligned} \overline{A} &= M(\overline{x})^{-1}A(\overline{\nu}) \\ \overline{U} &= M(\overline{x})^{-1}U \\ \overline{P} &= M(\overline{x})^{-1}P. \end{aligned} \tag{3.19}$$

Note that $M(\overline{x})$ is an invertible matrix due to its diagonal form with strictly positive entries. Equations (3.17) and (3.18) are commonly referred to as the regulator equations.

As a preliminary step we assume that $x(t) = \overline{x}$ and $\nu(t) = \overline{\nu}$ for which we prove that a controller of the form (3.16) exist and solves Problem 3.1. After that we extend these results by showing that assuming $x(t) = \overline{x}$ and $\nu(t) = \overline{\nu}$ is not required to draw the same conclusions.

Theorem 3.7 (Output regulation with constant volumes and flows)**.** *Let $x = \overline{x}$ and $\nu = \overline{\nu}$ with $\overline{x}$ and $\overline{\nu}$ as in (3.15), then there exist F, G, H and K such that the solutions of the closed-loop system (3.20)-(3.16) with exosystem (3.8) are bounded and satisfy (3.3), i.e.*

$$\lim_{t\to\infty} e(t) = 0.$$

Proof. Since $x = \overline{x}$ and $\nu = \overline{\nu}$, (3.9a), (3.9c) and (3.9d) take the form of the linear time invariant system

$$\begin{aligned} \dot{z} &= \overline{A}z + \overline{U}u + \overline{P}w \\ \dot{w} &= S\,w \\ e &= Cz + Qw. \end{aligned} \tag{3.20}$$

For this system it is well known (see *e.g.* (Isidori et al. 2003)) that a controller of the

form (3.16) solves the robust output regulation problem if there exists Π, Σ and R such that (3.17) and (3.18) are satiesfied. Lemma 1.4.2 in (Isidori et al. 2003) states that the regulator equations have a solution for all $\overline{A}$, $\overline{U}$, $\overline{P}$, C and Q if and only if

$$\det\begin{pmatrix} \overline{A} - \lambda I & \overline{U} \\ C & 0 \end{pmatrix} \neq 0, \tag{3.21}$$

for all λ which are eigenvalues of S. Equivalently this is satisfied if and only if

$$\det\begin{pmatrix} -\nu_p - \lambda & 0 & \nu_p & \mathbf{0}_n^T & 1 \\ \nu_p & -\nu_p - \lambda & 0 & \mathbf{0}_n^T & 0 \\ 0 & 0 & -\mathbf{1}_n^T \nu_c - \lambda & {\nu_c}^T & 0 \\ \mathbf{0}_n & \nu_c & \mathbf{0}_n & -[\nu_c] - \lambda I_n & \mathbf{0}_n \\ 0 & 1 & 0 & \mathbf{0}_n^T & 0 \end{pmatrix} \neq 0. \tag{3.22}$$

Observe that both the last row and column have only one non-zero entry. For this reason condition (3.21) holds, if and only if

$$\det\begin{pmatrix} \nu_p & 0 & \mathbf{0}_n^T \\ 0 & -\mathbf{1}_n^T \nu_c - \lambda & {\nu_c}^T \\ \mathbf{0}_n & \mathbf{0}_n & -[\nu_c] - \lambda I_n \end{pmatrix} \neq 0. \tag{3.23}$$

Due to the upper triangular form, (3.23) reduces to

$$\nu_p \left(\mathbf{1}_n^T \nu_c + \lambda\right) \prod_{j=1}^{n} \left(\nu_{c,j} + \lambda\right) \neq 0, \tag{3.24}$$

where $\nu_{c,j}$ is the j-th element of vector ν_c. By Assumption 3.4 we have that all eigenvalues of S have zero real part which implies that λ is purely imaginary. Since $\nu_p > 0$ and $\nu_{c,j} > 0$, it follows that (3.24) is satisfied, which implies there exists Π, Σ and R such that (3.17) and (3.18) are satisfied and therefore proves the thesis. ■

Remark 3.8 (Parametric uncertainties of $\overline{A}$)**.** *Note that $\overline{A}$ in (3.19) is assumed to be available to the controller. However, $\overline{A}$ depends on $\overline{\nu}$, which might not be known. Fortunately, as shown in (Isidori et al. 2003), the controller in (3.16) is robust against model parametric uncertainties, and, hence, against uncertainty in the estimate of $\overline{\nu}$.*

3.3 Stability analysis of the closed loop system

In this section we will show that (3.11) and (3.16) in closed loop with (3.9) solve Problem 3.1. The block diagram of the closed loop system is depicted in Figure 3.1. The main

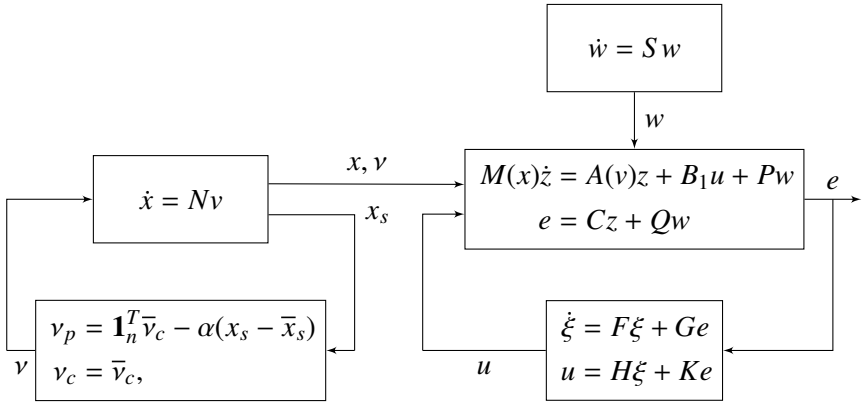

Figure 3.1: Block diagram of the closed loop system.

idea behind the controller design and stability analysis is that there is no feedback from the blocks on the right of Figure 3.1 to the blocks on the left. This implies that x and ν converge towards constant values independent of w, u, z and e. In turn it follows that (3.9a) asymptotically converges to a linear system. Consequently, we are required to analyse the internal based controller in closed loop with linear system that contains a time varying perturbation that converges asymptotically towards a constant.

The first step is to write (3.9a) in closed loop with controller (3.16) to obtain the nonlinear system

$$\begin{aligned} M(x)\dot{z} &= (A(v) + UKC)z + UH\xi + (UKQ + P)w \\ \dot{\xi} &= GCz + F\xi + GQw. \end{aligned} \tag{3.25}$$

Note that applying controller (3.11) ensures that $M(x(t))$ is invertible for all $t \geq 0$ due to Lemma 3.6. Therefore we can define

$$\begin{aligned} A_e(t) &= M(x)^{-1}A(v) - \overline{A} \\ B_e(t) &= M(x)^{-1}U - \overline{U} \\ P_e(t) &= M(x)^{-1}P - \overline{P}, \end{aligned} \tag{3.26}$$

with $\overline{A}$, $\overline{U}$ and $\overline{P}$ being as in (3.19). Now we perform the coordinate change

$$\zeta := \begin{pmatrix} z - \Pi w \\ \xi - \Sigma w \end{pmatrix}. \tag{3.27}$$

Bearing in mind (3.17) and (3.18), (3.27) allows us to write closed loop system (3.25) as

$$\dot{\zeta} = (A' + F'(t))\zeta + B'(t)w, \tag{3.28}$$

with

$$A' = \begin{pmatrix} \overline{A} + \overline{U}K\overline{C} & \overline{U}H \\ GC & F \end{pmatrix} \tag{3.29}$$

$$F'(t) = \begin{pmatrix} A_e(t) + B_e(t)KC & B_e(t)H \\ 0 & 0 \end{pmatrix} \tag{3.30}$$

$$B'(t) = \begin{pmatrix} P_e(t) + B_e(t)R + A_e(t)\Pi \\ 0 \end{pmatrix}. \tag{3.31}$$

Note that in contrast to what happens in linear time invariant systems, (3.31) only vanishes in case $x = \overline{x}$ and $\nu = \overline{\nu}$. Consider now (3.27) with system (3.28) and observe that $\zeta = 0$ implies that $z = \Pi w$. Due to (3.18) we know that $C\Pi + Q = 0$ and therefore also that

$$e = Cz + Qw = 0.$$

For this reason a sufficient condition such for (3.3) being satisfied is that ζ is bounded and $\lim_{t\to\infty} \zeta = 0$. Since in Section 3.2.1 it was already proven that (3.2) holds, this would also imply that Problem 3.1 is solved.

Theorem 3.9 (Convergence of (3.28))**.** *Consider system (3.28) where w is as in (3.8). Then, for any initial condition, ζ is bounded and satisfies*

$$\lim_{t\to\infty} \zeta(t) = 0.$$

Proof. First we define

$$u' := B'w, \tag{3.32}$$

such that system (3.28) becomes

$$\dot{\zeta} = (A' + F'(t))\zeta + u'. \tag{3.33}$$

We know by Lemma B.3 that the origin of (3.33) is uniformly exponentially stable when $u' = 0$. For this reason (see for instance (Rugh 1996)), there exists a state transition matrix $\Phi(t, s)$ and parameters $\mu \in \mathbb{R}_{>0}$ and $\lambda \in \mathbb{R}_{>0}$ such that

$$\|\Phi(t, t_0)\| \leq \mu e^{-\lambda(t-t_0)}, \tag{3.34}$$

and that the solution $\zeta(t)$ is given by

$$\zeta(t) = \Phi(t, t_0)\zeta(t_0) + \int_{t_0}^{t} \Phi(t, \tau)u'(\tau)d\tau.$$

Since we can bound $\|B'(t)w(t)\| < \gamma < \infty$ for any $t > 0$ we can also bound $\|\zeta\|$ by (see *e.g.* (Khalil 2002))

$$\begin{aligned}\|\zeta\| &\leq \|\Phi(t, t_0)\zeta(t_0) + \int_{t_0}^{t} \Phi(t, \tau)u'(\tau)d\tau\| \\ &\leq \mu e^{-\lambda(t-t_0)}\|\zeta(t_0)\| + \int_{t_0}^{t} \mu e^{-\lambda(t-\tau)}\|u'(\tau)\|d\tau \\ &\leq \mu e^{-\lambda(t-t_0)}\|\zeta(t_0)\| + \frac{\mu\gamma}{\lambda} \sup_{\tau\in[t_0,t)} \|u'(\tau)\|,\end{aligned}$$

implying that $\|\zeta\|$ is bounded. Now consider the defined input (3.32). Since $\lim_{t\to\infty} x = \overline{x}$ and $\lim_{t\to\infty} \nu = \overline{\nu}$ we know that $\lim_{t\to\infty} A_e(t) = 0$, $\lim_{t\to\infty} B_e(t) = 0$ and $\lim_{t\to\infty} P_e(t) = 0$. This implies $\lim_{t\to\infty} B'(t) = 0$ from which we conclude

$$\lim_{t\to\infty} \|u'\| = \lim_{t\to\infty} \|B'w\| = 0. \tag{3.35}$$

By the boundedness of $\|\zeta\|$ and (3.35), we conclude that $\lim_{t\to\infty} \|\zeta\| = 0$, which proves the thesis. ■

3.4 Case study

In order to illustrate the model and the proposed controller we consider a case study. A second case study is presented in Appendix C.

We consider a case study with three different consumers, each having a time varying heat demand. Energy can be stored in a stratified thermal storage which is designed to operate at a constant temperature of $85°C$. The stored amount of energy is regulated by setting a desired setpoint for the volume. Two time intervals are considered in which we store energy in the first interval after which the same amount of energy is drained in the second interval. Motivated by the operating temperature we take the setpoint and inital condition of the storage temperature equal to $\overline{z}_s = z_s(0) = 85°C$. The density and specific heat are given by $\rho = 975kg/m^3$ and $C_p = 4190J/Kg°C$, respectively. The total volume of the storage tank is $V^{\max} = 1000m^3$ and the volume of the hot layer is initialized at $x_s(0) = 100m^3$. Each heat exchanger has a volume of $V_i^c = V^p = \frac{2}{100}m^3$ and the temperatures of the heat exchangers of the producer and consumers are initialized at $z_p(0) = 70°C$ and $z_c(0) = \mathbb{1} \cdot 30°C$, respectively.

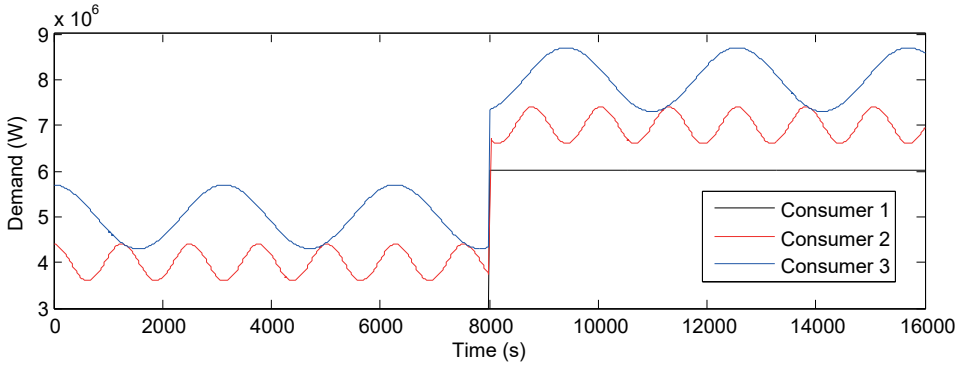

Figure 3.2: Time varying demand pattern.

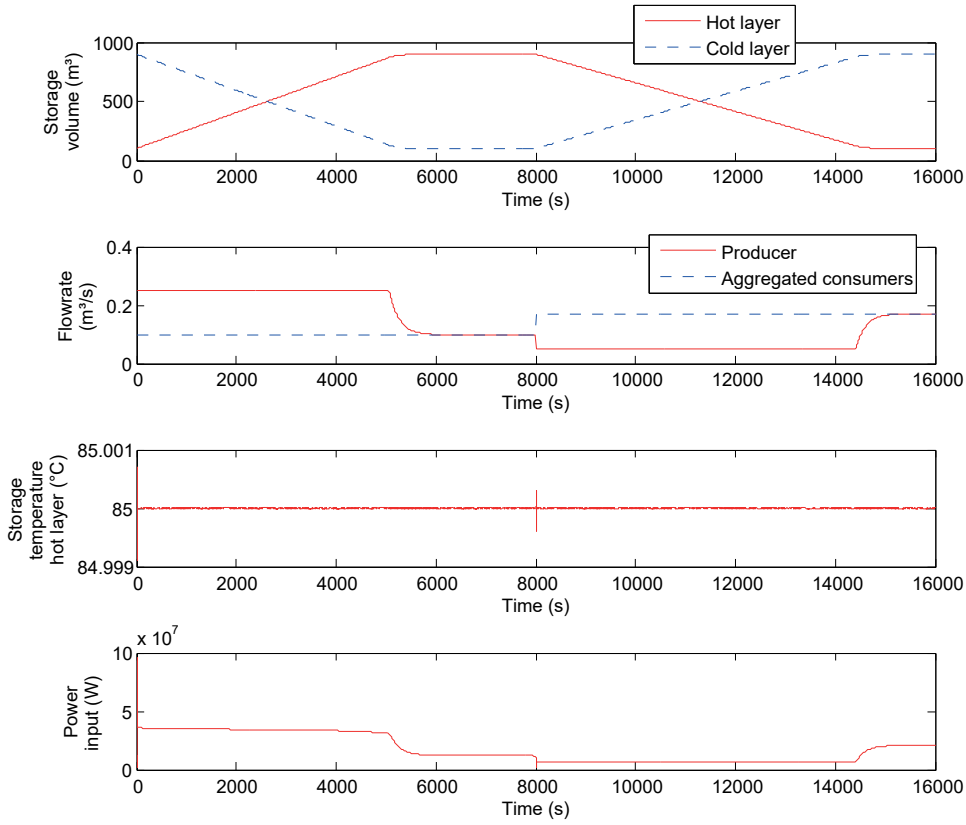

Figure 3.3: Three consumers with time varying demand.

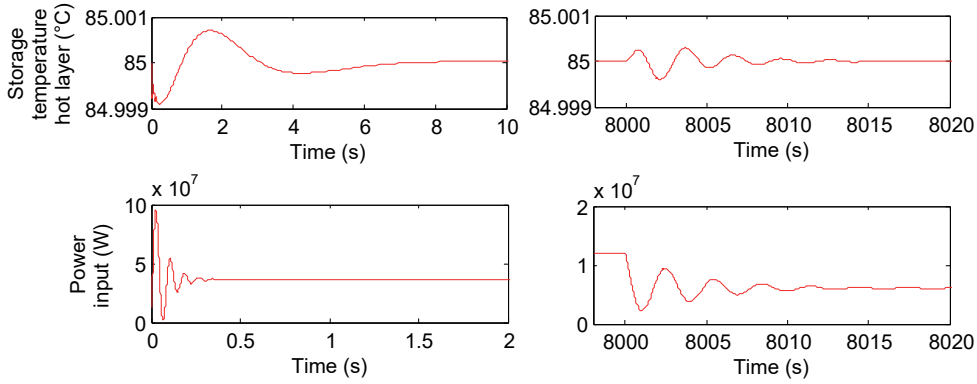

Figure 3.4: Magnification of Figure 3.3. Storage temperature and the power injection from $t = 0$ and $t = 8000$.

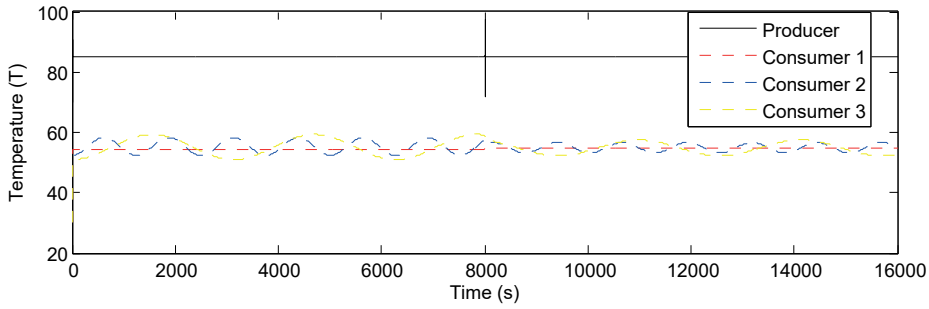

Figure 3.5: Temperatures of the heat exchangers under time varying demand.

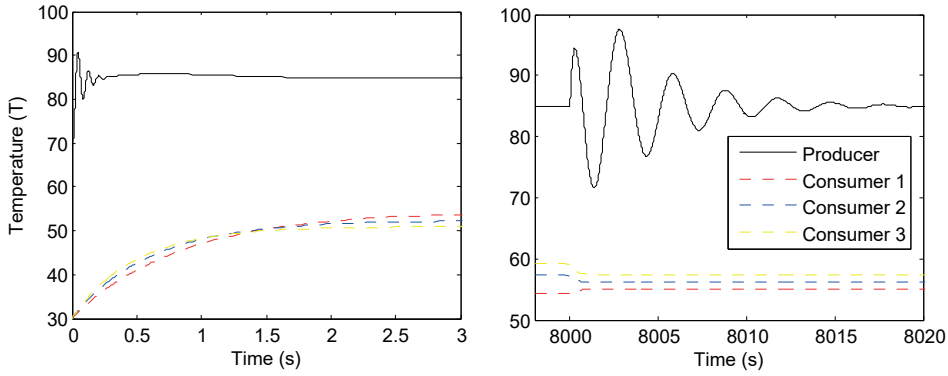

Figure 3.6: Magnification of Figure 3.5. Temperatures of the heat exchangers from $t = 0$ and $t = 8000$.

The numerical values of controller (3.16) are obtained by following the design procedure detailed in (Isidori et al. 2003, Section 1.5). These values are given by

$$F = \begin{pmatrix} 4 & -10 & 10 & -5 & 1 & -90 & -900 \\ 1 & -1 & 0 & 0 & 0 & 0 & 0 \\ 0 & 1 & -1 & 0 & 0 & 0 & 0 \\ 0 & 0 & 1 & -1 & 0 & 0 & 0 \\ 0 & 0 & 0 & 1 & -1 & 0 & 0 \\ 0 & 0 & 0 & 0 & 0 & -600 & 1 \\ 0 & 0 & 0 & 0 & 0 & -90000 & 0 \end{pmatrix}$$

$$G = \begin{pmatrix} 0 & 0 & 0 & 0 & 0 & 600 & 90000 \end{pmatrix}^T$$

$$H = \begin{pmatrix} 5 & -10 & 10 & -5 & 1 & -90 & -900 \end{pmatrix},$$

and $K = 0$. The gain υ in (3.11) regulating the flow is set to $\upsilon = 0.005$. To avoid nonpositive and too high flow rates, we impose a saturation on the corresponding control input and is given by $0.05m^3/s \leq \nu_p \leq 0.25m^3/s$. Note that this saturation is not considered analysis of this chapter, but in chapters 4 and 5 an analysis that includes input saturations in a related problem is addressed.

The domain of the two time intervals that we consider is given by $0s \leq t < 8000s$ and $8000s \leq t < 16000s$. The volume setpoints are $\overline{x}_s = 900m^3$ and $\overline{x}_s = 100m^3$ for the first and second time interval, respectively. The demand of the three consumers is given in Figure 3.2. The flowrates of the consumers in the first time interval are given by $\overline{v}_c = \begin{pmatrix} 0.024 & 0.033 & 0.041 \end{pmatrix}^T m^3/s$ and in the second time interval they are set to $\overline{v}_c = \begin{pmatrix} 0.049 & 0.057 & 0.065 \end{pmatrix}^T m^3/s$. Figure 3.4 shows that the temperature in the storage is approximately $z_s = 85°C$ within ten seconds despite the time varying demand. Furthermore Figure 3.3 shows that also the volume converges asymptotically towards the desired setpoints during each time interval. We observe some transient behaviour of the heat injection at $t = 8000s$ due to a change in setpoints, flowrates and extraction rates. In Figure 3.5 the temperatures of the heat exchangers of the consumers show the impact of the time-varying demand. Finally in Figure 3.6 we again see a transient behaviour at $t = 0s$ and $t = 8000s$ due to a change in setpoints, flowrates and demand.

Remark 3.10 (Performance with respect to frequency uncertainties.)**.** *Additional simulations have shown that the performance of the controller is not significantly deteriorated in the presence of small-range frequency uncertainties (around 20%) in the consumer demand pattern. The reason is that the controller that regulates the heat injection has a large integral gain and the system has slow dynamics due to the large volume in the storage tank. Moreover, in case the performance is deteriorated due to uncertainties in*

the frequency, adaptive and robust methods can be used to compensate for the frequency uncertainties (Isidori et al. 2003).

Chapter 4

Volume regulation and quasi-optimal production of multiple producers

Abstract

In this chapter we consider a flow network for which the goal is to solve a practical optimal regulation problem in the presence of input saturation. Based on Lyapunov arguments we propose distributed controllers which guarantee global convergence to an arbitrarily small neighborhood of the desired optimal steady state while fulfilling the constraints for all the time. As a case study we apply our distributed controller to a district heating network.

Regulation of flow networks recently received much attention due to its many different applications, see *e.g.* (Lovisari et al. 2014, Burbano and Di Bernardo 2014, Bauso et al. 2013). Moreover, there are several dynamical networks that share similar models and control problems. Some of these examples are DC networks (Zhao and Dörfler 2015), heating, ventilation and air conditioning (HVAC) systems (Gupta et al. 2015), compartmental flow systems (Blanchini et al. 2016), multi-agent systems (Zheng et al. 2011), hydraulic networks (De Persis and Kallesoe 2011), (De Persis et al. 2014), and power grids (Trip et al. 2016).

In flow networks it is often desirable to have optimal flows, according to some cost function. Static optimization problems associated with networks have been discussed in great detail (see *e.g.* (Bertsekas 1998), (Boyd and Vandenberghe 2004) and (Rockafellar 1984), and are commonly referred to as the mathematical theory of *network optimization*. Moreover, it is useful to solve these optimization problems in a distributed fashion, such as in (Gharesifard and Cortés 2014), in order to avoid excessive communication and computation times. However, most real networks have to react dynamically to changes in the network, which requires feedback controllers. This is for example done in (Bauso et al. 2013) where controllers are designed for linear systems to achieve asymptotic optimality. In (Bürger et al. 2014) and (Kim and De Persis 2015) this is extended to nonlinear systems by using passivity arguments. Rather than including an optimality condition on the flow, (Trip et al. 2016) assigns a cost function to the inputs and guarantees optimal state regulation for power networks. This approach is also combined with

optimal flows in (Bürger et al. 2015), which additionally considers capacity constraints on the transportation lines. However, these constraints depend on the initial conditions, which is not desirable in networks that have, *e.g.* physical constraints. Accordingly, the motivation arises to consider input and state constraints in regulation problems for flow networks for which the constraints are never violated, independent of the initial conditions. Model predictive control (MPC) handles input and state constraints in a natural way, as has been shown in (Danielson et al. 2013), where a capacity maximization and balancing problem is solved. However, the stability of MPC systems is often hard to analyze and running MPC algorithms is computationally intensive. A solution that avoids the use of MPC but does not consider any optimality is provided in (Bürger et al. 2013). In this paper the authors show that there exists a strong relation between clustering, optimal network flow problems and output agreement. The stability of flow networks under time-varying disturbances can be guaranteed by means of internal model based controllers on the edges, as has been shown in (Bürger and De Persis 2015) and (De Persis 2013). It is well know that these controllers can also be implemented in a distributed fashion, such as in (Como et al. 2013).

Port-Hamiltonian (PH) systems have also proven to be a powerful tool for the modeling and control of nonlinear networked systems (van der Schaft and Jeltsema 2014). These PH systems have been used extensively to model physically interconnected dynamical systems as well as to synthesize controllers that ensure output regulation (van der Schaft and Wei 2012, Romero et al. 2013, Ortega et al. 2008, Jayawardhana et al. 2007). In (Wei and van der Schaft 2013) a flow network is modeled as a PH system and necessary and sufficient conditions are provided to guarantee load balancing in the presence of input constraints but with no optimality. It is shown that if the graph has uni-directional flow due to the saturation, a sufficient condition for output agreement is that the associated directed graph is strongly connected. The same authors recently provided a result in which proportional-integral (PI) controllers are able to handle state constraints (Wei and van der Schaft 2014).

The model we consider is related to the one in Chapter 3. However, motivated by the slow temperature dynamics which can be made approximately constant by adequate control of the heat injection, we neglect the temperature dynamics in this Chapter. This allows us to design controllers for a more complex network and provide a stability certificate for the resulting closed loop system. To this end, we consider a control problem in which the goal is to achieve output regulation in flow networks. Motivated by capacity constraints and directional constraints we consider transient constraints on both the inputs at the nodes and flows on the links.

The main contributions of this chapter are twofold. First, we provide two distributed controllers, one that regulates the input on each node and one that controls the flows

on the edges. Similar as in (Wei and van der Schaft 2013) we equip the controllers with integral action. Building upon (Trip et al. 2016), (Bürger and De Persis 2015) and (Bürger et al. 2015), we show that these distributed controllers guarantee convergence to a quasi-optimal steady state, that is, to a steady state that is arbitrarily close to the optimal one. Second, we extend this result in the presence of heterogenous saturation on both inputs. In particular, we can enforce positivity constraints on the link flows, obtaining a network with unidirectional flows. In both cases we provide sufficient conditions for global asymptotic stability based on Lyapunov arguments. Finally, we apply these results to a district heating system with storage devices. This chapter can be considered as a preliminary work for Chapter 5 in which a similar control problem is solved. The similarities and differences between the control problem and corresponding control design are highlighted in that chapter.

The structure of the chapter is as follows. In Section 4.1 we introduce the model and two problem formulations. The first problem considers state regulation with optimality conditions on the steady state inputs, whereas the second one is an extension, in which we additionally consider saturation on the inputs and the flows. The solution to the first problem is given in Section 4.2 and the one to the second problem is given in Section 4.3. Finally, we present a case study in Section 4.4.

4.1 Output regulation and quasi-optimal steady state inputs

In this chapter we consider model (2.7) with $E = I$ (*i.e.* all nodes are actuated) and $h(x) = x$ such that we obtain

$$T_x \dot{x} = -B\lambda + u - d \tag{4.1a}$$

$$y = x, \tag{4.1b}$$

where $T_x \in \mathbb{R}^{n\times n}_{>0}$ is a diagonal matrix, $B \in \mathbb{R}^{n\times m}$ is the incidence matrix of the graph $\mathcal{G}$, $\lambda \in \mathbb{R}^m$ are the flows, $u \in \mathbb{R}^p$ are the inputs and $d \in \mathbb{R}^n$ the unmeasured disturbance. Moreover, for convenience we repeat Assumption 2.5:

Assumption 4.1 (Connectedness)**.** *The graph $\mathcal{G}$ is connected.*

We discuss two control objectives. The first objective is concerned with the output (4.1b), at steady state.

Objective 4.2 (Output regulation)**.** *Let $\overline{y}$ be a desired constant setpoint, then the output y of (4.1) asymptotically converges to $\overline{y}$, i.e.*

$$\lim_{t\to\infty} \|x(t) - \overline{y}\| = 0. \tag{4.2}$$

Remark 4.3 (Tracking of a ramp)**.** *The assumption that $\overline{y} = \overline{x}$ in (4.2) is a constant setpoint can be relaxed to a the possibility of tracking a linear transition between the current setpoint $\overline{x}(t_1)$ to a new setpoint $\overline{x}(t_2)$ with $t_2 > t_1$. To do so, the desired reference signal is modelled as a ramp, i.e.*

$$\overline{x}(t) = \overline{x}(t_1) + \frac{t - t_1}{t_2 - t_1}(\overline{x}(t_2) - \overline{x}(t_1)). \tag{4.3}$$

After a coordinate transformation $\tilde{x}(t) = x(t) - \overline{x}(t)$, we obtain a system of the same form as (2.7a), where the evolution of $\tilde{x}$ is described by

$$T_x \dot{\tilde{x}} = -B\lambda + Eu - \tilde{d}. \tag{4.4}$$

The corresponding constant disturbance is now given by

$$\tilde{d} = d + \frac{1}{t_2 - t_1}(\overline{x}(t_2) - \overline{x}(t_1)). \tag{4.5}$$

Note that boundedness of $\tilde{x}_i$ does not imply boundedness of x_i as $\overline{x}_i(t)$ increases or decreases constantly over time. Therefore, the used invariance principle in the later sections is not immediately applicable if we consider the original variables of the system. Nevertheless, the subsequent analysis can be applied to the incremental system (4.4) if we consider $\tilde{x}$ as the state.

At a state where $\overline{y} = \overline{x}$ is constant, system (4.1a) necessarily satisfies

$$\mathbf{0} = -B\lambda + u - d. \tag{4.6}$$

Premultiplying (4.6) with $\mathbb{1}_n^T$ results in

$$0 = \mathbb{1}_n^T Eu - \mathbb{1}_n^T d, \tag{4.7}$$

such that at a steady state the total input to the network needs to be equal to the total disturbance. It is therefore natural to wonder if the total input can be coordinated optimally among the nodes. Optimal coordination is discussed in Section 2.4 and from Lemma 2.17 we obtain that the optimal input $\overline{u}$ is given by (2.37) which we repeat here

$$\overline{u} = Q^{-1}\left(E^T \frac{\mathbb{1}_n \mathbb{1}_n^T}{\mathbb{1}_p^T Q^{-1} \mathbb{1}_p}(d + EQ^{-1}r) - r\right), \tag{4.8}$$

where $Q = \operatorname{diag}(q_1, \ldots, q_n)$ and $r = (r_1, \ldots, r_n)^T$ with q_i and r_i the quadratic and linear costs respectively corresponding to input u_i (see also (2.33)). This leads to the second

control objective we consider.

Objective 4.4 (Optimal feedforward input)**.** *The input at the nodes asymptotically converge to the solution to (2.36), i.e.*

$$\lim_{t\to\infty} \|u(t) - \overline{u}\| = 0, \tag{4.9}$$

with $\overline{u}$ as in (4.8).

In order to guarantee (4.9) without relying on a centralized controller we introduce a communication network. This network is introduced in more detail in Section 4.2. For convenience, we summarize the objectives and constraints yielding the following controller design problem.

Problem 4.5 (Controller design problem)**.** *Design distributed controllers that regulate inputs u at the nodes and the flows λ on the edges for system (4.1), such that*

$$\begin{aligned} \lim_{t\to\infty} \|x(t) - \overline{y}\| &= 0 \\ \lim_{t\to\infty} \|u(t) - \overline{u}\| &= 0, \end{aligned} \tag{4.10}$$

where $\overline{y}$ is the desired setpoint and $\overline{u}$ is as in (4.8). □

We now turn our attention to possible constraints on the control inputs u and λ under which the objectives should be reached. First, in physical systems the input u is generally constrained by a minimum value (often zero, preventing a negative input) and a maximum value, representing *e.g.* a production capacity.

Constraint 4.6 (Input limitations)**.** *The inputs at the nodes satisfy*

$$u_i^- < u_i(t) < u_i^+, \tag{4.11}$$

for all $i \in \mathcal{V}$ and all $t \geq 0$, with $u_i^-, u_i^+ \in \mathbb{R}$ being suitable constants.

Second, the flows on the edges are often constrained to be unidirectional and to be within the capacity of the edges. For this reason we consider the following constraint on the flows on the edges:

Constraint 4.7 (Flow capacity)**.** *The flows on the edges satisfy*

$$0 < \lambda_k(t) < \lambda_k^+, \tag{4.12}$$

for all $k \in \mathcal{E}$ and all $t \geq 0$, with $\lambda_k^+ \in \mathbb{R}_{>0}$ being a suitable constant.

Note that physical limitations and safety requirements demand that the constraints should be satisfied *for all time* and not only at steady state. Summarizing, the second control problem is formulated as follows:

Problem 4.8 (Constrained output regulation)**.** *For any given positive (arbitrarily small) numbers ϵ_x and ϵ_u, design distributed controllers that regulate the flows on the edges λ and input u at the nodes of system (4.1) such that*

$$\lim_{t\to\infty} \|x(t) - \overline{y}\| < \epsilon_x \tag{4.13}$$

$$\lim_{t\to\infty} \|u(t) - \overline{u}\| < \epsilon_u, \tag{4.14}$$

where $\overline{u}$ is as in (4.8) and $\overline{y} \in \mathbb{R}^n$ is a constant setpoint. Furthermore,

$$u^- \leq u(t) \leq u^+ \tag{4.15}$$

$$0 \leq \lambda(t) \leq \lambda^+, \tag{4.16}$$

should hold for all $t \geq 0$. □

Remark 4.9 (Practical convergence)**.** *In contrast to asymptotical convergence as is considered in Problem 4.5, we resort to practical convergence in order to guarantee (4.15) and (4.16). For a study of asymptotic stability we refer the reader to Chapter 5 in which a similar control problem is considered.*

Remark 4.10 (Positive systems)**.** *A common requirement is that, additionally to Problem 4.5 and Problem 4.8, the state x has to be nonnegative, i.e. $x(t) \geq \mathbf{0}$ for all t (see e.g. (Rami and Tadeo 2007) (Rantzer 2011)). Although, achieving output regulation (Objective 4.2), with $\overline{x} > \mathbf{0}$, is in practical cases sufficient to ensure that $x(t) \geq \mathbf{0}$ for all t, when the system suitably initialized, a theoretical guarantee is difficult to obtain, due to the presence of an unknown and constant disturbance d. An interesting future endeavor is to study the design of controllers solving Problem 4.5 and Problem 4.8 within the setting of so-called positive systems (Benvenuti and Farina 2002).*

We will now provide a solution to Problem 4.5 in Section 4.2 followed by a solution to Problem 4.8 in Section 4.3.

4.2 Unconstrained case

In this section we provide a solution to Problem 4.5, which also sets the ground for the controller design and analysis that solves Problem 4.8.

To solve Problem 4.5 we propose two controllers, one generating λ and one providing u. The former controller takes the outputs of the incident nodes as its input and takes the form of a standard PI controller. This controller is given by

$$\begin{aligned} \dot{\mu} &= \gamma_\mu B^T y \\ \lambda &= -\gamma_c B^T y - \gamma_\mu \mu, \end{aligned} \tag{4.17}$$

where $\gamma_\mu, \gamma_c \in \mathbb{R}_{>0}$ are suitable gains[1]. The latter controller, takes its local error measurement y as an input. To guarantee an optimal input at steady state we assign a state variable θ_i to each node. This state is communicated via a connected communication network that is represented by[2] L_c. In order to guarantee that Problem 4.5 can be solved we make the following assumption:

Assumption 4.11 (Communication network)**.** *The graph reflecting the communication topology is undirected and connected.*

We propose the following controller:

$$\dot{\theta} = -\gamma_l L^{com}\theta - \gamma_\theta Q^{-1} y \tag{4.18a}$$

$$u = Q^{-1}(\gamma_\theta \theta - r), \tag{4.18b}$$

where $\gamma_l, \gamma_\theta \in \mathbb{R}_{>0}$ are suitable gains. The controller is distributed due to the diagonal form of Q^{-1} and diffusive coupling between the states θ. This coupling is required in order to achieve consensus of θ and we will prove that this implies that u converges to the optimal steady state (4.8) despite the presence of disturbances.

Before we state the main theorem of this section we introduce the following lemma, in which an incremental form of (4.1), in closed loop with controllers (4.17) and (4.18) is obtained.

Lemma 4.12 (Incremental form of the closed loop system)**.** *Let Assumptions 4.1 and 4.11 be satisfied and let*

$$\overline{\theta} = -\frac{1}{\gamma_\theta}\frac{\mathbb{1}\mathbb{1}^T}{\mathbb{1}^T Q^{-1}\mathbb{1}}(d - Q^{-1}r), \tag{4.19}$$

and $\overline{\mu}$ be any solution to

$$\gamma_\mu B\overline{\mu} = \left(I - \frac{Q^{-1}\mathbb{1}\mathbb{1}^T}{\mathbb{1}^T Q^{-1}\mathbb{1}}\right)\left(d - Q^{-1}r\right), \tag{4.20}$$

[1] μ is introduced with some abuse of notation since there is no relation with the control input in (2.23).

[2] Note that the graph represented by L^{com} does not necessarily have to coincide with the graph represented by L.

then the incremental states

$$\begin{aligned}\tilde{x} &= x - \overline{x}\\ \tilde{\theta} &= \theta - \overline{\theta}\\ \tilde{\mu} &= \mu - \overline{\mu},\end{aligned} \tag{4.21}$$

with x, θ and μ as a solution to system (4.1), in closed loop with controllers (4.17) and (4.18), satisfy

$$\begin{aligned}\dot{\tilde{x}} &= -\gamma_c BB^T\tilde{x} - \gamma_\mu B\tilde{\mu} + \gamma_\theta Q^{-1}\tilde{\theta}\\ \dot{\tilde{\theta}} &= -\gamma_l L^{com}\tilde{\theta} - \gamma_\theta Q^{-1}\tilde{x}\\ \dot{\tilde{\mu}} &= \gamma_\mu B^T\tilde{x}.\end{aligned} \tag{4.22}$$

Furthermore, a solution to (4.20) always exists.

Proof. We combine (4.1) with (4.17) and (4.18), to obtain the closed loop system

$$\begin{aligned}\dot{x} =& -\gamma_c BB^T(x-\overline{x}) - \gamma_\mu B\mu\\ &+ Q^{-1}(\gamma_\theta\theta - r) + d\\ \dot{\theta} =& -\gamma_l L^{com}\theta - \gamma_\theta Q^{-1}(x-\overline{x})\\ \dot{\mu} =& \gamma_\mu B^T(x-\overline{x}).\end{aligned} \tag{4.23}$$

In light of (4.21) it follows directly from (4.23) that (4.22) is satisfied. Lastly we prove that there exists a $\overline{\mu}$ that satisfies (4.20). Since $\mathrm{Im}(B) = \ker(B^T)^\perp = \mathrm{span}(\mathbb{1})^\perp$ and $\mathbb{1}^T\left(I - \frac{Q^{-1}\mathbb{1}\mathbb{1}^T}{\mathbb{1}^T Q^{-1}\mathbb{1}}\right) = 0$, we know that there always exists a $\overline{\mu}$ that satisfies (4.20), which concludes the proof. ∎

Remark 4.13 (No damping in (4.22))**.** *The closed loop dynamics (4.22) are similar to the linear version of the closed loop dynamics of power grids, as studied in (Trip et al. 2016). The main difference in the model considered here, which requires a modification of the analysis, is the lack of damping terms.*

We will now state the following theorem which gives sufficient conditions to solve Problem 4.5.

Theorem 4.14 (Sufficient conditions for solving Problem 4.5)**.** *Let Assumptions 4.1 and 4.11 be satisfied and let there exists a pair of entries q_i, q_j such that $q_i \neq q_j$, then controllers (4.17) and (4.18), in closed loop with (4.1), solve Problem 4.5.*

Proof. In order to analyse the stability of the system, we use a standard quadratic Lyapunov function

$$V(\tilde{x},\tilde{\mu},\tilde{\theta}) = \frac{1}{2}\|\tilde{x}\|^2 + \frac{1}{2}\|\tilde{\theta}\|^2 + \frac{1}{2}\|\tilde{\mu}\|^2. \tag{4.24}$$

From Assumption 4.11 we know that the communication graph is undirected implying that $L^{com} = B_c B_c^T$ with B_c is the corresponding incidence matrix. It follows, using (4.22), that the derivative of $V(\tilde{x}, \tilde{\mu}, \tilde{\theta})$ is given by

$$\dot{V}(\tilde{x}, \tilde{\mu}, \tilde{\theta}) = -\gamma_c \|B^T \tilde{x}\|^2 - \gamma_l \|B_c^T \tilde{\theta}\|^2, \tag{4.25}$$

Due to the quadratic form of V, it is clear that V is positive definite and radially unbounded. Using LaSalle's invariance principle we can conclude that $(\tilde{x}, \tilde{\mu}, \tilde{\theta})$ converges to the largest invariant set where $\dot{V}(\tilde{x}, \tilde{\mu}, \tilde{\theta}) = 0$, which is given by

$$\mathcal{S} := \left\{ (\tilde{x}, \tilde{\mu}, \tilde{\theta}) | B^T \tilde{x} = 0, B_c^T \tilde{\theta} = 0 \right\}. \tag{4.26}$$

Next we characterize the dynamics on this invariant set $\mathcal{S}$. These, in light of (4.22), are given by

$$\dot{\tilde{x}} = -\gamma_\mu B \tilde{\mu} + \gamma_\theta Q^{-1} \tilde{\theta} \tag{4.27a}$$

$$\dot{\tilde{\theta}} = -\gamma_\theta Q^{-1} \tilde{x} \tag{4.27b}$$

$$\dot{\tilde{\mu}} = 0. \tag{4.27c}$$

From Assumptions 4.1 and 4.11 it follows that $\ker(B^T) = \mathrm{Im}(\mathbb{1})$ and $\ker(B_c^T) = \mathrm{Im}(\mathbb{1})$ such that on $\mathcal{S}$ both $\tilde{x}(t) = \mathbb{1}\tilde{x}^*(t)$ and $\tilde{\theta}(t) = \mathbb{1}\tilde{\theta}^*(t)$ are satisfied with $\tilde{x}^*(t)$ and $\tilde{\theta}^*(t)$ are undetermined scalar functions. Together with (4.27b) we therefore conclude that

$$\gamma_\theta (q_j^{-1} - q_i^{-1}) \tilde{x}^* = 0 \quad \text{for all } i, j. \tag{4.28}$$

By assumption there exist an i and j such that $q_j^{-1} \neq q_i^{-1}$, which implies, together with (4.28), that $\tilde{x}^* = 0$ and therefore also that $\dot{\tilde{\theta}}^* = 0$. By evaluating the dynamics of (4.27) we obtain

$$\tilde{x} = 0 \tag{4.29}$$

$$\tilde{\theta} = \frac{\gamma_\mu}{\gamma_\theta} Q B \tilde{\mu}, \tag{4.30}$$

from which it follows that $\mathbb{1}^T Q^{-1} \tilde{\theta} = 0$. Since we also know from (4.26) that $\tilde{\theta} = \mathbb{1}\tilde{\theta}_i$ for any i, this implies that $\tilde{\theta} = 0$. From this and (4.18b) we can now conclude that

$$\overline{u} = -Q^{-1} \left(\frac{\mathbb{1}\mathbb{1}^T}{\mathbb{1}^T Q^{-1} \mathbb{1}} (d - Q^{-1} r) + r \right), \tag{4.31}$$

which coincides with the optimal steady state input in view of (4.8). By (4.29) and (4.31)

we conclude that Problem 4.5 is solved. ■

4.3 Constrained case

In this section we provide a solution to Problem 4.8 where, compared to Problem 4.5, we additionally consider constraints (4.15) and (4.16) on the inputs u and λ. We propose controllers that are similar to those presented in Section 4.2, while taking these additional constraints into account. To this end we modify (4.17) in order to satisfy (4.16) and propose the following controller to generate λ:

$$\dot{\mu} = \gamma_\mu B^T y \tag{4.32a}$$

$$\lambda = \text{sat}(-\gamma_c B^T y - \gamma_\mu \mu; 0, \lambda^+), \tag{4.32b}$$

where $\gamma_\mu, \gamma_c \in \mathbb{R}$ are appropriate gains. Note that the flows in the network are constrained to be uni-directional since the lower bound of the saturation is identically zero. The controller that regulates the input on the nodes u uses the same principles as (4.18), with some additions in order to satisfy (4.15). To this end, we saturate the output of this controller. However, this is not sufficient to guarantee convergence. For this reason we adjust the dynamics of the controller to

$$\dot{\theta} = -\gamma_l L^{com} \text{sat}\left(\theta; \frac{1}{\gamma_\theta} Q(u^- + r), \frac{1}{\gamma_\theta} Q(u^+ + r)\right) - \gamma_\theta Q^{-1} \left(y - \gamma_c B \lambda\right) \tag{4.33a}$$

$$u = \text{sat}(Q^{-1} \left(\gamma_\theta \theta - r\right); u^-, u^+), \tag{4.33b}$$

where L^{com} is the Laplacian of a connected communication graph, γ_c is as in (4.32) and $\gamma_l, \gamma_\theta \in \mathbb{R}$ are appropriate gains.

Remark 4.15 (Additional term compared to (4.18))**.** *Note that (4.33a) has $\gamma_\theta \gamma_c Q^{-1} B \lambda$ as an additional term compared to (4.18). We will show that this term play a key role to prove convergence but it also causes a steady state error. Interestingly, this error can be made arbitrarily small by adjusting the gains γ_c, γ_θ and γ_l. The consequence of this term is that the controller additionally needs to measure the difference between all the incoming and outgoing flows. Apart from the uniform gains, controller (4.33) is still distributed since only local measurements are required.*

Remark 4.16 (Existence of a solution to the closed loop system)**.** *We observe that (4.1) in closed loop with controllers (4.32) and (4.33) is globally Lipschitz. For this reason we can conclude that a solution exists for all time $t \geq 0$.*

Before we state our main theorem we define a change of coordinates in which we

distinguish the desired steady state and the steady state deviation from the desired one, which we denote with a bar and hat, respectively. To this end, we let

$$\begin{aligned}\tilde{x} &= x - \overline{x} - \hat{x}\\ \tilde{\mu} &= \mu - \overline{\mu} - \hat{\mu}\\ \tilde{\theta} &= \theta - \overline{\theta} - \hat{\theta},\end{aligned} \tag{4.34}$$

where $\overline{\theta}$ is as in (4.19), $\overline{\mu}$ is any solution to (4.20) and we define $\hat{x}$, $\hat{\mu}$ and $\hat{\theta}$ as the solution to

$$0 = B^T \hat{x} \tag{4.35a}$$
$$0 = -\gamma_\mu B\hat{\mu} + \gamma_\theta Q^{-1}\hat{\theta} \tag{4.35b}$$
$$0 = -\gamma_\theta Q^{-1}\hat{x} - \gamma_l L^{com}\hat{\theta} - \gamma_\theta\gamma_c\gamma_\mu Q^{-1}B(\hat{\mu} + \overline{\mu}). \tag{4.35c}$$

that has minimal Euclidean norm. Before we state the next lemmas let us define

$$\gamma := {\gamma_\theta}^2\frac{\gamma_c}{\gamma_l} \tag{4.36a}$$
$$\tilde{d} := d - Q^{-1}r \tag{4.36b}$$
$$\overline{Q} := \frac{Q^{-1}\mathbb{1}\mathbb{1}^T Q^{-1}}{\mathbb{1}^T Q^{-1}\mathbb{1}} - Q^{-1} \tag{4.36c}$$
$$\Phi := -L^{com}Q + \frac{1}{n}\mathbb{1}\mathbb{1}^T. \tag{4.36d}$$

We will show that the solutions to (4.35) always exist and derive an incremental form for system (4.1) in closed loop with (4.32) and (4.33) in suitable new coordinates.

Lemma 4.17 (Characterization of the steady state errors)**.** *Let Assumptions 4.1 and 4.11 be satisfied, then solutions $\hat{x}$, $\hat{\mu}$ and $\hat{\theta}$ to (4.35) always exist and are given by:*

$$\hat{\theta} = \frac{\gamma}{\gamma_\theta}Q\left(\gamma\overline{Q} + \Phi\right)^{-1}\overline{Q}^2 Q\tilde{d} \tag{4.37}$$
$$\hat{\mu} = \frac{\gamma}{\gamma_\mu}B^\dagger\left(\gamma\overline{Q} + \Phi\right)^{-1}\overline{Q}^2 Q\tilde{d} \tag{4.38}$$
$$\hat{x} = \gamma_c\frac{\mathbb{1}\mathbb{1}^T Q^{-1}}{\mathbb{1}^T Q^{-1}\mathbb{1}}\left(I - \gamma\left(\gamma\overline{Q} + \Phi\right)^{-1}\overline{Q}\right)\overline{Q}Q\tilde{d}, \tag{4.39}$$

where γ, $\tilde{d}$, $\overline{Q}$ and Φ are as in (4.36).

Proof. From (4.35a) and (4.35b) we obtain that

$$\hat{x} = \mathbb{1}\hat{x}^* \tag{4.40}$$
$$0 = \mathbb{1}^T Q^{-1}\hat{\theta}, \tag{4.41}$$

for some function $\hat{x}^*(t) \in \mathbb{R}$. From (4.20) we can see that $\overline{\mu}$ is any solution to

$$\gamma_\mu B\overline{\mu} = -\overline{Q}Q\tilde{d}, \tag{4.42}$$

which combined this with (4.40), (4.35b) and (4.35c) results in

$$\left(L^{com} + {\gamma_\theta}^2\frac{\gamma_c}{\gamma_l}Q^{-2}\right)\hat{\theta} = -\frac{\gamma_\theta}{\gamma_l}Q^{-1}\mathbb{1}\hat{x}^* + \gamma_\theta\frac{\gamma_c}{\gamma_l}Q^{-1}\overline{Q}Q\tilde{d}. \tag{4.43}$$

By solving for $\hat{x}^*$ we obtain

$$\hat{x}^* = -\gamma_c\frac{\mathbb{1}^T Q^{-1}}{\mathbb{1}^T Q^{-1}\mathbb{1}}\left(\gamma_\theta Q^{-1}\hat{\theta} - \overline{Q}Q\tilde{d}\right). \tag{4.44}$$

Substituting (4.44) in (4.43) and combining this with (4.41) yields

$$\tilde{Q}Q^{-1}\hat{\theta} = \begin{pmatrix} \gamma_\theta\frac{\gamma_c}{\gamma_l}\overline{Q} \\ 0 \end{pmatrix}\overline{Q}Q\tilde{d}. \tag{4.45}$$

where $\overline{Q}$ is as in (4.36c) and $\tilde{Q}$ is defined as

$$\tilde{Q} := \begin{pmatrix} \gamma\overline{Q} - L^{com}Q \\ \mathbb{1}^T \end{pmatrix}. \tag{4.46}$$

Due to Lemma B.4 in Appendix B we know that $(\tilde{Q}^T\tilde{Q})^{-1}$, $(\gamma\overline{Q} - L^{com}Q + \mathbb{1}\mathbb{1}^T)^{-T}$ and $(\gamma\overline{Q} - L^{com}Q + \frac{1}{n}\mathbb{1}\mathbb{1}^T)^{-1}$ exist. This implies that the solution of (4.45) is given by (4.37), since

$$\begin{aligned}
\hat{\theta} =& \frac{1}{\gamma_\theta}Q(\tilde{Q}^T\tilde{Q})^{-1}\tilde{Q}^T\begin{pmatrix} \gamma\overline{Q} \\ 0 \end{pmatrix}\overline{Q}Q\tilde{d} \\
=& \frac{\gamma}{\gamma_\theta}Q\left((\gamma\overline{Q} - L^{com}Q + \mathbb{1}\mathbb{1}^T)^T(\gamma\overline{Q} - L^{com}Q + \frac{\mathbb{1}\mathbb{1}^T}{n})\right)^{-1} \\
& \cdot\left(\gamma\overline{Q} - L^{com}Q + \mathbb{1}\mathbb{1}^T\right)^T\overline{Q}^2Q\tilde{d} \\
=& \frac{\gamma}{\gamma_\theta}Q\left(\gamma\overline{Q} - L^{com}Q + \frac{1}{n}\mathbb{1}\mathbb{1}^T\right)^{-1}\overline{Q}^2Q\tilde{d},
\end{aligned} \tag{4.47}$$

where we used the identities $\mathbb{1}^T\overline{Q} = 0$ and (B.36) in Appendix B. By combining (4.40), (4.44) and (4.47) we immediately observe that (4.39) is satisfied.

To find $\hat{\mu}$ we use (4.35b) and obtain

$$B\hat{\mu} = \frac{\gamma_\theta}{\gamma_\mu} Q^{-1}\hat{\theta}. \tag{4.48}$$

To prove that (4.48) has a solution we use the identity $\mathbb{1}^T(\gamma\overline{Q}+\Phi) = \mathbb{1}^T$ and from Lemma B.4 in Appendix B we know that $(\gamma\overline{Q} + \Phi)$ is invertible. This implies that $\mathbb{1}^T(\gamma\overline{Q} + \Phi)^{-1} = \mathbb{1}^T$ and therefore we have that $\mathbb{1}^T\left(\gamma\overline{Q} + \Phi\right)^{-1}\overline{Q} = 0$. Since $\mathrm{Im}(B) = \ker(B^T)^\perp = \mathrm{span}(\mathbb{1})^\perp$ we conclude that (4.48) has a solution. Moreover, a solution with the minimal Euclidean norm is given by

$$\hat{\mu} = B^\dagger \frac{\gamma_\theta}{\gamma_\mu} Q^{-1}\hat{\theta}, \tag{4.49}$$

and due to (4.47) it is easy to see that (4.49) coincides with (4.38). Lastly it can be checked that (4.37)-(4.39) satisfies (4.35) identically, which proves the thesis. ■

Suppose that the steady states are unsaturated and $y = 0$, then (4.32b) and (4.33b) at steady state read as

$$\overline{u} = \gamma_\theta Q^{-1}\overline{\theta} - r \tag{4.50}$$

$$\overline{\lambda} = -\gamma_\mu\overline{\mu}. \tag{4.51}$$

This implies, in view of (4.19) and (4.20) that

$$\overline{u} = -\frac{Q^{-1}\mathbb{1}\mathbb{1}^T}{\mathbb{1}^T Q^{-1}\mathbb{1}}\left(d - Q^{-1}r\right) - r \tag{4.52}$$

$$B\overline{\lambda} = \overline{Q}Q\left(d - Q^{-1}r\right), \tag{4.53}$$

where $\overline{Q}$ is as defined in (4.36c). We note that (4.50) is, in light of (4.8), the desired steady state input. Furthermore it is important to note that $\overline{u}$ and $\overline{\lambda}$ are independent of any gain parameters.

A sufficient condition to guarantee that the desired steady state exists is that the steady state inputs $\overline{u}$ and $\overline{\lambda}$ are unsaturated. Furthermore, we will show that a sufficient condition to guarantee that this steady state is attractive is that the steady state inputs are strictly unsaturated. For these reasons we introduce the following definition.

Assumption 4.18 (Feasibility condition)**.** *For a given disturbance d, linear cost vector r and diagonal quadratic cost matrix Q, its corresponding $\overline{u}$ as in (4.50) satisfies*

$$u_i^- < \overline{u}_i < u_i^+ \tag{4.54}$$

for all $i \in \mathcal{V}$. Furthermore, there exists at least one solution $\overline{\lambda}$ to

$$\mathbf{0} = -B\overline{\lambda} + \overline{u} - d, \tag{4.55}$$

that satisfies

$$0 < \overline{\lambda}_k < \lambda_k^+, \tag{4.56}$$

for all $k \in \mathcal{E}$.

Before we state the main result of this chapter let us define

$$\hat{u} := \gamma_\theta Q^{-1}\hat{\theta} \tag{4.57}$$

$$\hat{\lambda} := -\gamma_\mu \hat{\mu}, \tag{4.58}$$

with $\hat{\theta}$ and $\hat{\mu}$ as in (4.37) and (4.38), respectively. We refer to $\hat{u}$ and $\hat{\lambda}$ as the steady state input errors. Moreover, we introduce the following Lemma:

Lemma 4.19 (Lyapunov function for (B.37))**.** *Let Assumptions 4.1 and 4.11 be satisfied and let λ^+, u^- and u^+ satisfy the feasibility condition for a given d, r and Q. Given the Lyapunov function*

$$V(\tilde{x}, \tilde{\mu}, \tilde{\theta}) = \frac{1}{2}\|\tilde{x}\|^2 + \sum_{i=1}^{n} S_i^p + \sum_{i=1}^{m} S_i^e, \tag{4.59}$$

where

$$S_i^p := \int_0^{\tilde{\theta}_i} \operatorname{sat}\left(y, \left(\frac{1}{\gamma_\theta}Q(u^- + r) - (\overline{\theta} + \hat{\theta})\right)_i, \left(\frac{1}{\gamma_\theta}Q(u^+ + r) - (\overline{\theta} + \hat{\theta})\right)_i\right) dy, \tag{4.60}$$

and

$$S_i^e := \frac{1}{\gamma_\mu^2}\int_0^{-\chi_i} \operatorname{sat}(y, (-\gamma_\mu(\overline{\mu} + \hat{\mu}))_i, (\lambda^+ - \gamma_\mu(\overline{\mu} + \hat{\mu}))_i) dy, \tag{4.61}$$

with $\chi = \gamma_\mu\tilde{\mu} + \gamma_c B^T\tilde{x}$, then

$$\dot{V}(\tilde{x}, \tilde{\mu}, \tilde{\theta}) \leq 0, \tag{4.62}$$

and the set

$$\mathcal{Q} = \left\{(\tilde{x}, \tilde{\mu}, \tilde{\theta}) \,\middle|\, V(\tilde{x}, \tilde{\mu}, \tilde{\theta}) \leq D\right\}, \tag{4.63}$$

with $D \geq 0$, is nonempty, compact and forward invariant for system (B.37).

Proof [3]*:* We first prove (4.62), then we will show that $\mathcal{Q}$ is forward invariant and finally we prove that $\mathcal{Q}$ is compact and non-empty. By evaluating the partial derivatives of (4.59), we see that

$$\begin{aligned}\frac{\partial V}{\partial \tilde{x}} &= \tilde{x}^T - \gamma_c \text{sat}_\mu(\tilde{x}, \tilde{\mu})^T B^T \\ \frac{\partial V}{\partial \tilde{\theta}} &= \text{sat}_\theta(\tilde{\theta})^T \\ \frac{\partial V}{\partial \tilde{\mu}} &= -\frac{1}{\gamma_\mu}\text{sat}_\mu(\tilde{x}, \tilde{\mu})^T,\end{aligned} \tag{4.64}$$

where

$$\text{sat}_\mu(\tilde{x}, \tilde{\mu}) := \text{sat}(-\gamma_c B^T \tilde{x} - \gamma_\mu \tilde{\mu}; \mu^-, \mu^+) \tag{4.65}$$

$$\text{sat}_\theta(\tilde{\theta}) := \text{sat}(\tilde{\theta}; \theta^-, \theta^+), \tag{4.66}$$

with

$$\mu^- = \gamma_\mu(\overline{\mu} + \hat{\mu}) \tag{4.67a}$$

$$\mu^+ = \gamma_\mu(\overline{\mu} + \hat{\mu}) + \lambda^+ \tag{4.67b}$$

$$\theta^- = \frac{1}{\gamma_\theta} Q(u^- + r) - (\overline{\theta} + \hat{\theta}) \tag{4.67c}$$

$$\theta^+ = \frac{1}{\gamma_\theta} Q(u^+ + r) - (\overline{\theta} + \hat{\theta}). \tag{4.67d}$$

Hence, with the help of the closed loop dynamics as presented in Lemma B.5, we obtain

$$\dot{V} = -\gamma_c \|B\text{sat}_\mu(\tilde{x}, \tilde{\mu})\|^2 - \gamma_l \|B_c^T \text{sat}_\theta(\tilde{\theta})\|^2, \tag{4.68}$$

where B_c is the incidence matrix associated to the communication graph. From (4.68) it is easy to see that (4.62) is satisfied, which directly implies that $\mathcal{Q}$ is forward invariant.

Finally we will prove that (4.63) is compact. Note that this is equivalent to $\mathcal{S}$ being closed and bounded. From the definition of $\mathcal{S}$ it follows trivially that it closed, which leaves us with the proof that (4.63) is bounded.

By Lemma B.9 we know that there exists an open ball that contains the origin that lies within the bounds of the saturation functions in (4.60) and (4.61). Notice that this implies that $S_i^p \geq 0$ and $S_j^e \geq 0$ for all i and j. Now suppose that $|\tilde{x}_i| \to \infty$, then necessarily $V(\tilde{x}, \tilde{\mu}, \tilde{\theta}) \to \infty$, however this is in contradiction with (4.68) implying that $\tilde{x}$ is bounded. Now suppose that $|\tilde{\theta}_i| \to \infty$, then necessarily $S_i^p \to \infty$ due to (B.62). This

[3]This proof is an extension of a proof presented in (Wei and van der Schaft 2013). The proof in that paper does not consider the dynamics of θ as in this chapter, nor an input at the node with associated cost function, *i.e.* $\theta = 0$, $Q = 0$ and $r = 0$.

implies again that $V(\tilde{x}, \tilde{\mu}, \tilde{\theta}) \to \infty$ from which we can conclude that $\tilde{\theta}$ is bounded. Lastly we prove that $\tilde{\mu}$ is bounded. Suppose that $|\tilde{\mu}_i| \to \infty$ then also $|-(\gamma_\mu(\tilde{\mu}) + \gamma_c B\tilde{x})_i| \to \infty$ since $\tilde{x}$ is bounded. This, together with (B.62) implies that $S_j^e \to \infty$. Therefore also $\tilde{\mu}$ is bounded and we can therefore conclude that $\mathcal{Q}$ is compact. Lastly we prove that $\mathcal{Q}$ is non-empty. Note that $V(0,0,0) = 0$, this implies that the origin is contained in $\mathcal{Q}$, which concludes the proof. ∎

We are now ready to state the main result of this chapter.

Theorem 4.20 (Sufficient conditions for solving Problem 4.8)**.** *Let Assumption 4.1 and 4.18 be satisfied and let there exist at least one pair q_i, q_j such that $q_i \neq q_j$, then Problem 4.8 is solved by controllers (4.32)-(4.33) with a suitable choice of γ_c, γ_θ and γ_l.*

Proof. In order to prove Theorem 4.20 we will show that $\lim_{t\to\infty} \tilde{x} = 0$ and $\lim_{t\to\infty} \tilde{\theta} = 0$ and argue that this implies that Problem 4.8 is solved. Let V be as in Lemma 4.19 in Appendix B. Using this same Lemma we know that we can invoke LaSalle's invariance principle to show that $(\tilde{x}, \tilde{\mu}, \tilde{\theta})$ converges to the largest invariant set where $\dot{V} = 0$, which is given by

$$\mathcal{S} := \left\{ (\tilde{x}, \tilde{\mu}, \tilde{\theta}) \,\middle|\, B\text{sat}_\mu(\tilde{x}, \tilde{\mu}) = 0, B_c^T \text{sat}_\theta(\tilde{\theta}) = 0 \right\}, \tag{4.69}$$

with $\text{sat}_\mu(\tilde{x}, \tilde{\mu})$ as in (4.65) and $\text{sat}_\theta(\tilde{\theta})$ as in (4.66). In light of Lemma B.5 we can see that the dynamics on this invariant set $\mathcal{S}$ are given by

$$\dot{\tilde{x}} = \gamma_\theta Q^{-1} \text{sat}_\theta(\tilde{\theta}) \tag{4.70a}$$

$$\dot{\tilde{\theta}} = -\gamma_\theta Q^{-1} \tilde{x} \tag{4.70b}$$

$$\dot{\tilde{\mu}} = B^T \tilde{x}. \tag{4.70c}$$

First we will prove that on this invariant set $\mathcal{S}$, necessarily $\tilde{\theta} = 0$.

Let θ^- and θ^+ be as in (4.67c) and (4.67d), respectively, then by Lemma B.9 in Appendix B we know that $\theta^- < 0$ and $\theta^+ > 0$. Now assume by contradiction that there exists a $\tilde{\theta}_i$, which is not identically equal to zero. Now consider two cases, either $\tilde{\theta}_j = 0$ for all $j \neq i$ or there exists at least one other $\tilde{\theta}_j$, with $i \neq j$, which is not identically equal to zero. In the first case we have that

$$\text{sat}(\tilde{\theta}_j; \theta_j^-, \theta_j^+) = 0, \tag{4.71}$$

for each $j \neq i$, since $\theta_j^- < 0$, $\theta_j^+ > 0$ for all $j \neq i$. Furthermore, due to Assumption 4.11 B_c is the incidence matrix of a connected graph, it holds that $B_c^T \text{sat}_\theta(\tilde{\theta}) = 0$, which implies that

$$\text{sat}(\tilde{\theta}_i; \theta_i^-, (\theta^+)_i) = \text{sat}(\tilde{\theta}_j; \theta_j^-, \theta_j^+), \tag{4.72}$$

for each i and j. From (4.71) and (4.72) we can now conclude that $\tilde{\theta}_i = 0$ since also $\theta_i^- < 0, \theta_i^+ > 0$. Therefore we have a contradiction and necessarily $\tilde{\theta}_i = 0$.

Now consider the second case, where we assume that there exists at least another $\tilde{\theta}_j$, with $i \neq j$, which is not identically equal to zero. By (4.70a) and (4.70b) we obtain that $\ddot{\tilde{\theta}} = -\gamma_\theta{}^2 Q^{-2} \mathrm{sat}_\theta(\tilde{\theta})$, which implies that for each element i we have that

$$\ddot{\tilde{\theta}}_i = \begin{cases} -\gamma_\theta{}^2 q_i^{-2} \theta_i^- & \text{if } \tilde{\theta}_i \leq \theta_i^- \\ -\gamma_\theta{}^2 q_i^{-2} \theta_i^+ & \text{if } \theta_i^+ \leq \tilde{\theta}_i \\ -\gamma_\theta{}^2 q_i^{-2} \tilde{\theta}_i & \text{otherwise.} \end{cases} \tag{4.73}$$

Let $p^- := \max_i\{\theta_i^-\}$ and $p^+ := \min_i\{\theta_i^+\}$. The solution $\tilde{\theta}_i$ to (4.73) consists of a trajectory that consists of sinusoidal or parabolic parts depending on the state $\tilde{\theta}_i$. The intervals in which the solution $\tilde{\theta}_i$ follows a pure parabolic trajectory have a finite length, since $\ddot{\tilde{\theta}}_i < 0$ if $\tilde{\theta}_i > 0$ and $\ddot{\tilde{\theta}}_i > 0$ if $\tilde{\theta}_i < 0$, guarantee that θ_i enters the unsaturated range in finite time. Furthermore, in all other intervals the solution $\tilde{\theta}_i$ follows a pure sinusoidal trajectory, which forces $\tilde{\theta}_i$ to cross the origin in finite time. For this reason there exists an interval (T_1, T_2) such that

$$p^- \leq \tilde{\theta}_i \leq p^+, \tag{4.74}$$

which implies that

$$\mathrm{sat}(\tilde{\theta}_i; \theta_i^-, \theta_i^+) = \tilde{\theta}_i, \tag{4.75}$$

due to the definition of p^- and p^+. Moreover, from $B_c^T \mathrm{sat}_\theta(\tilde{\theta}) = 0$ and (4.75), we obtain that

$$\tilde{\theta}_i = \mathrm{sat}(\tilde{\theta}_j; \theta_j^-, \theta_j^+), \tag{4.76}$$

for all j. Since $\theta_j^- \leq p^- \leq \tilde{\theta}_i \leq p^+ \leq \theta_j^+$) it follows that $\tilde{\theta}_i = \tilde{\theta}_j$ for all j, or equivalently $\tilde{\theta} = \mathbb{1}\alpha(t)$, where $\alpha(t) \in \mathbb{R}$. Due to (4.70a) and (4.70b), we have that

$$\mathbb{1}\ddot{\alpha}(t) = -Q^{-2}\mathbb{1}\alpha(t), \tag{4.77}$$

which implies that

$$-q_i^{-2}\alpha(t) = -q_j^{-2}\alpha(t), \tag{4.78}$$

for some i, j. Now, by assumption we know that there exists an i and a j such that $q_i \neq q_j$, which implies that necessarily $\alpha(t) = 0$. It follows that $\tilde{\theta}(t) = 0$ for $t \in (T_1, T_2)$. Also note that $\tilde{\theta}_i$ enters the interval (T_1, T_2) in finite time and by (4.73) we see that $\tilde{\theta}_i$ is locally Lipschitz continuous, hence cannot undergo jumps. This implies that $\tilde{\theta}(t) = 0$ for all $t \geq 0$ on the invariant set $\mathcal{S}$ which is a contradiction, implying that at most one $\tilde{\theta}_i$ is not identically equal to zero. As this case has already been ruled out, we obtain that $\tilde{\theta}(t) = 0$

for all $t \geq 0$ on the invariant set $\mathcal{S}$.

It is now trivial to prove that $\tilde{x} = 0$ on $\mathcal{S}$. Due to (4.70b) we can see that $0 = -Q^{-1}\tilde{x}$, which implies that $\tilde{x} = 0$. Finally, due to a suitable choice of γ_c, γ_θ and γ_l, Lemma B.7 in Appendix B and (4.34), we have that

$$\begin{aligned} \lim_{t\to\infty} \|x - \overline{x}\| &= \lim_{t\to\infty} \|\tilde{x} + \hat{x}\| = \|\hat{x}\| < \epsilon_x \\ \lim_{t\to\infty} \|u - \overline{u}\| &= \lim_{t\to\infty} \|\tilde{u} + \hat{u}\| = \|\hat{u}\| < \epsilon_u, \end{aligned} \tag{4.79}$$

and therefore the thesis follows. ■

From Theorem 4.8 we obtain that as long as the quadratic costs of at leat two producers are distinct, controllers (4.32)-(4.33) guarantee that both the volumes converge approximately to their setpoints and the inputs are approximately optimal at steady state. Moreover, by tuning the gains of the controller, the errors that correspond to these approximations can be made arbitrarily small. The controllers require only local measurement but in order to calculate the bounds on the gains, global information is required. In Chapter 5 a different control design is presented that does not require heterogeneous quadratic costs, guarantees zero steady state errors and does not require any tuning of the gains implying that the design and operation can be performed completely distributed.

Remark 4.21 (Characterization of the gains)**.** *The choice of γ_c, γ_θ and γ_l for which Problem 4.8 is solved are explicitly constructed in Lemma B.7 in Appendix B and a discussion on this choice can be found in Remark B.8.*

4.4 Case study

We provide a case study in which we consider a district heating system. The network is modeled by graph $\mathcal{G}$ and where each node has a producer, a consumer and a stratified storage tank as in Figure 2.2. Motivated by Remark 2.4 and Lemma 2.3 the corresponding model is given by (4.1). We perform a simulation over a 24 hour time interval and use a circle graph consisting of four nodes as in Figure 4.4. The entries of the quadratic cost functions are given by $Q = \text{diag}\begin{pmatrix} 1 & 0.7 & 0.3 & 0.1 \end{pmatrix}$, and s and r are zero vectors. We initialize the system at steady state, with the demand and the volume setpoint given by $d = -\begin{pmatrix} 0.03 & 0.03 & 0.03 & 0.03 \end{pmatrix}$ and $\overline{x} = \begin{pmatrix} 200 & 300 & 400 & 500 \end{pmatrix}$, respectively. Motivated by Remark 4.3 we investigate the response of the system to a ramp reference signal as well as to an increase in demand. First, at $t = 1h$ we switch from a constant reference signal to a ramp such that at $t = 6h$, $\overline{x}$ becomes $\overline{x} = \begin{pmatrix} 800 & 800 & 800 & 800 \end{pmatrix}$. Soon after this interval we increase the demand by 50% and keep the setpoints constant. The saturation bounds on the production and flows are given by $u^- = 0m^3/s$,

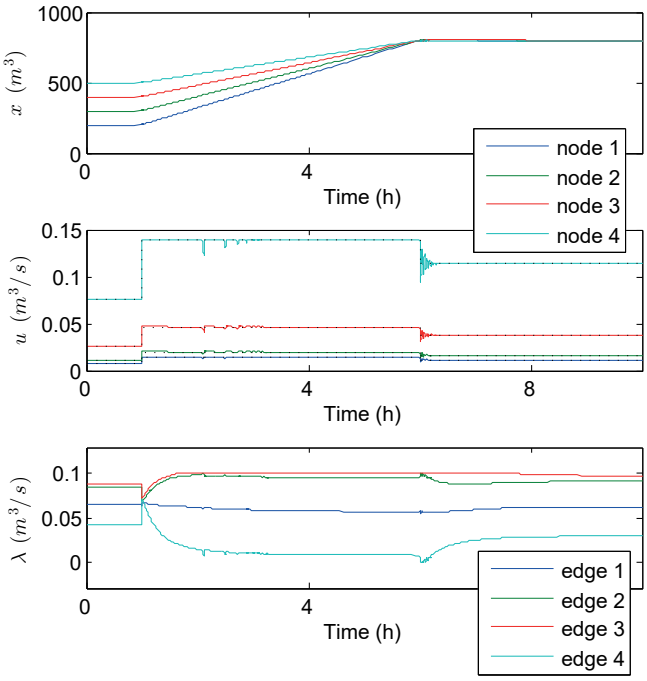

Figure 4.1: Volumes, flows and production in the presence of saturation.

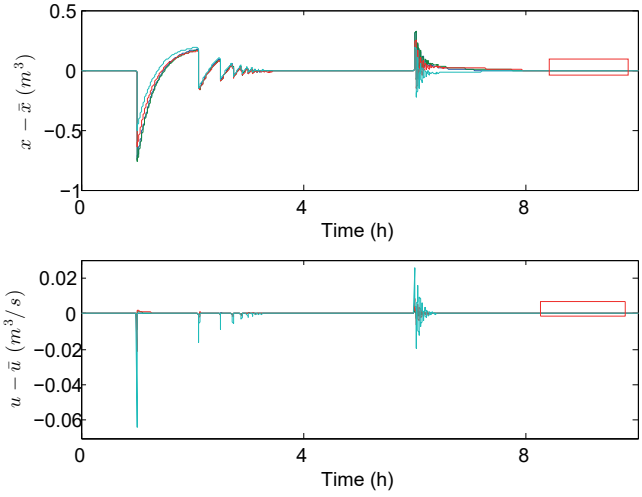

Figure 4.2: Deviations from the volume setpoints and optimal production. The highlighted area is depicted in Figure 4.3.

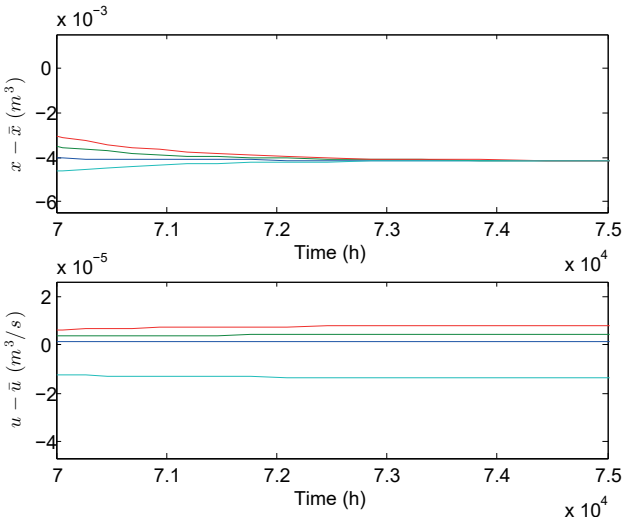

Figure 4.3: Enlargement of the highlighted areas of Figure 4.2.

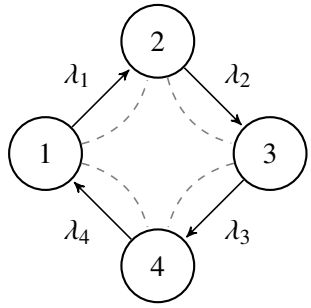

Figure 4.4: Topology of the considered heat network. The arrows indicate the required flow directions in the heat network, while the dashed lines represent the communication network used by the controllers.

$u^+ = 0.14m^3/s$ and $\lambda^+ = 0.1m^3/s$, respectively. Moreover, the error bounds, as defined in (4.13) and (4.14), are set to $\epsilon_x = 10^{-2}$ and $\epsilon_u = 10^{-4}$.

Based on Lemma B.7 in Appendix B we can explicitly calculate the bounds on γ_c, γ_θ and γ_l (see (B.52a) and (B.52b)). To illustrate how these gains are found, we investigate them for the first interval (*i.e.* between $0h$ and $1h$). In that case the numerical value of the right hand side of (B.52a) is 0.1324 and $\|\Phi^{-1}\overline{Q}^2 Q\tilde{d}\| = 0.7773$. Furthermore, we have that $\frac{\|\Phi^{-1}\overline{Q}^2 Q\tilde{d}\|}{\|\Phi^{-1}\overline{Q}\|} = 0.0676$ and by taking $\theta = 0.9985$ this implies that $\delta_\theta = 10^{-4}$. Additionally we have that $\delta_\theta = 0.0058$ and $\delta_\mu = 0.0087$ which means that $\min\left\{\delta_\theta, \delta_\mu, \delta_\theta, \epsilon_u\right\} = \epsilon_u$. The conditions in (B.52) are satisfied if $\gamma_c < 0.1109$ and ${\gamma_\theta}^2/\gamma_l < 1.90 \cdot 10^{-4}$, and therefore we take $\gamma_\theta = 0.01$, $\gamma_l = 0.53$, $\gamma_\mu = 0.01$ and $\gamma_c = 0.11$.

Plots of the resulting simulations can be found in Figure 4.1, in which we see that in all intervals $\lim_{t\to\infty} x \approx \overline{x}$ and $\lim_{t\to\infty} u \approx \overline{u}$. The optimal production $\overline{u}$ in the middle plot is given by the dotted black line from which one can see that the jumps in the reference signal (corresponding to a transition to a charging phase) affects the optimal production levels. In the top plot of Figure 4.1 we can see that x is able to track the piecewise constant reference signal $\overline{x}$. The flow injected by the producers, depicted in the middle plot, show some transient behaviour after the switch to the charging phase and increase of demand. In the interval $1 \leq t \leq 4$, we can also see that the production on node 4 and the flows on edge 3 are subject to saturation which cause some wind-up phenomena.

In Figure 4.2 we see in the upper plot the deviation of x from $\overline{x}$ and in the bottom plot the deviation of u from $\overline{u}$. Again the transient behaviour after $t = 1$ and $t = 6$ is clearly visible as well as the wind-up phenomena for $1 \leq t \leq 4$. Finally, an enlargement of the highlighted areas in Figure 4.2 can be found in Figure 4.3. From this Figure we can clearly see that at the end of the last interval we have that $\|x(t) - \overline{x}(t)\| < \epsilon_x$ and $\|u(t) - \overline{u}\| < \epsilon_u$, respectively.

Chapter 5

Volume regulation and optimal production of multiple producers

Abstract

This chapter investigates the control of flow networks, where the control objective is to regulate the measured output (e.g storage levels) towards a desired value. We present a distributed controller that dynamically adjusts the inputs and flows, to achieve output regulation in the presence of unknown disturbances (e.g. demand), while satisfying given input and flow constraints. Optimal coordination among the inputs, minimizing a suitable cost function, is achieved by exchanging information over a communication network. Exploiting an incremental passivity property, the desired steady state is proven to be globally asymptotically stable under the closed loop dynamics. Two case studies (a district heating system and a multi-terminal HVDC network) show the the effectiveness of the proposed solution.

In this chapter we extend the results of Chapter 4. The control problem and control design are similar to the ones proposed in that chapter, so we highlight the differences here. First we consider a control problem in which only a subset of nodes has a controllable input located at the nodes. Second, the controllers are adapted such that they include an additional state. Third, the saturation functions are changed to nonlinear strictly increasing functions with a possible upper and lower bounded range. These changes allow us to prove asymptotic stability with respect to the optimal steady state in a more general setting. Consequently we propose a *distributed* controller, dynamically adjusting inputs and flows, to achieve *optimal output regulation* under *capacity constraints* on the input and the flows and in the presence of *unknown* demand (disturbances).

The results presented in this chapter show some advantages over existing ones. Specifically, the proposed control scheme coordinates the inputs optimally to satisfy the total demand. Although these objectives have been separately addressed before, the way how we incorporate all of them within a coherent approach is new. Building upon (Bürger et al. 2015), (Scholten et al. 2016b) and (Trip et al. 2016), the controllers on the edges render the flow network incrementally passive with respect to the desired steady state. This passivity property is then exploited in the design of a distributed controller acting on

the nodes. Optimal coordination among the inputs, minimizing a suitable cost function, is achieved by exchanging relevant information over a communication network, whereas the constraints are enforced by using suitably selected nonlinear functions. Global convergence to the desired steady state is proven relying on Lyapunov arguments and an invariance principle. Furthermore, we provide two case studies (a district heating system and a multi-terminal HVDC network) to illustrate how physical systems are described as a flow network and to demonstrate the performance of the proposed solution.

The chapter is structured as follows. In Section 5.1 we introduce the model and state our control objective. The controller design is presented in Section 5.2, followed by the stability analysis of the closed loop system in Section 5.3. An extension of the considered plant and controller dynamics is stated and analyzed in Section 5.4 and finally two case studies are presented in Section 5.5.

5.1 Output regulation and optimal steady state inputs

In this section we consider the dynamics as in (2.7) which we repeat for convenience

$$T_x \dot{x} = -B\lambda + Eu - d \tag{5.1a}$$

$$y = h(x). \tag{5.1b}$$

where $T_x \in \mathbb{R}^{n\times n}_{>0}$ is a diagonal matrix, $B \in \mathbb{R}^{n\times m}$ is the incidence matrix of the graph $\mathcal{G}$, $\lambda \in \mathbb{R}^m$ are the flows, $u \in \mathbb{R}^p$ are the inputs and $d \in \mathbb{R}^n$ the unmeasured disturbance. Moreover, $E \in \mathbb{R}^{n\times p}$ is of the form

$$E = \begin{pmatrix} I_{p\times p} \\ \mathbf{0}_{(n-p)\times p} \end{pmatrix}, \tag{5.2}$$

and for convenience we repeat Assumptions 2.5 and 2.7:

Assumption 5.1 (Connectedness)**.** *The graph $\mathcal{G}$ is connected.*

Assumption 5.2 (Controllable inputs)**.** *There is at least one node that has a controllable input, i.e. $p \geq 1$.*

We discuss two control objectives and various input and flow constraints under which the objectives should be reached. We start with discussing the two objectives, which are similar to those in Chapter 4.1. The first objective is concerned with the output $y = h(x)$ in (5.1), at steady state.

Objective 5.3 (Output regulation)**.** *Let $\overline{y} \in \mathcal{R}(h(x))$ be a desired constant setpoint, then the output $y = h(x)$ of (5.1) asymptotically converges to $\overline{y}$, i.e.*

$$\lim_{t\to\infty} \|h(x(t)) - \overline{y}\| = 0. \tag{5.3}$$

Remark 5.4 (Tracking of a ramp)**.** *In case that $h(x) = x$ we can extend Objective 5.3, similar as in Remark 4.3, to the possibility of tracking a linear transition between the current setpoint $\overline{y}(t_1)$ to a new setpoint $\overline{y}(t_2)$ with $t_2 > t_1$. To do so, the desired reference signal is modelled as a ramp, i.e.*

$$\overline{y}(t) = \overline{y}(t_1) + \frac{t - t_1}{t_2 - t_1}(\overline{y}(t_2) - \overline{y}(t_1)). \tag{5.4}$$

After a coordinate transformation $\tilde{x}(t) = x(t) - \overline{y}(t)$, we obtain a system of the same form as (5.1a), where the evolution of $\tilde{x}$ is described by

$$T_x \dot{\tilde{x}} = -B\lambda + Eu - \tilde{d}. \tag{5.5}$$

The corresponding constant disturbance is now given by

$$\tilde{d} = d + \frac{1}{t_2 - t_1}(\overline{y}(t_2) - \overline{y}(t_1)). \tag{5.6}$$

Note that boundedness of $\tilde{x}_i$ does not imply boundedness of x_i as $\overline{y}_i(t)$ increases or decreases constantly over time. Therefore, the used invariance principle in the later sections is not immediately applicable if we consider the original variables of the system. Nevertheless, the subsequent analysis can be applied to the incremental system (5.5) if we consider $\tilde{x}$ as the state.

In order to guarantee that Objective 5.3 can be achieved we make the following assumption

Assumption 5.5 (Range of function h)**.** *Function h_i is such that $\overline{y}_i \in \mathcal{R}(h_i)$ for all $i \in \mathcal{V}_e$.*

Similar as in Objective 4.4 of Chapter 4, it is natural to wonder if the total input can be coordinated optimally among the nodes. Note however that optimal coordination is only possible if there are two or more controllable inputs at the nodes (*i.e.* $p \geq 2$). The related optimization problem is discussed in Section 2.4 and from Lemma 2.17 we obtain that the optimal steady state input $\overline{u}$ is given by (2.37) which we repeat here

$$\overline{u} = Q^{-1}\left(E^T \frac{\mathbb{1}_n \mathbb{1}_n^T}{\mathbb{1}_p^T Q^{-1} \mathbb{1}_p}(d + EQ^{-1}r) - r\right). \tag{5.7}$$

We are now ready to state the second control objective.

Objective 5.6 (Optimal feedforward input)**.** *The input at the nodes asymptotically converge to the solution to (2.36), i.e.*

$$\lim_{t\to\infty} \|u(t) - \overline{u}\| = 0, \tag{5.8}$$

with $\overline{u}$ as in (5.7).

We consider a similar constraint on the control inputs u as in Constraint 4.6 with the difference that only the nodes contained in $\mathcal{V}_e$ include a controllable input.

Constraint 5.7 (Input limitations)**.** *The inputs at the nodes satisfy*

$$u_i^- < u_i(t) < u_i^+, \tag{5.9}$$

for all $i \in \mathcal{V}_e$ and all $t \geq 0$, with $u_i^-, u_i^+ \in \mathbb{R}$ being suitable constants.

Moreover, similar to Constraint 4.7 in Chapter 4 we let the flows on the edges be constrained within the capacity of the edges.

Constraint 5.8 (Flow capacity)**.** *The flows on the edges satisfy*

$$\lambda_k^- < \lambda_k(t) < \lambda_k^+, \tag{5.10}$$

for all $k \in \mathcal{E}$ and all $t \geq 0$, with $\lambda_k^-, \lambda_k^+ \in \mathbb{R}$ being suitable constants.

Note that in Chapter 4 λ_k^- was taken as $\lambda_k^- = 0$ which we relax in this chapter. The physical limitations and safety requirements demand that the constraints should be satisfied *for all time* and not only at steady state.

Remark 5.9 (Special cases)**.** *The unconstrained case can be regarded as a particular example of the considered setting. This is obtained by taking $-\infty$ as a lower and ∞ as an upper bound for both u_i and λ_k. Moreover, if we take $\lambda_k^- \geq 0$ or $\lambda_k^+ \leq 0$, the flow on edge k is constrained to be unidirectional.*

In many applications it is desirable to have a distributed control architecture where controllers rely only on local information to decrease communications, to increase robustness and to improve the scalability of the control scheme. We therefore require that the controllers to be designed only depend on information available from adjacent nodes in the physical flow network or adjacent nodes in a digital communication network that is deployed to ensure optimality (see the next section, Objective 2).

For convenience, we summarize the objectives and constraints yielding the following controller design problem.

Problem 5.10 (Controller design problem)**.** *Design distributed controllers that regulate inputs u at the nodes and the flows λ on the edges, such that*

$$\begin{aligned} \lim_{t\to\infty} \|h(x(t)) - \overline{y}\| &= 0 \\ \lim_{t\to\infty} \|u(t) - \overline{u}\| &= 0, \end{aligned} \tag{5.11}$$

where $\overline{y}$ is the desired setpoint and $\overline{u}$ is as in (5.7). Furthermore,

$$\begin{aligned} \lambda_k^- < \lambda_k(t) < \lambda_k^+ \\ u_i^- < u_i(t) < u_i^+, \end{aligned} \tag{5.12}$$

for all $k \in \mathcal{E}$, $i \in \mathcal{V}_e$ and $t \geq 0$. □

Remark 5.11 (Positive systems)**.** *A common requirement is that, additionally to Objective 5.3 and Objective 5.6, the state x has to be nonnegative, i.e. $x(t) \geq \mathbf{0}$ for all t. Although, achieving output regulation (Objective 5.3), with $\overline{x} > \mathbf{0}$, is in practical cases sufficient to ensure that $x(t) \geq \mathbf{0}$ for all t, when the system suitably initialized (see also the case studies in Section 5.5), a theoretical guarantee is difficult to obtain, due to the presence of an unknown and constant disturbance d. An interesting future endeavor is to study the design of controllers achieving Objective 5.3 and Objective 5.6 within the setting of so-called positive systems (Benvenuti and Farina 2002) (Rami and Tadeo 2007).*

5.2 Design of distributed and optimal controllers

In this section we propose *distributed* input and flow controllers that achieve the various objectives under the constraints discussed in the previous section. The controllers will be designed to enjoy a passivity property and asymptotic stability of the closed loop system will derive from a suitable power preserving interconnection of the flow network and the controllers. Both the passivity property as well as the stability of the closed loop system will be discussed in the next section.

Before we introduce the controllers we observe two things. First we notice that left-multiplying (5.1a) by $\mathbb{1}_n^T$ gives

$$\mathbb{1}_n^T T_x \dot{x} = \mathbb{1}_n^T (Eu - d), \tag{5.13}$$

which shows that the aggregated storage level cannot be affected by the flows λ. However, from (5.1a) we can see that individual storage levels x_i are changed by the flows λ.

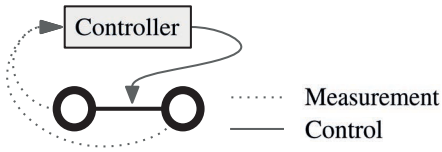

Figure 5.1: The controller that is located at the edge has access to the outputs of its adjacent nodes. Using these measurements as inputs, the controller generates the flow rate λ on the edge.

Second, at steady state, the state variable x is constant and (5.13) becomes

$$\mathbf{0} = \mathbb{1}_n^T(E\overline{u} - d), \tag{5.14}$$

which implies that a balance between the total input and disturbance is required at steady state in order to satisfy Objective 5.3. Motivated by the first observation we design the controller that regulates the flows λ such that the error $y - \overline{y}$ is balanced. After that we will design a controller that regulates u such that Problem 5.10 is satisfied, *i.e.* the error $y - \overline{y}$ will go to zero and will satisfy (5.14) at steady state.

5.2.1 Flows between the nodes

We design a controller that regulates the flows on the edges such that we achieve consensus in the error $y - \overline{y}$. We guarantee that the controller has the passivity property and that the controller is distributed by considering it of the following form[1]

$$\begin{aligned} T_\mu \dot{\mu} &= B^T(h(x) - \overline{y}) - (f(\mu) - \xi) \\ T_\xi \dot{\xi} &= f(\mu) - \xi \\ \lambda &= f(\mu), \end{aligned} \tag{5.15}$$

where $T_\mu, T_\xi \in \mathbb{R}^{m\times m}_{>0}$ are diagonal matrices with strictly positive entries, $\mu, \xi \in \mathbb{R}^m$ and the mapping $f(\cdot) : \mathbb{R}^m \to \mathbb{R}^m$, with $f(\mu) = (f_1(\mu_1), \ldots, f_m(\mu_m))^T$, has suitable properties discussed in Assumptions 5.15 and 5.16 below. Moreover, B is the incidence matrix reflecting the topology of the physical network, which implies that the flow controller on edge k only requires information from its adjacent nodes (see also Figure 5.1). It therefore follows that the controller is distributed.

[1] μ is introduced with some abuse of notation since there is no relation with the control input in (2.23).

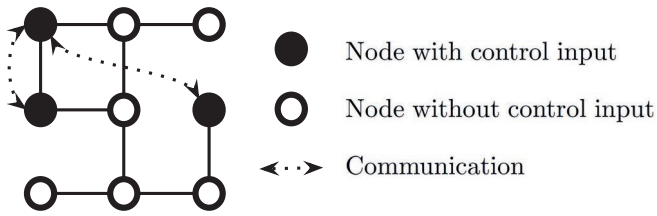

Figure 5.2: Example of a flow network including a communication graph.

5.2.2 Inputs at the nodes

Next, we design an input controller u_i at each node i that adjusts the external input to the network. Inspired by the result in (Trip and De Persis 2017), where a similar control problem is considered in the setting of power networks, we propose the controller

$$\begin{aligned} T_\theta \dot{\theta} &= -E^T(h(x) - \bar{y}) - (g(\theta) - \phi) \\ T_\phi \dot{\phi} &= g(\theta) - \phi - QL^{com}(Q\phi + r) \\ u &= g(\theta), \end{aligned} \tag{5.16}$$

where $T_\theta, T_\phi \in \mathbb{R}^{p\times p}_{>0}$ are diagonal matrices with strictly positive entries, $\theta, \phi \in \mathbb{R}^p$ with $p = |\mathcal{V}_e|$ and the mapping $g(\cdot) : \mathbb{R}^p \to \mathbb{R}^p$ with $g(\theta) = (g_1(\theta_1) \dots g_p(\theta_p))^T$, has suitable properties that will be discussed in Assumptions 5.15 and 5.16 below. Moreover, L^{com} is the Laplacian matrix reflecting the communication topology (see also Figure 5.2). This communication ensures that at steady state a consensus is obtained in the marginal costs, *i.e.* $Qg(\bar{\theta}) + r \in \mathrm{Im}(\mathbb{1})$. In order to guarantee that all marginal costs converge to the same value we make the following assumption on the communication network.

Assumption 5.12 (Communication network)**.** *The graph reflecting the communication topology is balanced*[2] *and strongly connected.*

Lemma 5.13 (Consequences of Assumption 5.12)**.** *If Assumption 5.12 is satisfied, then L^{com} is a positive semi-definite matrix and*

$$x^T L^{com} x = 0, \tag{5.17}$$

if and only if $x \in \mathrm{Im}(\mathbb{1})$.

Proof. The proof follows immediately from (Olfati-Saber and Murray 2004, Theorem 7). Specifically, since the communication graph is balanced, L^{com} is positive semi-definite

[2] A directed graph is balanced if the (weighted) in-degree is equal to the (weighted) out-degree of every node.

and (5.17) satisfies

$$x^T L^{com} x = \frac{1}{2} x^T (L^{com} + (L^{com})^T) x = x^T \hat{L}^{com} x, \tag{5.18}$$

where $\hat{L}^{com}$ is a Laplacian matrix corresponding to the communication network with *undirected* edges. Furthermore, $\mathrm{Ker}(\hat{L}^{com}) = \mathrm{Im}(\mathbb{1})$, due to the connectedness of the communication network. ■

Remark 5.14 (Local and exchanged information)**.** *According to (5.16), every controller at node $i \in \mathcal{V}_p$, measures $y_i = h_i(x_i)$ and compares it with the desired set point $\overline{y}_i$. Information on the marginal costs $(q_i\phi_i + r_i)$ is exchanged among neighbours over a communication network with a topology described by L^{com}. Controller (5.16) is therefore fully distributed. The output $g_i(\theta_i)$ is chosen to satisfy Constraint 1, and is discussed in more detail in the next subsection.*

5.2.3 Feasibility of the control problem

In order to guarantee that controllers (5.16) and (5.15) in closed loop with (5.1) solve Objectives 5.6 and 5.3 we require that f and g satisfy certain properties. There properties are related to a steady state of the closed loop system and is given in the following assumption:

Assumption 5.15 (Properties of f and g)**.** *Functions f_k and g_i, in respectively (5.15) and (5.16), are continuously differentiable and strictly increasing. Moreover, let $\overline{u}$ be as in (5.7), then f_k is such that there exists a $\omega \in \mathbb{R}^m$ where $[B^\dagger(E\overline{u} - d) + (I - B^\dagger B)\omega]_k \in \mathcal{R}(f_k)$ for all $k \in \mathcal{E}$, and g_i satisfies $\overline{u}_i \in \mathcal{R}(g_i)$ for all $i \in \mathcal{V}_e$.*

Moreover, controllers (5.16) and (5.15) are designed to guarantee the fulfilment of Constraints (5.9) and (5.10) by properly selecting $f(\mu)$ and $g(\theta)$. Since $\lambda = f(\mu)$ and $u = g(\theta)$, the following assumption is sufficient to ensure that the inputs and flows do not exceed their limitations.

Assumption 5.16 (Bounded controller outputs)**.** *Functions $f_k(\cdot)$ and $g_i(\cdot)$, in respectively (5.15) and (5.16) satisfy*

$$\begin{aligned} \mathcal{R}(f_k) &\subseteq (\lambda_k^-, \lambda_k^+) \\ \mathcal{R}(g_i) &\subseteq (u_i^-, u_i^+) \end{aligned} \tag{5.19}$$

for all $k \in \mathcal{E}$ and $i \in \mathcal{V}_e$.

Possible choices for $f_k(\mu_k)$ and $g_i(\theta_i)$ that satisfy Assumptions 5.15 and 5.16 include *e.g.* the function $\gamma(z) = z$ in absence of any constraints, and also the constraint enforcing functions $\gamma(z) = \tanh(z)$, $\gamma(z) = \arctan(z)$ (see also the case studies in Section 5.5).

Before we analyse the stability of the system we investigate the properties of the steady state. To do so, we write system (5.1) in closed loop with controllers (5.15) and (5.16), obtaining

$$\begin{aligned} T_x\dot{x} &= -Bf(\mu) + Eg(\theta) - d \\ T_\mu\dot{\mu} &= B^T(h(x) - \overline{y}) - (f(\mu) - \xi) \\ T_\xi\dot{\xi} &= f(\mu) - \xi \end{aligned} \tag{5.20a}$$

$$\begin{aligned} T_\theta\dot{\theta} &= -E^T(h(x) - \overline{y}) - (g(\theta) - \phi) \\ T_\phi\dot{\phi} &= g(\theta) - \phi - QL^{com}(Q\phi + r). \end{aligned} \tag{5.20b}$$

Any equilibrium of system (5.20) satisfies

$$\mathbf{0} = -Bf(\overline{\mu}) + Eg(\overline{\theta}) - d \tag{5.21a}$$

$$\mathbf{0} = B^T(h(\overline{x}) - \overline{y}) - (f(\overline{\mu}) - \overline{\xi}) \tag{5.21b}$$

$$\mathbf{0} = f(\overline{\mu}) - \overline{\xi} \tag{5.21c}$$

$$\mathbf{0} = -E^T(h(\overline{x}) - \overline{y}) - (g(\overline{\theta}) - \overline{\phi}) \tag{5.21d}$$

$$\mathbf{0} = (g(\overline{\theta}) - \overline{\phi}) - QL^{com}(Q\overline{\phi} + r). \tag{5.21e}$$

We will now show that under Assumptions 5.1–5.15 there exists at least one solution to (5.21) and all solutions (5.21) satisfy the control objectives.

Lemma 5.17 (Fulfilment of Objectives 1 and 2)**.** *Let Assumptions 5.1–5.15 hold. Then, there exists an equilibrium $(\overline{x}, \overline{\mu}, \overline{\xi}, \overline{\theta}, \overline{\phi})$ of system (5.20). Moreover, any equilibrium is such that $h(\overline{x}) = \overline{y}$ and $g(\overline{\theta}) = \overline{u}$, where $\overline{u}$ is the optimal control input given by (5.7).*

Proof. To prove the statement, we first show that at least one equilibrium of system (5.20) exists. Since the graph is connected, due to Assumption 5.1, it follows that $\mathrm{Im}(B) = \ker(B^T)^\perp = \mathrm{span}(\mathbb{1})^\perp$. Moreover, by definition of $\overline{u}$ as in (5.7) and Assumption 5.2, we have that

$$\mathbb{1}_n^T(E\overline{u} - d) = 0, \tag{5.22}$$

and it therefore follows that $(E\overline{u} - d) \in \mathrm{Im}(B)$. For this reason

$$\overline{\lambda} = B^\dagger(E\overline{u} - d) + (I - B^\dagger B)\omega, \tag{5.23}$$

is a solution to

$$-B\overline{\lambda} + E\overline{u} - d = \mathbf{0}, \tag{5.24}$$

for any $\omega \in \mathbb{R}^m$. By Assumption 5.15 there exists at least one ω such that $\overline{\lambda} \in \mathcal{R}(f_k)$ ensuring that $\overline{\mu} = f^{-1}(\overline{\lambda})$. Moreover, again by Assumption 5.15 there exists a $\overline{\theta} = g^{-1}(\overline{u})$ and by Assumption 5.5 it follows that there exists a $\overline{x} = h^{-1}(\overline{y})$. Defining $\overline{\xi} = \overline{\lambda}$ and $\overline{\phi} = \overline{u}$, shows that there exists a state $(\overline{x}, \overline{\mu}, \overline{\xi}, \overline{\theta}, \overline{\phi})$ that satisfies the equation (5.21) and is therefore an equilibrium of (5.20).

Next we show that any equilibrium $(\overline{x}, \overline{\mu}, \overline{\xi}, \overline{\theta}, \overline{\phi})$ necessarily satisfies $h(\overline{x}) = \overline{y}$ and $g(\overline{\theta}) = \overline{u}$, where $\overline{u}$ is the optimal control input given by (5.7). From (5.21c), $\overline{\xi} = f(\overline{\mu})$ holds and we will show that this implies that necessarily $h(\overline{x}) = \overline{y}$. By (5.21e), bearing in mind that L^{com} is the Laplacian of a balanced and strongly connected graph, due to Assumption 5.12 it follows from Lemma 5.13 that $\mathbb{1}_p^T Q^{-1}(g(\overline{\theta}) - \overline{\phi}) = 0$. This, together with (5.21d), implies that $\mathbb{1}_p^T Q^{-1} E^T (h(\overline{x}) - \overline{y}) = 0$. By (5.21b) and $\overline{\xi} = f(\overline{\mu})$, we also have $B^T(h(\overline{x}) - \overline{y}) = \mathbf{0}$. Hence,

$$\begin{pmatrix} \mathbb{1}_p^T Q^{-1} E^T \\ B^T \end{pmatrix} (h(\overline{x}) - \overline{y}) = \mathbf{0}. \tag{5.25}$$

We now prove that the matrix above has full-column rank. Suppose, *ad absurdum*, that there exists $v \neq \mathbf{0}$ such that

$$\begin{pmatrix} \mathbb{1}_p^T Q^{-1} E^T \\ B^T \end{pmatrix} v = \mathbf{0}. \tag{5.26}$$

By Assumption 5.1 it follows that $v = \mathbb{1}_n v_*$ with v_* a scalar. Then $\mathbb{1}_p^T Q^{-1} E^T \mathbb{1}_n v_* = 0$, which is, by definition of E in (5.2) and Assumption 5.2, equivalent to $\mathbb{1}_p^T Q^{-1} \mathbb{1}_p v_* = 0$ and implies that $v_* = 0$, contradicting that $v = \mathbb{1}_n v^* \neq \mathbf{0}$. Hence, necessarily $h(\overline{x}) - \overline{y} = \mathbf{0}$ and by strict monotonicity of $h(\cdot)$, we must have that $\overline{x} = h^{-1}(\overline{y})$.

Since $h(x) = \overline{y}$, it follows from (5.21d) that $g(\overline{\theta}) = \overline{\phi}$, and by strict monotonicity of $g(\theta)$, that $\overline{\theta} = g^{-1}(\overline{\phi})$. Moreover, from (5.21e) we obtain that $L^{com}(Q\overline{\phi} + r) = \mathbf{0}$ and since the communication graph is strongly connected due to Assumption 5.12, we have that $Q\overline{\phi} + r \in \mathrm{Im}(\mathbb{1}_p)$. Since $\mathbb{1}_n^T B = \mathbf{0}$, we obtain from (5.21a) that $\mathbb{1}_n^T (Eg(\overline{\theta}) - d) = 0$. Bearing in mind that $\overline{u}$ satisfies $Q\overline{u} + r \in \mathrm{Im}(\mathbb{1}_p)$ and $\mathbb{1}_n^T (E\overline{u} - d) = 0$, we have consequently that $g(\overline{\theta}) = \overline{\phi} = \overline{u}$, with $\overline{u}$ as in (5.7).

■

As a consequence of Lemma 5.17 we have that if Assumptions 5.1–5.15 hold, system

(5.20) is equivalent to

$$\begin{aligned} T_x\dot{x} &= -B(f(\mu) - f(\overline{\mu})) + E(g(\theta) - g(\overline{\theta})) \\ T_\mu\dot{\mu} &= B^T(h(x) - h(\overline{x})) - ((f(\mu) - f(\overline{\mu})) - (\xi - \overline{\xi})) \end{aligned} \tag{5.27a}$$

$$\begin{aligned} T_\xi\dot{\xi} &= (f(\mu) - f(\overline{\mu})) - (\xi - \overline{\xi}) \\ T_\theta\dot{\theta} &= -E^T(h(x) - h(\overline{x})) - (g(\theta) - g(\overline{\theta})) + (\phi - \overline{\phi}) \\ T_\phi\dot{\phi} &= (g(\theta) - g(\overline{\theta})) - (\phi - \overline{\phi}) - QL^{com}Q(\phi - \overline{\phi}), \end{aligned} \tag{5.27b}$$

a form that will be exploited in the stability analysis.

5.3 Stability analysis of the closed loop system

In this section we analyze the stability of the closed-loop system (5.20). The analysis is foremost based on LaSalle's invariance principle and exploits useful properties of interconnected incrementally passive systems. To facilitate the discussion, we first recall the following definition:

Definition 5.18 (Incremental passivity)**.** *System*

$$\begin{aligned} \dot{x} &= f(x, u) \\ y &= h(x), \end{aligned} \tag{5.28}$$

with $x \in \mathcal{X}$, $\mathcal{X}$ the state space and $u, y \in \mathbb{R}^n$, is incrementally passive[3] *with respect to a constant triplet $(\overline{x}, \overline{u}, \overline{y})$ satisfying*

$$\begin{aligned} \mathbf{0} &= f(\overline{x}, \overline{u}) \\ \overline{y} &= h(\overline{x}), \end{aligned} \tag{5.29}$$

if there exists a continuously differentiable and radially unbounded function $V(x, \overline{x}) : \mathcal{X} \to \mathbb{R}$, such that for all $x \in \mathcal{X}$, $u \in \mathbb{R}^m$ and $y = h(x)$, $\overline{y} = h(\overline{x})$

$$\dot{V}(x, u, \overline{x}, \overline{u}) = \frac{\partial V}{\partial x} f(x, u) + \frac{\partial V}{\partial \overline{x}} f(\overline{x}, \overline{u}) \leq (y - \overline{y})^T (u - \overline{u}). \tag{5.30}$$

We now proceed with establishing the incremental passivity property of (5.20a), that is the proposed flow controller (5.15) renders the network dynamics (5.1) incrementally passive with respect to the input $Eg(\theta)$ and output $h(x)$.

[3] The definition of incremental passivity property holds with respect to any solution (Pavlov and Marconi 2008). However, with some abuse of terminology, we state the incremental passivity property with respect to a steady state solution. This is also referred to as *shifted passivity* (van der Schaft 2012).

Lemma 5.19 (Incremental passivity of (5.20a))**.** *Let Assumptions 5.1–5.15 hold. System (5.20a) with input $Eg(\theta)$ and output $h(x)$ is incrementally passive with respect to the constant $(\overline{x}, \overline{\mu}, \overline{\xi})$ satisfying (5.21a)-(5.21c). Namely, the radially unbounded storage function $V_1(x, \overline{x}, \mu, \overline{\mu}, \xi, \overline{\xi})$ satisfies*

$$\dot{V}_1(x, \overline{x}, \mu, \overline{\mu}, \xi, \overline{\xi}) = (h(x) - h(\overline{x}))^T E(g(\theta) - g(\overline{\theta})) - (f(\mu) - \xi)^T (f(\mu) - \xi), \tag{5.31}$$

along the solutions to (5.20a).

Proof. Consider the storage function

$$\begin{aligned} V_1(x, \overline{x}, \mu, \overline{\mu}, \xi, \overline{\xi}) = &\sum_{i \in \mathcal{V}} T_{x_i} \int_{\overline{x}_i}^{x_i} h_i(y) - h_i(\overline{x}_i) dy + \sum_{k \in \mathcal{E}} T_{\mu_k} \int_{\overline{\mu}_k}^{\mu_k} f_k(y) - f_k(\overline{\mu}_k) dy \\ &+ \frac{1}{2} (\xi - \overline{\xi})^T T_\xi (\xi - \overline{\xi}). \end{aligned} \tag{5.32}$$

Since $h_i(x_i)$ and $f_k(\mu_k)$ are strictly increasing functions, the incremental storage function $V_1(x, \overline{x}, \mu, \overline{\mu}, \xi, \overline{\xi})$ is radially unbounded. Furthermore, $V_1(x, \overline{x}, \mu, \overline{\mu}, \xi, \overline{\xi})$ satisfies along the solutions to (5.20a), or equivalently along the solutions to (5.27a),

$$\begin{aligned} \dot{V}_1(x, \overline{x}, \mu, \overline{\mu}, \xi, \overline{\xi}) &= (h(x) - h(\overline{x}))^T T_x \dot{x} + (\xi - \overline{\xi})^T T_\xi \dot{\xi} + (f(\mu) - f(\overline{\mu}))^T T_\mu \dot{\mu} \\ &= (h(x) - h(\overline{x}))^T E(g(\theta) - g(\overline{\theta})) \\ &\quad - ((f(\mu) - f(\overline{\mu})) - (\xi - \overline{\xi}))^T ((f(\mu) - f(\overline{\mu})) - (\xi - \overline{\xi})), \end{aligned} \tag{5.33}$$

and since $f(\overline{\mu}) = \overline{\xi}$, $V_1(x, \overline{x}, \mu, \overline{\mu}, \xi, \overline{\xi})$ indeed satisfies (5.31) along the solutions to (5.20a). ∎

We now prove a similar result for (5.20b), that is the controller (5.16) is incrementally passive with respect to the input $-h(x)$ and output $Eg(\theta)$.

Lemma 5.20 (Incremental passivity of (5.20b))**.** *Let Assumptions 5.1–5.15 hold. System (5.20b) with input $-h(x)$ and output $Eg(\theta)$ is incrementally passive with respect to $(\overline{\theta}, \overline{\phi})$ satisfying (5.21d)-(5.21e). Namely, the radially unbounded storage function $V_2(\theta, \overline{\theta}, \phi, \overline{\phi})$ satisfies*

$$\begin{aligned} \dot{V}_2(\theta, \overline{\theta}, \phi, \overline{\phi}) = &- (g(\theta) - \phi)^T (g(\theta) - \phi) - (\phi - \overline{\phi})^T Q L^{com} Q (\phi - \overline{\phi}) \\ &- (g(\theta) - g(\overline{\theta}))^T E^T (h(x) - h(\overline{x})), \end{aligned} \tag{5.34}$$

along the solutions to (5.20b).

Proof. Consider the storage function

$$V_2(\theta,\overline{\theta},\phi,\overline{\phi}) = \sum_{i\in\mathcal{V}} T_{\theta_i}\int_{\overline{\theta}_i}^{\theta_i} g_i(y) - g_i(\overline{\theta}_i)dy + \frac{1}{2}(\phi-\overline{\phi})^T T_\phi(\phi-\overline{\phi}). \tag{5.35}$$

Note that since $g_i(\theta_i)$ is a strictly increasing function, the incremental storage function $V_2(\theta,\overline{\theta},\phi,\overline{\phi})$ is radially unbounded. Furthermore, $V_2(\theta,\overline{\theta},\phi,\overline{\phi})$ satisfies along the solutions to (5.20b), or equivalently along the solutions to (5.27b),

$$\begin{aligned}
\dot{V}_2(\theta,\overline{\theta},\phi,\overline{\phi}) &= (g(\theta)-g(\overline{\theta}))^T T_\theta\dot{\theta} + (\phi-\overline{\phi})^T T_\phi\dot{\phi}\\
&= (g(\theta)-g(\overline{\theta}))^T\cdot\Big(-(g(\theta)-g(\overline{\theta})) + (\phi-\overline{\phi}) - E^T(h(x)-\overline{y})\Big)\\
&\quad + (\phi-\overline{\phi})^T(-(\phi-\overline{\phi}) + (g(\theta)-g(\overline{\theta})) - QL^{com}Q(\phi-\overline{\phi}))\\
&= -(g(\theta)-g(\overline{\theta}))^T(g(\theta)-g(\overline{\theta})) + 2(g(\theta)-g(\overline{\theta}))^T(\phi-\overline{\phi})\\
&\quad - (\phi-\overline{\phi})^T(\phi-\overline{\phi}) - (\phi-\overline{\phi})^T QL^{com}Q(\phi-\overline{\phi})\\
&\quad - (g(\theta)-g(\overline{\theta}))^T E^T(h(x)-\overline{y}),
\end{aligned} \tag{5.36}$$

Since $g(\overline{\theta}) = \overline{\phi}$, $V_2(\theta,\overline{\theta},\phi,\overline{\phi})$ indeed satisfies (5.34) along the solutions to (5.20b). ∎

Exploiting the previous lemmas, we are now ready to prove the main result of this chapter.

Theorem 5.21 (Solving Problem 5.10 for dynamics (5.1))**.** *Let Assumptions 5.1–5.16 hold. The solutions of system (5.1), in closed loop with (5.15) and (5.16), globally approaches the set*

$$\Upsilon_1 = \left\{ x,\mu,\xi,\theta,\phi \;\middle|\; \begin{array}{l} B(f(\mu)-f(\overline{\mu})) = \mathbf{0},\ B(\xi-\overline{\xi}) = \mathbf{0},\\ x=\overline{x},\ \theta=\overline{\theta},\ \phi=\overline{\phi}\end{array} \right\}, \tag{5.37}$$

where $\lambda = f(\mu)$ is a constant, $h(x) = \overline{y}$ and where $u = g(\theta) = \overline{u}$, with $\overline{u}$ the optimal input given by (5.7). Moreover, $u = g(\theta)$ and $\lambda = f(\mu)$ satisfy constraints (5.9) and (5.10) for all $t \geq 0$. Therefore, controllers (5.15) and (5.16) solve Problem 5.10 for the flow network (5.1).

Proof. Satisfying constraints (5.9) and (5.10) for all $t \geq 0$ follows from the design of $g(\theta)$ and $f(\mu)$ and Assumption 5.16. Let

$$V(x,\overline{x},\mu,\overline{\mu},\xi,\overline{\xi},\theta,\overline{\theta},\phi,\overline{\phi}) = V_1(x,\overline{x},\mu,\overline{\mu},\xi,\overline{\xi}) + V_2(\theta,\overline{\theta},\phi,\overline{\phi}), \tag{5.38}$$

with $V_1(x,\overline{x},\mu,\overline{\mu},\xi,\overline{\xi})$ and $V_2(\theta,\overline{\theta},\phi,\overline{\phi})$ given in Lemma 5.19 and Lemma 5.20, respecti-

vely. Consequently, $V(\cdot)$ satisfies

$$\begin{aligned}\dot{V}(x,\overline{x},\mu,\overline{\mu},\xi,\overline{\xi},\theta,\overline{\theta},\phi,\overline{\phi}) = &-(\phi-\overline{\phi})^T QL^{com}Q(\phi-\overline{\phi}) - (g(\theta)-\phi)^T(g(\theta)-\phi)\\ &-(f(\mu)-\xi)^T(f(\mu)-\xi),\end{aligned} \tag{5.39}$$

along the solutions to (5.20). From (5.39) and Lemma 5.13 we have that $\dot{V}(\cdot) \leq 0$ and since $V(\cdot)$ is radially unbounded, the solutions to (5.20) approach the largest invariant set contained entirely in the set $\mathcal{S}_1$, where $\dot{V}(\cdot) = 0$. This set is characterized by

$$\mathcal{S}_1 = \left\{x,\mu,\xi,\theta,\phi \,\middle|\, \phi = g(\theta),\, \xi = f(\mu),\, Q(\phi-\overline{\phi}) \in \mathrm{Im}(\mathbb{1}) \right\}, \tag{5.40}$$

where $Q(\phi+\overline{\phi}) \in \mathrm{Im}(\mathbb{1}_p)$ follows from Lemma 5.13. It follows that the dynamics of system (5.20) on the set $\mathcal{S}_1$ satisfy

$$T_x\dot{x} = -B(f(\mu)-f(\overline{\mu})) + E(\phi-\overline{\phi}) \tag{5.41a}$$
$$T_\mu\dot{\mu} = B^T(h(x)-h(\overline{x})) \tag{5.41b}$$
$$T_\xi\dot{\xi} = \mathbf{0} \tag{5.41c}$$
$$T_\theta\dot{\theta} = -E^T(h(x)-h(\overline{x})) \tag{5.41d}$$
$$T_\phi\dot{\phi} = \mathbf{0}. \tag{5.41e}$$

Due to (5.40), (5.41c) and (5.41e) we have that

$$\dot{\mu} = \left(\frac{\partial f(\mu)}{\partial \mu}\right)^{-1}\dot{\xi} = \mathbf{0} \tag{5.42}$$
$$\dot{\theta} = \left(\frac{\partial g(\theta)}{\partial \theta}\right)^{-1}\dot{\phi} = \mathbf{0}, \tag{5.43}$$

where we note that $\frac{\partial f(\mu)}{\partial \mu} \neq \mathbf{0}$ and $\frac{\partial g(\theta)}{\partial \theta} \neq \mathbf{0}$. It follows now from (5.41b), (5.41d), (5.42) and (5.43) that

$$\begin{pmatrix} B^T \\ -E^T \end{pmatrix}(h(x)-h(\overline{x})) = \mathbf{0}. \tag{5.44}$$

From Lemma 2.8 we know that $\begin{pmatrix} B & -E \end{pmatrix}^T$ has full column rank and therefore has a left inverse. As a result, we have that necessarily $h(x) - h(\overline{x}) = \mathbf{0}$, *i.e.* $h(x) = \overline{y}$. By strict monotonicity of $h(x)$, it follows that on the invariant set $x = \overline{x}$ and that $\dot{x} = \mathbf{0}$. Premultiplying both sides of (5.41a) by $\mathbb{1}_p^T$, yields $0 = \mathbb{1}_p^T(\phi-\overline{\phi})$ and since $Q(\phi-\overline{\phi}) \in \mathrm{Im}(\mathbb{1}_p)$, where Q is a diagonal matrix with only strictly positive entries, it follows that on the set where $\dot{V} = 0$ necessarily $\phi = \overline{\phi}$. From (5.40) and (5.41a) it therefore follows that $B(f(\mu) - f(\overline{\mu})) = \mathbf{0}$ and $B(\xi - \overline{\xi}) = \mathbf{0}$. Moreover, since on the set $\mathcal{S}_1$, $\phi = g(\theta)$

and $\overline{\phi} = g(\overline{\theta})$, we also have that $g(\theta) = g(\overline{\theta}) = \overline{u}$ (see also Lemma 5.17). Consequently, system (5.20) indeed approaches the set where $h(x) = \overline{y}$ and where $u = g(\theta) = g(\overline{\theta}) = \overline{u}$, with $\overline{u}$ the optimal input given by (5.7).

Note that the incremental storage function $V(\cdot)$ can be defined with respect to any equilibrium in Υ_1, and since $\dot{V}(\cdot) \leq 0$, every point in $\mathcal{Q}_1$ is a Lyapunov stable equilibrium of system (5.20). Consequently, every positive limit set associated with any solution to system (5.20) contains a Lyapunov stable equilibrium. It then follows by (Haddad and Chellaboina 2008, Proposition 4.7)[4] that this positive limit set is a singleton, which proves convergence to a point. Therefore, the system (5.20) approaches the set where μ, ξ, and consequently λ, are constant. ■

Remark 5.22 (Uniqueness of μ)**.** *In the case that the graph $\mathcal{G}$ contains no cycles, i.e. the graph is a tree, then there exists a unique solution of μ to $B(f(\mu) - f(\overline{\mu})) = \mathbf{0}$.*

Remark 5.23 (Locally increasing mappings)**.** *Note that the global convergence result is a consequence of the strictly increasing behavior of the nonlinear functions $f_k(\mu_k)$, $g_i(\theta_i)$ and $h_i(x_i)$. In case the functions are increasing on a finite interval, a local result of Theorem 5.21 can be derived. An important class of functions for which this holds are functions that are not necessary increasing on the whole domain, such as sinusoidal functions.*

Remark 5.24 (Avoiding oscillations)**.** *In the proof of Theorem 5.21, we exploited the dynamics of the additional control variables ξ and ϕ to conclude that on the invariant set $\dot{\mu} = \dot{\theta} = \mathbf{0}$. It is natural to wonder if these additional controller states are essential to obtain the convergence result of Theorem 5.21. Therefore, we compare (5.15) and (5.16) with controllers of the form*

$$\begin{aligned} T_\mu \dot{\mu} &= B^T(h(x) - \overline{y}) \\ \lambda &= f(\mu) \end{aligned} \tag{5.45}$$

$$\begin{aligned} T_\theta \dot{\theta} &= -QL^{com}(Qg(\theta) + r) - (h(x) - \overline{y}) \\ u &= g(\theta), \end{aligned} \tag{5.46}$$

as both (5.15)-(5.16) and (5.45)-(5.46) admit a steady state where $h(\overline{x}) = \overline{y}$ and $g(\overline{\theta}) = \overline{u}$. However, in contrast to (5.20), for which we have proven global convergence to the

[4] See also the errata and addenda for the corrected version.

desired state, system

$$\begin{aligned} T_x\dot{x} &= -Bf(\mu) + Eg(\theta) - d \\ T_\mu\dot{\mu} &= B^T(h(x) - \overline{y}) \\ T_\theta\dot{\theta} &= -QL^{com}(Qg(\theta) + r) - (h(x) - \overline{y}), \end{aligned} \tag{5.47}$$

can converge (depending on Q) to a limit cycle exhibiting oscillatory behavior as has been shown in (Scholten et al. 2016b).

To illustrate this claim, consider the linear case, where $f(\mu) = \mu$, $g(\theta) = \theta$ and $h(x) = x$ with $E = I$. Introducing $\tilde{x} = x - \overline{x}$, $\tilde{\mu} = \mu - \overline{\mu}$, $\tilde{\theta} = \theta - \overline{\theta}$, and assuming $Q = \overline{q}I$ with $\overline{q} \in \mathbb{R}$, system (5.47) *results in*

$$\begin{pmatrix} \dot{\tilde{x}} \\ \dot{\tilde{\mu}} \\ \dot{\tilde{\theta}} \end{pmatrix} = \begin{pmatrix} \mathbf{0} & -B & I \\ B^T & \mathbf{0} & \mathbf{0} \\ -I & \mathbf{0} & -\overline{q}^2 L^{com} \end{pmatrix} \begin{pmatrix} \tilde{x} \\ \tilde{\mu} \\ \tilde{\theta} \end{pmatrix}. \tag{5.48}$$

It can be readily confirmed that the solution to (5.48), with initial conditions $\tilde{x}(0) = \mathbf{0}$, $\tilde{\mu}(0) = \mathbf{0}$ and $\tilde{\theta}(0) = \mathbb{1}_p$, is given by

$$\tilde{x}(t) = \mathbb{1}_p \sin(t) \tag{5.49}$$

$$\tilde{\theta}(t) = \mathbb{1}_p \cos(t) \tag{5.50}$$

$$\tilde{\mu}(t) = \mathbf{0}, \tag{5.51}$$

which indeed clearly exhibits oscillatory behavior.

5.4 Extensions and adjustments to the control problem

In the previous discussion we focussed on the design of dynamical flow controllers. On the other hand, flows in networks might follow from underlying physical principles that are not accurately described by (5.15). An important example is the case where the flow λ_k directly depends on the states x_i of its adjacent nodes. This is common in *e.g.* compartmental systems (see *e.g.* (Blanchini et al. 2016), (Bauso et al. 2013) and (Lee et al. 2017)). Another example is when a change of λ is induced by the dynamics of the system, instead of a controller that is up to design. We discuss in Subsection 5.4.2 an important example where the flow dynamics are induced by 'potential differences'. First we discuss how certain compartmental systems fit within the presented setting.

5.4.1 Additional links without a control input

Model (5.1) shows big similarities with those in compartmental systems (see (Blanchini et al. 2016)). Therefore, it is natural to wonder how these models are related. Compared to (5.1), compartmental systems have additional dynamics that model state dependent inflows, outflows and flows between nodes. In this section we incorporate such dynamics in our framework by augmenting (5.1), resulting in

$$T_x \dot{x} = \Psi(x) - B\lambda + Eu - d \tag{5.52a}$$

$$y = h(x), \tag{5.52b}$$

where

$$\Psi(x) = -B_c \gamma(B_c^T h(x)) - E_c \eta(E_c^T h(x)). \tag{5.53}$$

Here, B_c[5] is the incidence matrix of a (not necessarily connected) graph $\mathcal{G}_c = (\mathcal{V}, \mathcal{E}_c)$. Moreover, the set of nodes that have a state dependent inflow/outflow is given by $\mathcal{V}_c \subseteq \mathcal{V}$, with cardinality $p_c := |\mathcal{V}_c|$. Matrix $E_c \in \mathbb{R}^{n \times p_c}$ models the p_c state dependent inflows/outflows and its entries are defined as

$$(e_c)_{ik} = \begin{cases} 1 & \text{if the } k\text{-th flow is located at node } i \\ 0 & \text{otherwise.} \end{cases}$$

Let $l := |\mathcal{E}_c|$. The mapping $\gamma(B_c^T h(x)) : \mathbb{R}^l \to \mathbb{R}^l$ is given by $\gamma(B_c^T h(x)) = (\gamma_1(a_1) \dots \gamma_l(a_l))^T$, with $a_k = [B_c^T h(x)]_k$ and $\gamma_k(a_k)$ is increasing and continuously differentiable for all $k \in \mathcal{E}_S$. The mapping $\eta(E_c^T h(x)) : \mathbb{R}^{e_c} \to \mathbb{R}^{e_c}$ is given by $\eta(E_c^T h(x)) = (\eta_1(b_1) \dots \eta_{e_c}(b_{e_c}))^T$, with $b_i = [E_c^T h(x)]_i$ and $\eta_i(b_i)$ is increasing and continuously differentiable for all $i \in \mathcal{V}_c$.

Remark 5.25 (Interpretation of $\Psi(x)$)**.** *In compartmental systems the flow between two nodes can be proportional to a potential difference between two nodes. Moreover, inflows and outflows from the system are often considered proportional to the potential at the corresponding node. The additional term $\Psi(x)$ in (5.52) models these dynamical effects. More specifically, $B_c \gamma(B_c^T h(x))$ models the former dynamics and $E_c \eta(E_c^T h(x))$ the latter. Note that (5.52) models a compartmental system with additional actuated edges (flows controlled by a pump) and actuated inputs (production or injection). The actuation allows us to achieve output regulation and an optimal coordination among the inputs at the nodes while previously only asymptotic stability with respect to an arbitrary steady*

[5] B_c is introduced with some abuse of notation. In Chapter 4 it was used to denote the incidence matrix of the communication network, while in this section it refers to the incidence matrix of the network that models the unactuated flows.

state was considered (see e.g. (Blanchini et al. 2016) and (Como 2017)). In (Blanchini et al. 2016) flows between two nodes are considered that are proportional to a potential at a single node (for example the outflow of a reservoir due to gravity). We do not consider these dynamics in this chapter and leave the stability analysis in that setting as future work.

The optimal control allocation problem (2.36) for the considered dynamics (5.52) becomes

$$\begin{aligned} \underset{u,\lambda}{\text{minimize}} \quad & C(u) \\ \text{subject to} \quad & \mathbf{0} = \Psi(\overline{x}) - B\lambda + Eu - d. \end{aligned} \tag{5.54}$$

Similar to Lemma 2.17, the following can be immediately shown:

Lemma 5.26 (Solution to optimization problem (5.54))**.** *The solution to (5.54) is given by*

$$\hat{u} = Q^{-1}(\hat{\kappa} - r), \tag{5.55}$$

where

$$\hat{\kappa} = E^T \frac{\mathbb{1}_n \mathbb{1}_n^T}{\mathbb{1}_p^T Q^{-1} \mathbb{1}_p} (\hat{d} + EQ^{-1} r), \tag{5.56}$$

and $\hat{d} = d + E_c \eta(E_c^T h(\overline{x}))$.

Proof. The proof follows similar arguments as the proof of Lemma 2.17. We introduce the Lagrangian

$$L(u, \zeta) = C(u) + \zeta(\Psi(\overline{x}) - B\lambda + Eu - d), \tag{5.57}$$

where $\zeta \in \mathbb{R}$ is the Lagrange multiplier. The saddle point $(\overline{u}, \overline{\zeta})$, which corresponds to the solution of $\max_\zeta \min_u L(u, \zeta)$, satisfies

$$\begin{aligned} \mathbf{0} &= \nabla C(\overline{u}) + \mathbb{1}_p \overline{\zeta} \\ \mathbf{0} &= \Psi(\overline{x}) - B\lambda + E\overline{u} - d. \end{aligned} \tag{5.58}$$

For this reason and by definition of $\Psi(x)$ as in (5.53) it follows that

$$\mathbb{1}_p^T \overline{u} = \mathbb{1}_n^T (d - E_c \eta(E_c^T h(\overline{x}))) = \mathbb{1}_n^T \hat{d}, \tag{5.59}$$

as $\mathbb{1}_p^T B_c \gamma(B_c^T h(x)) = 0$. It follows by the same argumentation as in the proof of Lemma 2.17 that (5.55) is satisfied. ∎

Assumption 5.27 (Properties of f and g revisited)**.** *Functions f_k and g_i, in respectively (5.15) and (5.16), are continuously differentiable and strictly increasing. Moreover, let $\hat{u}$*

be as in (5.55), then f_k is such that there exists a $\omega \in \mathbb{R}^m$ where $[B^\dagger(\Psi(h(\overline{x})) + E\hat{u} - d) + (I - B^\dagger B)\omega]_k \in \mathcal{R}(f_k)$ for all $k \in \mathcal{E}$, and g_i satisfies $\hat{u}_i \in \mathcal{R}(g_i)$ for all $i \in \mathcal{V}_e$.

Theorem 5.28 (Solving Problem 5.10 for dynamics (5.52))**.** *Let Assumptions 5.1–5.12 and 5.16–5.27 hold. The solutions of system (5.52), in closed loop with (5.15) and (5.16), converge globally to a point in the set*

$$\Upsilon_2 = \left\{ x, \mu, \xi, \theta, \phi \;\middle|\; \begin{array}{l} B(f(\mu) - f(\overline{\mu})) = \mathbf{0},\ B(\xi - \overline{\xi}) = \mathbf{0}, \\ x = \overline{x},\ \theta = \overline{\theta},\ \phi = \overline{\phi} \end{array} \right\}, \tag{5.60}$$

where $\lambda = f(\mu)$ is a constant, $h(x) = \overline{y}$ and $u = g(\theta) = \hat{u}$, with $\hat{u}$ given by (5.55). Moreover, $u = g(\theta)$ and $\lambda = f(\mu)$ satisfy constraints (5.9) and (5.10) for all $t \geq 0$. Therefore, controllers (5.15) and (5.16) solve Problem 5.10 for the flow network (5.52).

Proof. First, the fulfilment of the the constraints (5.9) and (5.10) for all $t \geq 0$ is guaranteed by the design of the controllers. Second, similar to Lemma 5.17 Assumptions 5.1–5.12 and 5.27 guarantee that a steady state exists and all steady states satisfy $h(x) = \overline{y}$ and $u = g(\theta) = \hat{u}$, with $\hat{u}$ given by (5.55). Third, a straightforward adjustment of the arguments of Theorem 5.21 shows that the same incremental storage function (5.38), used in Theorem 5.21, now satisfies

$$\begin{aligned} \dot{V}(\cdot) = (h(x) - h(\overline{x}))^T(\Psi(x) - \Psi(\overline{x})) - (\phi - \overline{\phi})^T Q L^{com} Q(\phi - \overline{\phi}) \\ - (g(\theta) - \phi)^T(g(\theta) - \phi) - (f(\mu) - \xi)^T(f(\mu) - \xi), \end{aligned} \tag{5.61}$$

along the solutions to (5.52) in closed loop with (5.15) and (5.16). We continue by showing that the additional term in $\dot{V}(\cdot)$ (comparing with the expression of $\dot{V}(\cdot)$ in (5.39)) satisfies

$$(h(x) - h(\overline{x}))^T(\Psi(x) - \Psi(\overline{x})) \leq 0. \tag{5.62}$$

Next we use Hadamard's lemma which states that for any smooth, real-valued function $f : \mathbb{R}^n \to \mathbb{R}^n$ it holds that

$$f(x) = f(a) + \sum_{i=1}^{n} (x_i - a_i) \int_0^1 \frac{\partial f}{\partial x_i}(a + t(x - a))\, dt, \tag{5.63}$$

with $a = (a_1, ..., a_n)$, and $x = (x_1, ..., x_n)$. It follows that

$$\begin{aligned}(h(x) - h(\overline{x}))^T(\Psi(x) - \Psi(\overline{x})) = & -(h(x) - h(\overline{x}))^T B_c(\gamma(B_c^T h(x)) - \gamma(B_c^T h(\overline{x})) \\ & -(h(x) - h(\overline{x}))^T E_c(\eta(E_c^T h(x)) - \eta(E_c^T h(\overline{x}))) \\ = & -(h(x) - h(\overline{x}))^T B_c \Gamma^b(x) B_c^T (h(x) - h(\overline{x})) \\ & -(h(x) - h(\overline{x}))^T E_c \Gamma^e(x) E_c^T (h(x) - h(\overline{x})) \leq 0,\end{aligned}$$

where $\Gamma^b(x)$ and $\Gamma^e(x)$ are diagonal matrices with entries

$$\Gamma^b_{kk}(x) = \int_0^1 \left.\frac{\partial \gamma_k(y_k)}{\partial y_k}\right|_{y_k = \tau(\chi_k^b(x) - \chi_k^b(\overline{x})) + \chi_k^b(\overline{x})} d\tau \tag{5.64}$$

$$\Gamma^e_{ii}(x) = \int_0^1 \left.\frac{\partial \eta_i(y_i)}{\partial y_i}\right|_{y_i = \tau(\chi_i^e(x) - \chi_i^e(\overline{x})) + \chi_i^e(\overline{x})} d\tau, \tag{5.65}$$

with $\chi_k^b(x) = [B_c^T h(x)]_k$ and $\chi_i^e(x) = [E_c^T h(x)]_i$. In fact, since $\gamma_k(\cdot)$ and $\eta_i(\cdot)$ are increasing functions for all $k \in \mathcal{E}_c$ and all $i \in \mathcal{V}_c$ it follows that that $\Gamma^b_{kk}(x), \Gamma^e_{ii}(x) \geq 0$ for any x. Therefore, $V(\cdot)$ satisfies

$$\begin{aligned}\dot{V}(\cdot) \leq & -(\phi - \overline{\phi})^T Q L^{com} Q(\phi - \overline{\phi}) - (g(\theta) - \phi)^T (g(\theta) - \phi) \\ & -(f(\mu) - \xi)^T (f(\mu) - \xi),\end{aligned} \tag{5.66}$$

along the solutions to (5.52) in closed loop with (5.15) and (5.16). Note that expression (5.66) is identical to (5.39), that is used to prove Theorem 5.21. Similar to that proof we can argue that $x = \overline{x}$, by exploiting the relations (5.41b) – (5.41e). Therefore, on the invariant set where $\dot{V}(\cdot) = 0$,

$$T_x \dot{x} = \Psi(x) - \Psi(\overline{x}) - B(f(\mu) - f(\overline{\mu})) + E(\phi - \overline{\phi}), \tag{5.67}$$

reduces to (5.41a), such that system (5.52) in closed loop with (5.15) and (5.16), is on the invariant set identical to (5.41). From here, the proof follows the same steps as the proof of Theorem 5.21. ■

5.4.2 Potential induced flows on the links

While in Section 5.2.1 the dynamics for the flows on the edges were up to design we consider in this subsection that they are given by the following expression:

$$\begin{aligned}T_\mu \dot{\mu} &= B^T(h(x) - \overline{y}) \\ \lambda &= f(\mu).\end{aligned} \tag{5.68}$$

This is motivated by networks in which the flow dynamics are induced by physics such as the behaviour of inductive lines in an electric network (see the case study on a multi-terminal high voltage direct current network in Subsection 5.5.2). In such networks $h(x) - \bar{y}$ denotes the potential at the nodes, μ the state variable at the link and λ the flow on the link as a result of a possible difference in potential. Similar dynamics as (5.68) have been studied in the context of networked systems in *e.g.* (van der Schaft and Wei 2012), (Bürger et al. 2014) and (Bürger et al. 2015). Note however that none of these studies included the controllers at the nodes as in (5.16) which is included in the analysis here.

The dynamics (5.68) coincide with (5.15), if one neglects the terms depending on the now missing state ξ. In fact, (5.68) can generate the same steady state output as (5.15) and also shares an incremental passivity property. However, as we pointed out in Remark 5.24, the state ξ is essential to derive the convergence result in Theorem 5.21. On the other hand, by carefully selecting nodes that have a controllable external input, the controllers (5.16) and (5.68) still solve Problem 5.10 for the flow network (5.1). This choice is based on the notion of a zero forcing set (see *e.g.*, (Hogben 2010), (Monshizadeh et al. 2014)), which we review next. Consider the graph $\mathcal{G}$ and let us initially color each of its nodes either black or white. The color of the nodes then changes according to the following coloring rule:

Graph coloring rule *If node i is colored black and has exactly one neighbor j which is white, then the color of node j is changed to black.*

Let $\mathcal{V}_0 \subseteq \mathcal{V}$ be the set of nodes which are initially colored black, while the remaining ones are white, and let $C(\mathcal{V}_0)$ be the set of black node obtained by applying the color changing rule until no more changes are possible. A zero forcing set is then defined as:

Definition 5.29 (Zero forcing set)**.** *If $\mathcal{V}_z \subseteq \mathcal{V}$ satisfies $C(\mathcal{V}_0) = \mathcal{V}$ then $\mathcal{V}_z$ is a zero forcing set for $\mathcal{G}$.*

We now make a connection between a zero forcing set and the set $\mathcal{V}_e$ of nodes that have actuation (*i.e.,* all nodes that correspond to the rows of E that contain a non-zero entry).

Assumption 5.30 ($\mathcal{V}_e$ is a zero forcing set)**.** *The set $\mathcal{V}_e$ is a zero forcing set for $\mathcal{G}$.*

An example of a zero forcing set is provided in Figure 5.2, where the black nodes form a zero forcing set for the physical network. We are now ready to state the second result of this section.

Theorem 5.31 (Solving Problem 5.10 with dynamics (5.68))**.** *Let Assumptions 5.1–5.16 and 5.30 hold. The solutions of system (5.1), in closed loop with the controllers (5.16)*

and (5.68), globally approaches the set

$$\Upsilon_3 = \left\{ x, \mu, \theta, \phi \,\middle|\, B(f(\mu) - f(\overline{\mu})) = \mathbf{0},\ x = \overline{x},\ \theta = \overline{\theta},\ \phi = \overline{\phi} \right\}, \tag{5.69}$$

where $\lambda = f(\mu)$ is a constant, $h(x) = \overline{y}$ and where $u = g(\theta) = \overline{u}$, with $\overline{u}$ given by (5.7). Moreover, $u = g(\theta)$ and $\lambda = f(\mu)$ satisfy constraints (5.9) and (5.10) for all $t \geq 0$. Therefore, controllers (5.16) and (5.68) solve Problem 5.10 for system (5.1).

Proof. Following the argumentation of the proof of Theorem 5.21, using the same incremental storage function (5.38), allows us to conclude that the solutions to the system (5.1), (5.16), (5.68) approach the largest invariant set contained in the set where $\dot{V}(\cdot) = 0$. This set where $\dot{V}(\cdot) = 0$ is characterized by

$$\mathcal{S}_3 = \left\{ x, \mu, \theta, \phi \,\middle|\, \phi = g(\theta), Q(\phi - \overline{\phi}) \in \mathrm{Im}(\mathbb{1}) \right\}. \tag{5.70}$$

System (5.1), (5.16), (5.68) satisfies on this set

$$T_x \dot{x} = -B(f(\mu) - f(\overline{\mu})) + E(\phi - \overline{\phi}) \tag{5.71a}$$

$$T_\mu \dot{\mu} = B^T (h(x) - h(\overline{x})) \tag{5.71b}$$

$$\mathbf{0} = -E^T (h(x) - h(\overline{x})) \tag{5.71c}$$

$$T_\phi \dot{\phi} = \mathbf{0}. \tag{5.71d}$$

We now prove by induction that $h_i(x_i) = h_i(\overline{x}_i)$ for all $i \in \mathcal{V}$. To this end, let us define the sequence of sets of nodes $\mathcal{V}_k \subseteq \mathcal{V}$, with $k \in \mathbb{N}_{\geq 0}$, having the properties:

(i) $\mathcal{V}_k$ is a zero forcing set;

(ii) on the largest invariant set for (5.1), (5.16), (5.68) contained in $\mathcal{S}_3$, it holds that $h_i(x_i) = h_i(\overline{x}_i)$ for all $i \in \mathcal{V}_k$.

Let the cardinality of $\mathcal{V}_k$ be denoted by n_k. In order to show that $h_i(x_i) = h_i(\overline{x}_i)$ for all $i \in \mathcal{V}$ we will prove that there exists an index $\overline{k}$ such that $n_{\overline{k}} = n$, where $\mathcal{V}_{\overline{k}}$ satisfies properties (*i*) and (*ii*). Recall that $|\mathcal{V}| = n$.

First, we note that Assumption 5.30 and (5.71c) imply that $\mathcal{V}_e$ satisfies properties (i) and (ii). For this reason, we can set $\mathcal{V}_0 = \mathcal{V}_e$ and $n_0 = p > 0$ that satisfies properties (i) and (ii). If $n_0 = n$, then $\overline{k} = 0$, otherwise $n_0 < n$ and we proceed as follows.

For a $k \in \mathbb{N}_{\geq 0}$, we consider a set of nodes $\mathcal{V}_k$ of cardinality n_k such that $0 < n_k < n$ and properties (i) and (ii) above are satisfied. We will show that this implies that there exists a set of nodes $\mathcal{V}_{k+1}$ that satisfies properties (i) and (ii) with $n_k < n_{k+1}$.

Let us define

$$B^{(k)} = \begin{pmatrix} B^{\mathcal{B}(k)} \\ B^{\mathcal{W}(k)} \end{pmatrix},$$

where the matrices $B^{\mathcal{B}(k)} \in \mathbb{R}^{n_k \times m}$ and $B^{\mathcal{W}(k)} \in \mathbb{R}^{(n-n_k)\times m}$ are obtained by collecting from B the rows indexed by $\mathcal{V}_k$ and $\mathcal{V}\backslash\mathcal{V}_k$ respectively. Note that $B^{(k)}$ is obtained from B by reordering of the rows and that $B^{\mathcal{B}(k)}$ are the rows of B corresponding to the black nodes and $B^{\mathcal{W}(k)}$ the ones corresponding to the white nodes. Similarly, for any vector $\chi \in \mathbb{R}^n$ let $\chi^{\mathcal{B}(k)} \in \mathbb{R}^{n_k}$ and $\chi^{\mathcal{W}(k)} \in \mathbb{R}^{n-n_k}$ be obtained by collecting from χ the elements indexed by $\mathcal{V}_k$ and $\mathcal{V}\backslash\mathcal{V}_k$ respectively. We note that by property (ii), on the largest invariant set, the set $\mathcal{V}_k$ fulfils $(h(x) - h(\overline{x}))^{\mathcal{B}(k)} = \mathbf{0}$, or more explicitly, $h_i(x_i) - h_i(\overline{x}_i) = 0$ for all $i \in \mathcal{V}_k$. By the strict monotonicity of $h_i(x_i)$, it follows that on the invariant set $x_i = \overline{x}_i$ for all $i \in \mathcal{V}_k$. Since $\frac{d}{dt}(\phi - \overline{\phi}) = \mathbf{0}$ due to (5.71d), by (5.71a) and (5.71b), on the invariant set we have that

$$T_x \begin{pmatrix} \mathbf{0} \\ \dot{x}^{\mathcal{W}(k)} \end{pmatrix} = -B^{(k)} \frac{\partial f(\mu)}{\partial \mu} B^{(k)^T} \begin{pmatrix} \mathbf{0} \\ (h(x) - h(\overline{x}))^{\mathcal{W}(k)} \end{pmatrix},$$

from which it follows that

$$\mathbf{0} = -B^{\mathcal{B}(k)} \frac{\partial f(\mu)}{\partial \mu} B^{\mathcal{W}(k)^T} (h(x) - h(\overline{x}))^{\mathcal{W}(k)}. \tag{5.72}$$

Note that $B^{\mathcal{B}(k)} \frac{\partial f(\mu)}{\partial \mu} B^{\mathcal{W}(k)^T}$ is the right-upper block of the Laplacian matrix $B^{(k)} \frac{\partial f(\mu)}{\partial \mu} B^{(k)^T}$ with strictly positive weight matrix, since $f_i(\mu_i)$ is strictly increasing, such that $\frac{\partial f_k(\mu_k)}{\partial \mu_k} > 0$ for all $k \in \mathcal{E}$. The non-zero entries in $B^{\mathcal{B}(k)} \frac{\partial f(\mu)}{\partial \mu} B^{\mathcal{W}(k)^T}$ correspond to pairs of exactly one black and one white node that are connected via an edge. Therefore we have that each row i of $B^{\mathcal{B}(k)} \frac{\partial f(\mu)}{\partial \mu} B^{\mathcal{W}(k)^T}$ (which corresponds to a black node) contains a strictly negative number at entry j if node $n_k + j$ is a neighbor of the node i. By Assumption 5.30 we have that $\mathcal{V}_k$ is a zero forcing set and that $\mathcal{V}_k \subsetneq \mathcal{V}$, which implies that there exists at least one row of $B^{\mathcal{B}(k)} \frac{\partial f(\mu)}{\partial \mu} B^{\mathcal{W}(k)^T}$ which contains exactly one non-zero entry. Let $\mathcal{U}_k$ be the set in which we collect the nodes that correspond to these rows and define $\mathcal{V}_{k+1} := \mathcal{V}_k \cup \mathcal{U}_k$. From (5.72), we have that $0 = h_i(x_i) - h_i(\overline{x}_i)$, for all $i \in \mathcal{U}_k$ and therefore for all $i \in \mathcal{V}_{k+1}$. Moreover, since $\mathcal{V}_k \subset \mathcal{V}_{k+1}$, and since we assume that $\mathcal{V}_k$ is a zero forcing set for $\mathcal{G}$, also $\mathcal{V}_{k+1}$ is a zero forcing set for $\mathcal{G}$. This concludes the proof that there exists a set of nodes $\mathcal{V}_{k+1}$ that satisfies properties (i) and (ii) with $n_k < n_{k+1}$.

Since the number of nodes is finite, in a finite number of iterations $\overline{k}$ we arrive at a set $\mathcal{V}_{\overline{k}}$ where $n_{\overline{k}} = n$, *i.e.* $\mathcal{V}_{\overline{k}}$ coincides with $\mathcal{V}$ and has the property that on the largest invariant set for (5.1), (5.16), (5.68) contained in Υ_3, $0 = h_i(x_i) - h_i(\overline{x}_i)$ for all $i \in \mathcal{V}_{\overline{k}} = \mathcal{V}$. From here, omitting the variable ξ, the proof follows, *mutatis mutandis*, the proof of Theorem 5.21 starting below (5.44). ∎

Remark 5.32 (Relaxing Assumption 5.30)**.** *In the case $f(\mu) = \mu$ and $h(x) = x$, succes-*

sive differentiations of (5.71c) yields

$$\mathbf{0} = \underbrace{\begin{pmatrix} -E^T \\ E^T Y \\ -E^T Y^2 \\ \vdots \\ (-1)^{n-1} E^T Y^{n-1} \end{pmatrix}}_{O} (h(x) - h(\overline{x})), \tag{5.73}$$

where $Y = T_x^{-1} B T_\mu^{-1} B^T$. *To conclude that* $h(x) = h(\overline{x})$, *it is sufficient that the matrix* O *has full column rank, that is the pair* (E^T, Y) *is observable. However, in the case of the nonlinear mappings* $f(\mu)$ *and* $h(x)$, *it not immediate to find a similar criterion that permits us to conclude* $h(x) = h(\overline{x})$.

After separately discussing the particular modifications to the flow network and controllers in Subsections 5.4.1 and 5.4.2, we briefly discuss the combination of both in the corollary below:

Corollary 5.33. *Let Assumptions 5.1–5.12 and 5.16–5.27 hold. Consider the flow network (5.52) and let* $\mathcal{V}_s \subseteq \mathcal{V}_c$, *be defined as*[6]

$$\mathcal{V}_s = \{ i \in \mathcal{V}_c \,\big|\, \eta_i(y_i) \text{ is } \textit{strictly} \text{ increasing in } y_i \}. \tag{5.74}$$

If $\mathcal{V}_e \cup \mathcal{V}_s$ *is a zero forcing set for* $\mathcal{G}$, *then system (5.52), in closed loop with the controllers (5.16) and (5.68), globally approaches the set*

$$\Upsilon_4 = \left\{ x, \mu, \theta, \phi \,\middle|\, \begin{array}{l} B(f(\mu) - f(\overline{\mu})) = \mathbf{0}, \\ x = \overline{x},\ \theta = \overline{\theta},\ \phi = \overline{\phi} \end{array} \right\}, \tag{5.75}$$

where $\lambda = f(\mu)$ *is a constant,* $h(x) = \overline{y}$ *and* $u = g(\theta) = \overline{u}$, *with* $\overline{u}$ *given by (5.7). Therefore, controllers (5.16) and (5.68) solve Problem 5.10 for the flow network (5.52).*

Proof. Following a similar argumentation as in the the proof of Theorem 5.31, $x_i = \overline{x}_i$ for all $i \in \mathcal{V}_e$. Moreover, the dynamics (5.52) give rise to an additional term in $\dot{V}(\cdot)$ in the same manner as in the proof of Theorem 5.28 (see (5.64)), namely:

$$-(h(x) - h(\overline{x}))^T E_c \Gamma^e(x) E_c^T (h(x) - h(\overline{x})) < 0. \tag{5.76}$$

Consequently, on the largest invariant set where $\dot{V}(\cdot) = 0$, also $x_i = \overline{x}_i$ for all $i \in \mathcal{V}_s$,

[6] In Theorem 5.28, we only required $\eta_i(y_i)$ to be increasing for $i \in \mathcal{V}_c$.

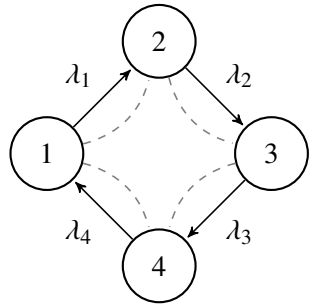

Figure 5.3: Topology of the considered heat network. The arrows indicate the required flow directions in the heat network, while the dashed lines represent the communication network used by the controllers.

since $\eta_i(y_i)$ is strictly increasing for all $i \in \mathcal{V}_s$. From here the proof continues along the lines of the proof of Theorem 5.31. ■

5.5 Case studies

To illustrate how various physical systems can be regarded as a flow network and to show the performance of the proposed controllers we consider two case studies. The first case study considers a district heating system, whereas the second case study considers a multi-terminal HVDC network.

5.5.1 District heating system

We consider a district heating system with a topology as depicted in Fig 5.3. Each node represents a producer, a consumer and a stratified storage tank as in Figure 2.2 and let the output of the system be $h_i(x_i) = x_i$. The various nodes are interconnected via a pipe network $\mathcal{G}$ resulting in the model (5.1) with $T_x = I$ and $E = I$.
We perform a simulation over a 40 hour time interval in which we evaluate the response to a change in demand at $t = 12$ and change in setpoint at $t = 24$. The cost functions of the four producers are purely quadratic, *i.e.* $s = r = \mathbf{0}$ and $Q = \operatorname{diag}\begin{pmatrix} 10 & 9 & 7 & 6 \end{pmatrix}$. Initially the volume is set to $x(0) = \begin{pmatrix}200 & 200 & 200 & 200\end{pmatrix}^T$ and the first setpoint $\overline{x}(t) = x(0)$, for all $t < 24$. The initial demand is given by $d = \begin{pmatrix}30 & 30 & 30 & 30\end{pmatrix}^T$, for all $t < 12$, which is increased to $d = \begin{pmatrix}35 & 35 & 35 & 35\end{pmatrix}^T$, for all $t \geq 12$. At $t = 24$ the setpoint for the volume $\overline{x}(t)$ is increased, such that $\overline{x}(t) = \begin{pmatrix}210 & 210 & 210 & 210\end{pmatrix}^T$ for all $t \geq 24$. To guarantee uni-directional flows and positive production we require $\lambda > 0$,

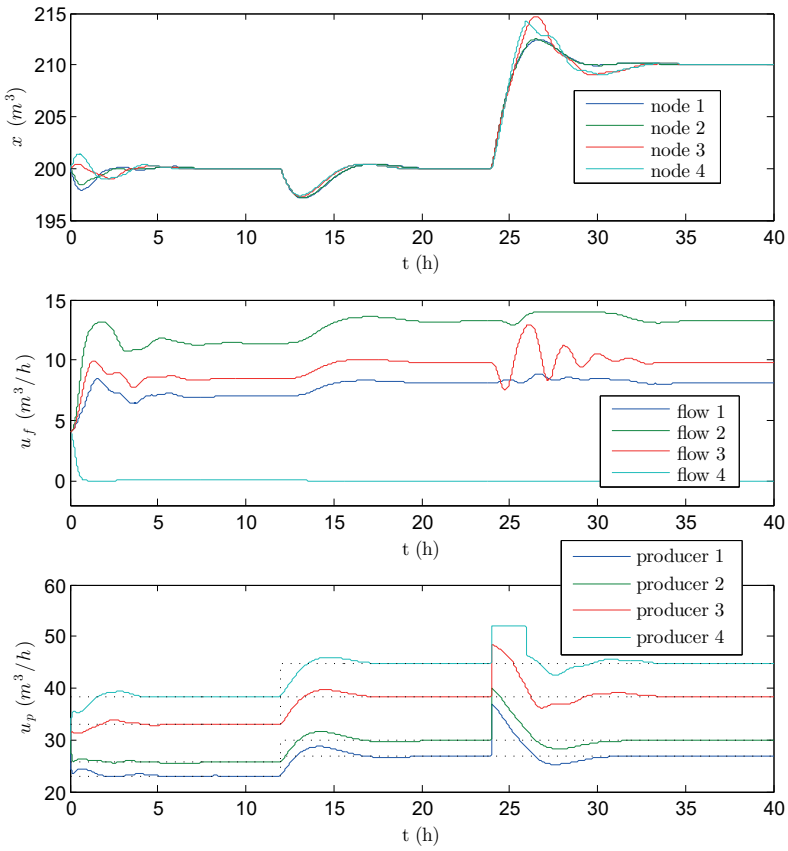

Figure 5.4: Volumes, flows and productions of the district heating system during a 40 hour period. The optimal production $\overline{u}_p$ as in (5.7) is indicated by dotted lines in the lower plot.

$u > 0$ and due to capacity constraints we additional require them to be upper bounded by 14 m^3/h and 52 m^3/h, respectively. To enforce these constraints the input is designed as

$$\lambda_i(\mu_i) = 7(\tanh(\mu_i) + 1)$$
$$u_i(\theta_i) = 26(\tanh(\theta_i) + 1),$$

where $\tanh(\cdot)$ is the hyperbolic tangent function. Finally we let $T_\mu = I$, $T_\theta = I$, $T_\phi = 0.005 \cdot I$ and we set all the weights of L^{com} to 10 and we let it be undirected which implies that L^{com} is balanced.

The resulting response of the system can be found in Figure 5.4, where we can clearly see the effects of the increased demand at $t = 12$ and change in setpoint at $t = 24$. More

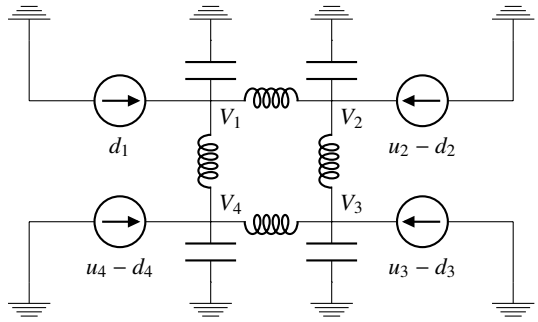

Figure 5.5: Topology of a four bus multi-terminal HVDC network. We take $C_i = 57\mu F$ and $\mathcal{L}_k = 0.0135H$ for $i, k \in \{1, \ldots, 4\}$.

specifically, in the upper plot we can see that the controllers indeed let the volumes in the four storage tanks to converge towards the desired setpoints of $200m^3$ ($t < 24$) and $210m^3$ ($t \geq 24$). In the middle plot we see that the flows in the pipes remain within the constraint $0 < \lambda_k < 14$ for all k throughout the entire simulation. Finally, in the bottom plot we see the production at the four nodes and the optimal productions denoted by the dotted lines. We observe that the production converges towards the optimal value $\overline{u}$ and satisfies $0 < u_i < 52$ for all i and for the entire simulation interval.

5.5.2 Multi-terminal high voltage direct current networks

As a second case study we consider multi-terminal high voltage direct current (HVDC) networks that have been recently studied in *e.g.* (Andreasson et al. 2016). We assume that the lines connecting the terminals are lossless, such that the overall network dynamics are given by

$$\begin{aligned} C\dot{V} &= -B\mu + u - d \\ \mathcal{L}\dot{\mu} &= B^T V, \end{aligned} \tag{5.77}$$

where V are the voltages at the terminals, μ are the currents through the lines, d are *uncontrollable* current loads and u are the *controllable* current injections. We consider a circuit of four nodes of which only nodes 2, 3 and 4 have a controllable current injection. The corresponding circuit is provided in Figure 5.5, where C_i is the capacitance at terminal i, and $\mathcal{L}_k$ is the inductance of line k. The first objective is to stabilize the voltage at terminal i around its desired setpoint $\overline{V}_i$, which is identical for each terminal. Therefore, $B^T V = B^T(V - \overline{V})$. The second objective is to share the controllable current injections equally among the terminals. Note that (5.77), is an example of the model studied in Subsection 5.4.2, and that the set of nodes with a controllable current injection is a zero

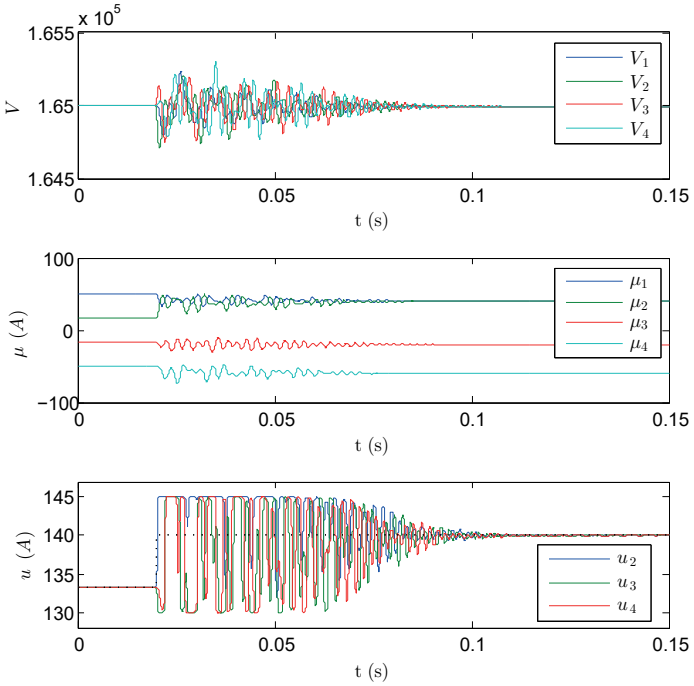

Figure 5.6: Voltages, current flows and current injections for a high voltage direct current network. The optimal production $\overline{u}_p$ as in (5.7) is indicated by dotted lines in the lower plot.

forcing set for the considered network. Therefore, Assumption 5.30 is satisfied and it follows from Theorem 5.31 that asymptotic stability of the desired state is guaranteed, if the controllers (5.16) are applied to control the current injections. In this case study, the controllers (5.16) are applied, with $q_i = 1, s_i = 0, r_i = 0$, $T_{\theta i} = 100$, $T_{\phi i} = 0.02$, for all $i \in \{1, \dots, 4\}$. The underlying communication network connects nodes $2-3$ and $3-4$, where each link has a weight of 10^4. The desired voltage is $\overline{V}_i = 165kV$ at all terminals throughout the simulation. Initially, all d_i have a value of $100A$. At $t = 0.02s$, the value of d_2 increased to $140A$, whereas d_3 is decreased to $80A$. To prevent low and high current injections during the transient we require at all terminals that $130A \leq u_i(t) \leq 145A$ is satisfied. To ensure this we let

$$u_i = g_i(\theta_i) = 130 + 7.5\,(\tanh(\theta_i) + 1)\,. \tag{5.78}$$

The response to the change in demand is given in Figure 5.6, from where we conclude that the voltages converge towards their set point of $165kV$, while u satisfies its constraints at all time.

Chapter 6

Pressure regulation with a single producer and positivity constraints

Abstract

In this chapter we investigate pressure regulation in large scale hydraulic networks with a multi-pump architecture. We propose distributed controllers that regulate the pressure drop at each end-user asymptotically towards desired set-points. We prove that the obtained closed-loop nonlinear system is locally asymptotically stable. In contrast to previous results, the proposed solution guarantees, besides pressure regulation, that the pumps generate only positive pressures (inputs), required by many (centrifugal) pumps that are commonly used in hydraulic networks.

Pressure regulation problems of a closed large scale hydraulic network with multiple pumps are common in district heating networks. In these heat networks a single heat source (producer) has to deliver heat to multiple end-users that have an uncertain and possibly changing demand. The heat is exchanged through heat exchangers while the pumps guarantee that the heat is transported through the fluid in the pipes. In order to reduce heat dispersion, the diameter of the pipes are kept as small as possible. However, smaller pipes can lead to a higher resistance, resulting in pressure losses throughout the network. In order to maintain a desirable pressure at all the end-users, a multi-pump architecture can be used (De Persis and Kallesoe 2011). In such an architecture each pump is equipped with a controller that maintains locally the desired pressure drop. Depending on the topology of the hydraulic network, additional coordination among the pumps may be needed.

Various solutions have been proposed to regulate the pressure in these multi-pump hydraulic networks with an unknown demand, such as PI controllers (Sloth and Wisniewski 2015), (De Persis et al. 2014) and nonlinear adaptive controllers (Hu et al. 2003), (Koroleva and Krstic 2005), (Koroleva et al. 2006). Additional objectives such as reducing the water leakage (Kallesøe et al. 2015), (Tahavori et al. 2014), or reducing the energy consumptions of the pumps (Sloth and Wisniewski 2015) have been considered as well. An important practical constraint is that (centrifugal) pumps that are used in most hydraulic networks can only generate a positive pressure, lowering the

practical applicability of solutions that do not take this constraint explicitly into account. This constrained control problem, where the input is quantized as well, has been previously addressed in (De Persis and Kallesoe 2011), but results in a steady state error in the desired pressure drops at the end-user valves.

In contrast to the flow networks considered in Chapters 4 and 5, hydraulic networks include the algebraic and dynamic relations between the pressures and flowrates. In this chapter we focus on the pressure regulation of a closed large scale hydraulic network with multiple pumps. The focus of this chapter is to extend previous results by guaranteeing the positivity constraint on the input (pump pressures), while regulating the pressures at the end-users to their desired values.

We propose a distributed control structure, where every local controller resembles the structure of a nonlinear PI controller. Related nonlinear PI controllers have been considered before in for example (Astolfi et al. 2007). In order to guarantee positivity constraint on the input, saturation functions and a state dependent integral gain are included in the controller. Furthermore, we prove that the state of desired pressure drops at the end-users is locally asymptotically stable. Since the considered model of the hydraulic network can be formulated as a port-Hamiltonian system (van der Schaft and Maschke 2013) or as a Euler-Lagrange system (Ortega et al. 2008), we believe that the obtained results on the regulation of hydraulic networks can offer an inspiration for solving control problems in other networked (energy) systems admitting a port-Hamiltonian or Euler-Lagrange model. Specifically, the way how the input constraints are enforced might offer new perspectives on general classes of controlled flow networks that have similar requirements (Wei and van der Schaft 2014), (Trip et al. 2017).

The chapter is structured as follows, in Section 6.1 we introduce the model and introduce the controller design. The corresponding stability analysis can be found in Section 6.3 and we end this chapter with a case study of a district heating system in Section 6.4.

6.1 Pressure drop regulation with positivity constraints

In this chapter we consider a hydraulic network modeled by (2.32) which we repeat for convenience

$$\begin{aligned} J\dot{q} =& - Df(D^T q) + u \\ y =& \mu_c(q), \end{aligned} \tag{6.1}$$

where D is the fundamental loop matrix, $\mathcal{J}$ is a diagonal matrix with non-negative entries, $J = D\mathcal{J}D^T$, Δh_p is the pressure drop at the end-users $u = D\Delta h_p$ is the input and $f(\cdot)$ and $\mu_c(\cdot)$ are a nonlinear mappings as in (2.27) and (2.30) respectively. The main objective is to maintain the pressure drop at the end-user valves $y = \mu_c(q)$, at a desired

value $r \in \mathbb{R}^n_{>0}$. In the case that there are no pressure constraints on the considered pumps this control problem has been satisfactory solved in (De Persis et al. 2014). However, the considered pumps in this chapter can only provide positive pressures. Therefore, the control input u is required to be positive, which complicates the controller design. The corresponding control problem is as follows:

Problem 6.1 (Pressure drop regulation with a positive input)**.** *Let $r \in \mathbb{R}^n_{>0}$, design controllers adjusting $u(t)$ given in (6.1), such that*

$$\lim_{t\to\infty} \|y(t) - r\| = 0, \tag{6.2}$$

while satisfying $u(t) \geq \mathbf{0}$ for all $t \geq 0$. Moreover, a controller that generates $u_i(t)$ can only access the measurement $y_i(t)$ and the reference signal r_i. □

Next, we propose a controller that solves Control problem 6.1 and analyse the stability of the obtained closed-loop system in Section 5.

6.2 Controller design

In order to design the controllers that satisfy the positivity constraint on $u(t)$ as in Problem 6.1, we define mappings $s(\theta)$ and $\sigma(x)$ as

$$\begin{aligned} s(\theta) &= \begin{pmatrix} s_1(\theta_1) \\ \vdots \\ s_n(\theta_n) \end{pmatrix} \\ \sigma(x) &= \begin{pmatrix} \sigma_1(x_1) \\ \vdots \\ \sigma_n(x_n) \end{pmatrix}, \end{aligned} \tag{6.3}$$

where function $s_i(\theta_i) \in C^1(\mathbb{R}; \mathbb{R})$ is strictly increasing and satisfies

$$\lim_{\theta_i\to-\infty} s_i(\theta_i) = 0, \tag{6.4}$$

for each $i \in \{1, \ldots, n\}$. The function $\sigma_i(\cdot) \in C^1(\mathbb{R}; \mathbb{R})$ is decreasing and

$$\sigma_i(x_i) = 0, \tag{6.5}$$

if $x_i \geq 0$ for each $i \in \{1, \dots, n\}$. Notice that with the definitions above we have that

$$\begin{aligned} \mathcal{R}(s(\cdot)) &\in \mathbb{R}^n_{\geq 0} \\ \mathcal{R}(\sigma(\cdot)) &\in \mathbb{R}^n_{\geq 0}. \end{aligned} \tag{6.6}$$

where $\mathcal{R}$ denotes the range. Consider a controller of the form

$$\dot{\theta} = -\left[\frac{\partial s(\theta)}{\partial \theta}\right]^{-1} (\mu_c(q) - r) \tag{6.7a}$$

$$u = s(\theta) + \sigma(\mu_c(q) - r), \tag{6.7b}$$

where $s(\cdot)$ and $\sigma(\cdot)$ are defined as in (6.3).

Remark 6.2 (Interpretation of controller (6.7))**.** *Note that (6.7) has the form of a PI controller where $u(t) \geq \mathbf{0}$ for all $t \geq 0$ due to the (6.6). Moreover, following the stability analysis in the next section, integrator (6.7a) includes the state dependent gain $[\frac{\partial s(\theta)}{\partial \theta}]^{-1}$, which is nonsingular since $s_i(\theta_i)$ is strictly increasing for each i.*

6.3 Stability analysis of the closed loop system

In this section we provide a stability analysis of system (6.1) interconnected with controller (6.7), resulting in

$$J\dot{q} = -Df(D^T q) + s(\theta) + \sigma(\mu_c(q) - r) \tag{6.8a}$$

$$\dot{\theta} = -\left[\frac{\partial s(\theta)}{\partial \theta}\right]^{-1} (\mu_c(q) - r). \tag{6.8b}$$

Before we study the stability of (6.8), we first determine its steady state.

6.3.1 Existence of a steady state

To guarantee the existence of a steady state of (6.8) we make the following assumption:

Assumption 6.3 (Feasibility condition)**.** *Setpoint r and mappings $\mu_c(\cdot)$ and $s(\cdot)$ satisfy*

$$\begin{aligned} r &\in \mathcal{R}(\mu_c(q)) \\ Df(D^T \mu_c^{-1}(r)) &\in \mathcal{R}(s(\theta)). \end{aligned} \tag{6.9}$$

Note that Assumption 6.3 is not restrictive since $s(\cdot)$ can be designed to satisfy (6.9) and $Df(D^T \mu_c^{-1}(r)) \in \mathbb{R}^n_{>0}$ for all $r \in \mathbb{R}^n_{>0}$. In the lemma below we prove that under

Assumption 6.3 there exists a *unique* steady state $(\overline{q}, \overline{\theta})$ satisfying

$$\mathbf{0} = -Df(D^T\overline{q}) + s(\overline{\theta}) + \sigma(\mu_c(\overline{q}) - r) \tag{6.10a}$$

$$\mathbf{0} = -\left[\left.\frac{\partial s(\theta)}{\partial \theta}\right|_{\theta=\overline{\theta}}\right]^{-1}(\mu_c(\overline{q}) - r). \tag{6.10b}$$

Lemma 6.4 (Existence of a steady state)**.** *Let Assumption 6.3 hold. There exists a unique $(\overline{q}, \overline{\theta})$ that satisfies (6.10) and is given by*

$$\overline{q} = \mu_c^{-1}(r) \tag{6.11a}$$

$$\overline{\theta} = s^{-1}\left(Df(D^T\mu_c^{-1}(r))\right). \tag{6.11b}$$

Proof. First note that (6.11) satisfies (6.10) and exists due to Assumption 6.3. Conversely, we prove that (6.11) is the only steady state that satisfies (6.10). Since $\mu_c(q)$ and $s(\theta)$ are strictly increasing they have a unique inverse and $[\frac{\partial s(\theta)}{\partial \theta}]^{-1} \neq \mathbf{0}$. Therefore, (6.10b) implies (6.11a). By design we have that $\sigma(\mathbf{0}) = \mathbf{0}$ such that $\sigma(\mu_c(\overline{q}) - r) = \mathbf{0}$ and it follows that necessarily (6.11b) is satisfied. ∎

Lemma 6.4 is essential to the stability analysis in the next subsection, since $\overline{q}$ as in (6.11) implies that $\|\mu_c(\overline{q}) - r\| = 0$ as is desired in Control problem 6.1. In order to solve Control problem 6.1 it is therefore sufficient to prove that (6.11) is a (locally) asymptotically stable equilibrium of (6.8).

6.3.2 Stability analysis of the desired steady state

This section investigates the stability of the desired steady state (6.10) under the closed loop dynamics (6.8). We consider the storage function (De Persis et al. 2014)

$$V = \sum_{i=1}^{n} \int_{\bar{q}_i}^{q_i} (\mu_c(\xi) - r)d\xi + \frac{1}{2}\dot{q}^T J\dot{q}. \tag{6.12}$$

Next, we derive two useful properties of the storage function V that allow us to derive the main result of this chapter.

Lemma 6.5 (Decreasing storage function)**.** *The storage function V satisfies*

$$\dot{V} \leq -\sum_{i=1}^{n} \dot{q}_i^2 \left.\frac{\partial \lambda_i(\tilde{q}_i)}{\partial \tilde{q}_i}\right|_{\tilde{q}_i=(D^T q)_i} \leq 0, \tag{6.13}$$

along the solutions to (6.8).

Proof. Along the solutions to system (6.8) we have that V satisfies

$$\begin{aligned}\dot{V} &= (\mu_c(q) - r)^T \dot{q} + \dot{q}^T J \ddot{q} \\ &= (\mu_c(q) - r)^T \dot{q} - \dot{q}^T \left[D\Gamma(q) D^T - \frac{\partial \sigma(\mu(q) - r)}{\partial \mu(q)} \frac{\partial \mu(q)}{\partial q} \right] \dot{q} + \dot{q}^T \frac{\partial s(\theta)}{\partial \theta} \dot{\theta},\end{aligned} \tag{6.14}$$

where

$$\Gamma(q) = \begin{bmatrix} \Gamma^c(q) & \mathbf{0} \\ \mathbf{0} & \Gamma^r(q) \end{bmatrix}, \tag{6.15}$$

with

$$\Gamma^c_{ii}(q) = \left. \frac{\partial \lambda_i(\tilde{q}_i)}{\partial \tilde{q}_i} \right|_{\tilde{q}_i = (D^T q)_i}, \tag{6.16}$$

for $i \in \{1, ..., n\}$ (representing all the end-user valves),

$$\Gamma^r_{ii}(q) = \left. \frac{\partial (\lambda_i(\tilde{q}_i) + \mu_i(\tilde{q}_i))}{\partial \tilde{q}_i} \right|_{\tilde{q}_i = (D^T q)_i}, \tag{6.17}$$

for $i \in \{n+1, ..., m\}$ (representing all other components in the network) and $\Gamma^c_{ij}(q) = \Gamma^r_{ij}(q) = 0$ for all $i \neq j$. Since $\sigma(\mu(q) - r)$ and $\mu(q)$ are decreasing and increasing mappings respectively, we have that

$$\frac{\partial \sigma(\mu(q) - r)}{\partial \mu(q)} \frac{\partial \mu(q)}{\partial q} \preceq \mathbf{0}. \tag{6.18}$$

Furthermore, (6.7a) implies

$$\frac{\partial s(\theta)}{\partial \theta} \dot{\theta} = -(\mu_c(q) - r), \tag{6.19}$$

such that we obtain from (6.14), (6.18) and (6.19) that

$$\dot{V} \leq -\dot{q}^T D\Gamma(q) D^T \dot{q} = -\dot{q}^T \Gamma^c(q) \dot{q} - \dot{q}^T F \Gamma^r(q) F^T \dot{q}, \tag{6.20a}$$

where we have exploited the structure of D given by (2.25). Since $\lambda_i(\cdot)$ and $\mu_i(\cdot)$ are strictly increasing functions, it follows that $\Gamma^c_{ii}(q) > 0$ and $\Gamma^r_{ii}(q) \geq 0$ for all i. Combining the latter with the observation that the last term in (6.20a) is a positive semidefinite quadratic form, we obtain (6.13). ∎

Lemma 6.6 (Positive definite Hessian matrix)**.** *The Hessian matrix $\mathcal{H}(V(q, \theta))$ of the storage function V in (6.12) evaluated at $(\overline{q}, \overline{\theta})$ as in (6.11) is positive definite, i.e.*

$$\mathcal{H}(V(q, \theta))|_{q=\bar{q}, \theta=\bar{\theta}} \succ \mathbf{0}. \tag{6.21}$$

Proof. From (6.12) we obtain

$$V = \frac{1}{2} z(q)^T J^{-1} z(q) + \frac{1}{2} s(\theta)^T J^{-1} s(\theta) + z(q)^T J^{-1} s(\theta) + \sum_{i=1}^{n} J_i \int_{\bar{q}_i}^{q_i} \mu_c(y) - r dy, \tag{6.22}$$

where $z(q) := \sigma(\mu_c(q) - r) - Df(D^T q)$. A straightforward calculation shows that

$$\mathcal{H}(V(q,\theta)) = \begin{bmatrix} \mathcal{A}(q,\theta) & \mathcal{B}(q,\theta) \\ \mathcal{B}^T(q,\theta) & C(q,\theta) \end{bmatrix}, \tag{6.23}$$

where

$$\begin{aligned} \mathcal{A}_{ij}(q,\theta) &= \frac{\partial^2}{\partial q_i \partial q_j} z(q)^T J^{-1} \left(\frac{1}{2} z(q) + s(\theta) \right) + \frac{\partial^2}{\partial q_i \partial q_j} \sum_{i=1}^{n} J_i \int_{\bar{q}_i}^{q_i} \mu_c(y) - r dy \\ &= \sum_{k=1}^{n} \left(\frac{\partial^2 z_k(q)}{\partial q_i \partial q_j} (z_k(q) + s_k(\theta_k)) + \frac{\partial z_k(q)}{\partial q_i} \frac{\partial z_k(q)}{\partial q_j} \right) J_k^{-1} + \frac{\partial \mu_{ci}(q_i)}{\partial q_j} J_i \end{aligned}$$

$$\mathcal{B}_{ij}(q,\theta) = \frac{\partial^2}{\partial q_i \partial \theta_j} z(q)^T J^{-1} s(\theta) = \frac{\partial z_j(q)}{\partial q_i} J_j^{-1} \frac{\partial s_j(\theta_j)}{\partial \theta_j}$$

$$C_{ij}(q,\theta) = J_i^{-1} \frac{\partial^2 s_i(\theta_i)}{\partial \theta_i \partial \theta_j} (s_i(\theta_i) + z_i(q)) + J_i^{-1} \frac{\partial s_i(\theta_i)}{\partial \theta_i} \frac{\partial s_i(\theta_i)}{\partial \theta_j}.$$

Note that $C_{ij}(q,\theta) = 0$ if $i \neq j$ since $\frac{\partial s_i(\theta_i)}{\partial \theta_j} = 0$. We now evaluate $\mathcal{H}(V(q,\theta))|_{q=\bar{q},\theta=\bar{\theta}}$, which we denote with a slight abuse of notation as

$$\mathcal{H}(V(q,\theta))|_{q=\bar{q},\theta=\bar{\theta}} = \begin{bmatrix} \mathcal{A}(\overline{q},\overline{\theta}) & \mathcal{B}(\overline{q},\overline{\theta}) \\ \mathcal{B}^T(\overline{q},\overline{\theta}) & C(\overline{q},\overline{\theta}) \end{bmatrix}. \tag{6.24}$$

From (6.10) we have $s(\overline{\theta}) + z(\overline{q}) = \mathbf{0}$ such that

$$\begin{aligned} \mathcal{A}_{ij}(\overline{q},\overline{\theta}) &= \sum_{k=1}^{n} J_k^{-1} \left. \frac{\partial z_k(q)}{\partial q_i} \right|_{q=\overline{q}} \left. \frac{\partial z_k(q)}{\partial q_j} \right|_{q=\overline{q}} + J_i \left. \frac{\partial \mu_{ci}(q_i)}{\partial q_j} \right|_{q=\overline{q}} \\ \mathcal{B}_{ij}(\overline{q},\overline{\theta}) &= J_j^{-1} \left. \frac{\partial z_j(q)}{\partial q_i} \right|_{q=\overline{q}} \left. \frac{\partial s_j(\theta_j)}{\partial \theta_j} \right|_{\theta_j=\overline{\theta}_j} \\ C_{ij}(\overline{q},\overline{\theta}) &= J_i^{-1} \left. \frac{\partial s_i(\theta_i)}{\partial \theta_i} \right|_{\theta_i=\overline{\theta}_i} \left. \frac{\partial s_i(\theta_i)}{\partial \theta_j} \right|_{\theta=\overline{\theta}}. \end{aligned} \tag{6.25}$$

Since $C(\overline{q},\overline{\theta}) \succ \mathbf{0}$, it is sufficient that the Schur complement of block $C(\overline{q},\overline{\theta})$ of matrix $\mathcal{H}(V(q,\theta))|_{q=\bar{q},\theta=\bar{\theta}}$ is positive definite in order to conclude that $\mathcal{H}(V(q,\theta))|_{q=\bar{q},\theta=\bar{\theta}} \succ \mathbf{0}$. This Schur complement $S(\overline{q},\overline{\theta})$ is given by

$$S(\overline{q},\overline{\theta}) := \mathcal{A}(\overline{q},\overline{\theta}) - \mathcal{B}(\overline{q},\overline{\theta})C(\overline{q},\overline{\theta})^{-1}\mathcal{B}^T(\overline{q},\overline{\theta}), \tag{6.26}$$

where

$$S_{ij}(\overline{q},\overline{\theta}) = \mathcal{A}_{ij}(\overline{q},\overline{\theta}) - \sum_{l=1}^{n}\left(\mathcal{B}_{il}(\overline{q},\overline{\theta})C_{ll}(\overline{q},\overline{\theta})^{-1}\mathcal{B}_{jl}(\overline{q},\overline{\theta})\right) = J_i\left.\frac{\partial\mu_{ci}(q_i)}{\partial q_j}\right|_{q=\overline{q}}.$$

Since $\frac{\partial\mu_{ci}(q_i)}{\partial q_j} > 0$ if $i = j$ and $\frac{\partial\mu_{ci}(q_i)}{\partial q_j} = 0$ otherwise, we have that $S(\overline{q},\overline{\theta}) \succ \mathbf{0}$ and we conclude that indeed $\mathcal{H}(V(q,\theta))|_{q=\bar{q},\theta=\bar{\theta}} \succ \mathbf{0}$. ■

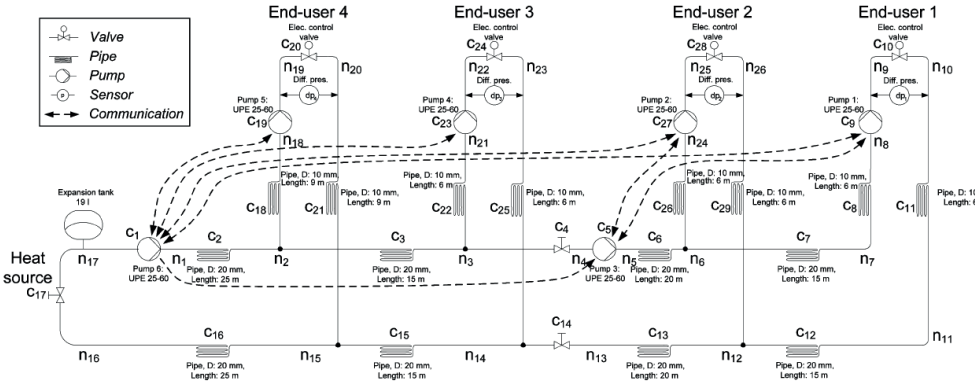

Figure 6.1: Topology of a four end-user network with a single producer (De Persis and Kallesoe 2011).

We are now ready to state the main result of this chapter.

Theorem 6.7 (Local asymptotic stability of (6.8))**.** *Let Assumption 6.3 hold, then equilibrium (6.11) of system (6.8) is locally asymptotically stable.*

Proof. It follows from Lemma 6.6 that the storage function V given by (6.12) has a strict local minimum at the desired steady state $(\overline{q},\overline{\theta})$. Since $\dot{V} \leq 0$ as a result of Lemma 6.5, there exists a forward invariant set Υ around $(\overline{q},\overline{\theta})$ and by LaSalle's invariance principle the solutions that start in Υ converge towards the largest invariant set contained in $\Upsilon \cap \mathcal{Q}$, where

$$\mathcal{Q} = \left\{ q \in \mathbb{R}^n, \theta \in \mathbb{R}^n \;\middle|\; 0 = \sum_{i=1}^{n} \dot{q}_i^2 \left.\frac{\partial\lambda_i(\tilde{q}_i)}{\partial\tilde{q}_i}\right|_{\tilde{q}_i=(D^Tq)_i} \right\}.$$

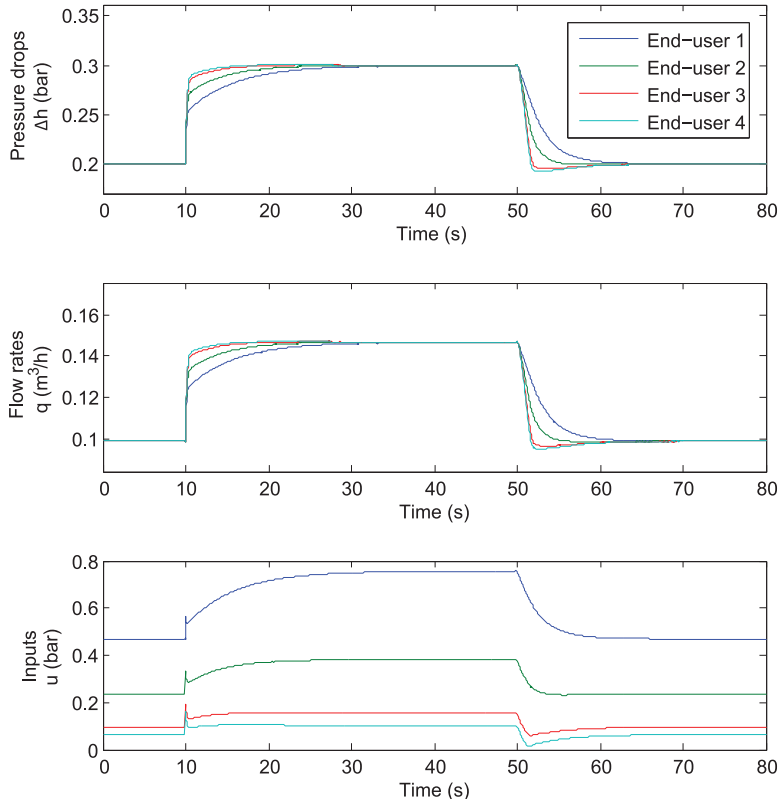

Figure 6.2: Evolution of the pressure drops (top) and flow rates (middle) at the end-users, as well as the total generated pump pressures (bottom) in the fundamental loops. The setpoint is increased at time $t = 10s$ and decreased at time $t = 50s$.

Since $\lambda_i(\cdot)$ is strictly increasing, it follows that on the invariant set $\dot{q} = \mathbf{0}$. In view of (6.8a), this implies that on this set

$$\mathbf{0} = -f(D^T q) + s(\theta) - \sigma(\mu(q) - r). \tag{6.27}$$

Differentiating (6.27) yields

$$\frac{\partial\Big(f(D^T q) + \sigma(\mu(q) - r)\Big)}{\partial q}\dot{q} = \frac{\partial s(\theta)}{\partial \theta}\dot{\theta}, \tag{6.28}$$

and since $\dot{q} = \mathbf{0}$, we conclude from (6.8b) that $\mu_c(q) - r = \mathbf{0}$ implying that $q = \overline{q}$ on the invariant set. Finally, from (6.27) we obtain that $Df(D^T q) = s(\theta)$ which implies that necessarily $\theta = \overline{\theta}$ on the invariant set. ■

Note that Theorem 6.7 shows that controllers (6.7) indeed solve Control problem 6.1,

provided that the initial conditions $q(\mathbf{0})$ and $\theta(\mathbf{0})$ are sufficiently close to the steady state (6.11). Moreover, controller (6.7) is designed in such a way that it can be implemented in a distributed fashion, meaning that it only requires measurements of y_i and setpoint r_i in order to generate u_i.

6.4 Case study

To illustrate the the proposed controller (6.7), we perform a case study where we simulate a network with four end-users as depicted in Figure 6.1. The functions σ_i and s_i are designed as

$$\sigma_i(x) = \begin{cases} -x - \frac{1}{40000} & \text{if } x < -0.005 \\ x^2 & \text{if } -0.005 \leq x < 0 \\ 0 & \text{if } 0 \leq x, \end{cases} \tag{6.29}$$

and

$$s_i(x) = \begin{cases} 0.0023e^{124.992x} & \text{if } x < 0.01 \\ 0.8\tanh(x) & \text{if } x \geq 0.01. \end{cases} \tag{6.30}$$

Note that σ_i and s_i are chosen such that they are continuous, have a continuous derivative and are non-negative. The functions λ_i and μ_i are given by

$$\lambda_i(x) = p_i(x^3 + x), \quad \mu_i(x) = v_i(x^3 + x), \tag{6.31}$$

where $v_i = 0.1$ for all i and $p_i = 0.0141$ if i corresponds to an end-user and $p_i = 0.4503$ otherwise. The matrix $\mathcal{J}$ is such that $\mathcal{J}_{ii} = 0.1$ for all i, resulting in

$$D^T\mathcal{J}D = \frac{1}{10}\begin{bmatrix} 7 & 4 & 4 & 4 \\ 4 & 9 & 6 & 6 \\ 4 & 6 & 12 & 9 \\ 4 & 6 & 9 & 14 \end{bmatrix}. \tag{6.32}$$

We investigate the response of the system during a change of the setpoint r. The initial setpoint for each end-user valve i is $r_i = 0.2$, which is increased to $r_i = 0.3$ at time $t = 10s$ and decreased to its initial value at time $t = 50s$. The results of the simulation can be found in Figure 6.2. In the upper plot we see that the pressures indeed converge to the desired setpoints after a transient response of approximately $20s$. From the bottom plot it can be seen that the inputs remain positive throughout the simulation.

Remark 6.8 (Required communication between the pumps)**.** *As discussed in Remark 2.16, the controller assigns the total required pressure to the sum of all the pumps in a*

cycle. For this reason communication between the pumps in each cycle is required to assign an input to an individual pump. The communication that is required is depicted in Figure 6.1 by the dashed lines and is explained in more detail in (De Persis and Kallesoe 2011).

Chapter 7

Geothermal reservoir implications of a time varying control

Abstract

This chapter provides a proof of concept in which the heat production of a geothermal system is controlled depending on the demand in a district heating network. A model predictive control strategy is designed, which uses volume measurements in the storage tank and predictions of the demand to regulate the production of the geothermal system in real time. The implications of such a time varying production for the reservoir are investigated using a 2D reactive transport reservoir model. As a case study, the Groningen geothermal project is considered for which the controller is tuned. The numerical data generated by the controller in closed loop with a modelled district heating network are used as input for the reservoir simulations. These make use of discrete parameter analysis to evaluate the effect of pressure depletion, reservoir permeability, flow rate, re-injection temperature and injection pH on the geothermal reservoir. The production using a model predictive control does not create adverse geochemical effects in the reservoir, instead the controller improves the efficiency of the geothermal heat extraction. The findings pave the way towards a stronger integration between heat networks and a more sustainable development of geothermal resources.

In a classical setup of a geothermal district heating system, geothermal systems always provide a baseload while backup systems provide excess demand (Sayegh et al. 2016). Recently it has been shown that periods of high and low production levels can be utilized as a means towards a more sustainable utilization of the geothermal resource (Axelsson 2010). Global historical data on direct use geothermal systems suggest that there is a capacity factor drop over time (Lund and Boyd 2016). This drop could be partly attributed to a better utilization of the produced geothermal heat by means of coupling supply and demand.

To match supply with demand in such systems, a storage component can be included to cope with daily fluctuation (Sayegh et al. 2016) (Kyriakis and Younger 2016), while the geothermal production can be adjusted to match the seasonal changes. However, a dynamic production rate can have several consequences, among which are changes in

chemical compositions, pressures and temperatures of the geothermal reservoir. Moreover, a dynamic production rate also has an effect in the cold front breakthrough time of the reservoir.

To avoid clogging of the reservoir due to salt precipitation, the rate of change of the production needs to be enforced. However, it is poorly investigated how these constraints can be obtained and moreover they are most likely dependent on the characteristics of the geothermal system and are therefore case specific. Finally, a geothermal system has upper and lower production constraints due to the capacity of the pipes, pumps and the reservoir permeability.

In order to satisfy all previously mentioned constraints while supplying a time varying heat demand, a storage device can be used to shift loads in time (Kyriakis and Younger 2016). To provide the geothermal system with time-varying production rates a controller should be designed that takes the production and storage capacity constraints into account. In case the demand has a periodic structure an internal model controller can be used such as in Chapter 3. In (Rosander 2012) several other controller designs are presented that do not require a periodic demand among which well-tuned proportional-integral-differential (PID) controllers and model predictive controllers (MPC) are the most promising. The PID controllers are very easy to implement and guarantee stability but cannot guarantee that the constraints are satisfied at all time. On the other hand, an MPC does have the capacity to guarantee that the constraints are satisfied at all time but the stability of these controllers is hard to prove. Moreover, these MPC mostly rely on ad-hoc tuning and experimental analysis (Siroky et al. 2011). Despite these drawbacks, MPC received a lot of attention (Siroky et al. 2011) (Campo and Morari 1989) (Mayne et al. 2000) and (Allgower et al. 1999), and have been also applied to the pressure control of geothermal systems (Darup and Renner 2016) and thermal energy storage for buildings (Ma et al. 2012).

An MPC solves an optimal control problem over a finite discrete time horizon, returning a sequence of control inputs of which only the first one is implemented. After this implementation the process is reiterated using a new finite horizon that is shifted one step forward. Since the future demand is often unknown, a prediction must be made to solve the optimization problem. These predictions can be based e.g., on historical data and weather predictions. Also a dynamic model of the system to control is required to implement an MPC. Therefore a model flow network as considered in Chapters 3, 4 and 5 can be used.

Motivated by the research objectives of the Flexiheat project, in this chapter we design a Model Predictive Controller (MPC) which is able to generate a real time production level of a geothermal system. The controller uses a storage level measurement and demand prediction as input and takes constraints into account for the production le-

vel, change in production level and storage level. The model uses a realistic, yearlong demand pattern for an equivalent of 10,000 households. The controller is simulated in closed loop with the geothermal reservoir, the storage devices and the network interconnecting them.

The resulting simulation is used together with a 2D reservoir model to obtain two insights. Firstly, it is investigated whether the geothermal doublet is able to provide the demanded energy (i.e. feasibility of delivery). Secondly, the long term effects of a variable, demand driven, seasonal production pattern on reservoir behavior (e.g. breakthrough time, reactive transport etc.) is compared to constant production rate data. The analysis makes use of the Groningen geothermal project (NE Netherlands) data and features, and considers uncertainty classes discussed in previous research (Daniilidis et al. 2016).

The chapter is structured as follows: in Section 7.1 the problem that is considered is explained along the corresponding controller design. In Chapter 7.2 a description of the model and corresponding characteristics of a reservoir located in Groningen is presented. An analysis of the performance of the controller in closed loop with the district heating network is carried out in Section 7.3 and in Section 7.4 the corresponding reservoir simulations are presented. Finally a discussion is presented in Section 7.5.

7.1 Problem setting and controller design

First we design a model predictive controller that is able to regulate the production of the geothermal system in real time. This controller is interconnected with a modelled storage device in order to analyze its performance. The demand pattern is predicted based on historical demand data and the MPC uses this prediction in combination with measurements from the storage device as inputs. Additionally, it takes the predetermined limitations of the reservoir into account in the form of constraints on the change of the production rate. This control structure is depicted in the upper part of Figure 7.1. It is designed such that it can be applied to any setup that includes a district heating network, storage device and geothermal system. The controller can be tuned in order to meet case specific requirements.

After the design of the controller we investigate in Section 7.2 the implications to the geothermal reservoir of this time varying production. To do this, a 2D reservoir model of the Groningen geothermal project is used. The production levels that are generated using the heat network were converted from an hourly to a monthly demand and used as input for a 50 year reservoir simulation. The bottom part of Figure 7.1 shows the model of the reservoir for which 243 scenarios were considered, each one corresponding to a different choice of parameters. The results with regards to the reservoir behavior in terms of pressure, permeability and power changes are investigated.

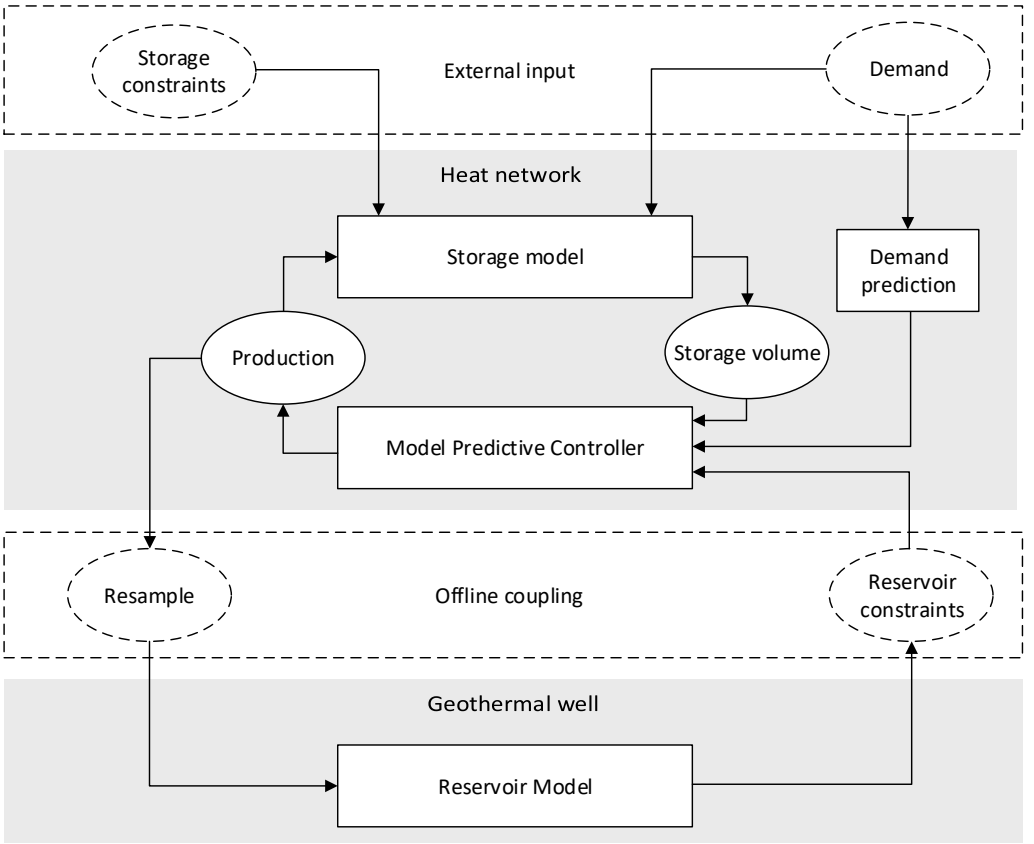

Figure 7.1: Overall flow chart of the simulation. The storage model and the MPC are connected in closed loop and where the static constraints from the reservoir model and storage are used. The aggregated demand in the heat network is predicted using historical data and used as input for the MPC and the actual demand is used as input for the storage model. The resulting production levels are used (offline) as an input for the reservoir simulations.

7.1.1 Heat demand

We consider a geothermal system that is connected to a storage tank via a heat exchanger. In turn, this storage tank is connected to a network with several consumers. These consumers have an aggregated demand $d_a(k)$ given in watt (W) where k denotes the discrete time step. However, the geothermal system has a maximum production rate u^{max} and in order to guarantee that the demand can be met with an admissible production rate, the demand is split in the demand covered by the geothermal well

$$d_g(k) = \begin{cases} u^{max} & \text{if} \quad d_a(k) \geq u^{\max} \\ d_a & \text{otherwise,} \end{cases} \tag{7.1}$$

and the excess demand that is covered by a backup system

$$d_b(k) \;=\; d_a(k) - d_g(k), \tag{7.2}$$

such as a gas fired boiler or biomass incinerator. For simplicity we consider the case in which the excess demand $d_b(k)$ can be ignored, which is the case when the backup systems automatically satisfies the excess demand. For optimal coordination of production in the multiple producer case the reader is referred to chapters 4 and 5.

In order to obtain a discrete time model for the storage device the demand is converted from W to m^3/h. This is done using:

$$d(k) = \frac{60^2}{c_P \rho \Delta T} d_g(k), \tag{7.3}$$

where d is the demand covered by the geothermal well in m^3/h, c_p is the specific heat in $J/kg \cdot K$, ρ is the density of the water in Kg/m^3 and ΔT is the temperature difference between the production and return pipes in the reservoir in Kelvin (K). It is assumed that temperature difference ΔT is independent of the time step k, which implies that $d_g(k)$ depends linearly on $d(k)$. Moreover, the temperature difference between the inflow and outflow of the heat exchanger is considered equal for both the compartments connected to the reservoir and district heating network. That is, we assume an ideal heat exchanger with no heat loss and equal flow rates through both compartments. Having defined our demand, the model of the storage is introduced.

7.1.2 Model of the storage tank

A storage model is considered, which is connected to a district heating grid with demand $d(k)$ and a geothermal well with production $u(k)$ (in m^3/h) at time k. The heated water

contained in the pipes of the district heating network can act as a buffer, but since it is assumed that ΔT is constant, the temperature dynamics of the fluids in the pipes can be neglected. The resulting model for the storage device takes the form of a difference equation and is given as

$$V(k+1) = V(k) + u(k) - d(k), \tag{7.4}$$

where V is the volume of the storage tank. The controllable input will be the production u while d is considered to be a disturbance. Same as in (7.3), the input $u(k)$ can be converted back to Watts using

$$u_g(k) = \frac{c_P \rho \Delta T}{60^2} u(k). \tag{7.5}$$

where $u_g(k)$ is the production of the geothermal well given in W.

In order to keep the volume of the storage tank between the minimal and maximal volume capacity, it is required that

$$V^{min} \leq V(k) \leq V^{max}, \tag{7.6}$$

for all $k \geq 0$. Furthermore, the pumps in the geothermal system have a minimal and maximal capacity. Therefore we also have that

$$u^{min} \leq u(k) \leq u^{max}, \tag{7.7}$$

for all $k \geq 0$, and where u^{max} is defined as in Section 7.1.1. Lastly, the porosity, and therefore also the pressure drop, in the geothermal reservoir (see (Daniilidis et al. 2017) for more details) can be affected by rapid changes in the flow rate. For this reason it is desirable to let the change in production rate of the geothermal system be upper and lower bounded, therefore let

$$\Delta u^{min} \leq u(k-1) - u(k) \leq \Delta u^{max}, \tag{7.8}$$

for all $k \geq 1$, with Δu^{min} and Δu^{max} reservoir specific constants. Let k_0 denote the current time step with corresponding input $u(k_0)$, $k_1 = k_0 + 1$ be the next time step and let $N_c \in \mathrm{N}$ be a control horizon. It is required that model dynamics (7.4) and constraints (7.6)-(7.8) are satisfied for all time $k \in \{k_1, \ldots, k_0 + N_c\}$. In order to write the model and constraints

in a more compact form the following state, input and auxiliary variables are defined

$$u = (u(k_1), \ldots, u(k_0 + N_c))^T$$
$$V = (V(k_1), ..., V(k_0 + N_c))^T.$$

Using this notation, (7.6) and (7.7) can now be written for $k \in \{k_1, \ldots, k_0 + N_c\}$ as

$$V^{min} \leq V \leq V^{max} \tag{7.9a}$$
$$u^{min} \leq u \leq u^{max}, \tag{7.9b}$$

where the inequality relations are to be intended component-wise. Moreover, again to facilitate a more compact form, the matrix $S \in \mathrm{R}^{N_c \times (N_c+1)}$ is defined as

$$S = \begin{pmatrix} 1 & -1 & 0 & \ldots & 0 & 0 \\ 0 & 1 & -1 & \ldots & 0 & 0 \\ 0 & 0 & 1 & \ldots & 0 & 0 \\ \vdots & \vdots & \vdots & \ddots & \vdots & \vdots \\ 0 & 0 & \ldots & \ldots & 1 & -1 \end{pmatrix}, \tag{7.10}$$

from which it follows that

$$\begin{pmatrix} u(k_0) - u(k_1) \\ u(k_1) - u(k_1 + 1) \\ \vdots \\ u(k_0 + N_c - 1) - u(k_0 + N_c) \end{pmatrix} = S \begin{pmatrix} u(k_o) \\ u \end{pmatrix}, \tag{7.11}$$

which implies that (7.8) for $k \in \{k_1, ..., k_0 + N_c\}$ reads as

$$\Delta u^{min} \leq S \begin{pmatrix} u(k_0) \\ u \end{pmatrix} \leq \Delta u^{max}. \tag{7.12}$$

Again using (7.10) it is possible to write (7.4) for $k \in \{k_1, ..., k_0 + N_c\}$as

$$0 = S \begin{pmatrix} V(k_0) \\ V \end{pmatrix} + u + d, \tag{7.13}$$

where

$$d = (d(k_1), \ldots, d(k_0 + N_c))^T. \tag{7.14}$$

Note that at time k_0, d is not known since it consists of future demands. To overcome

this, a prediction $\hat{d}$ is used for the implementation. These predictions can be based on weather forecasts, historical demand and/or known changes in the network such as planned maintenance or newly connected consumers. The controller that will be designed will in general perform better under more accurate predictions.

7.1.3 Model predictive controller design

In order to keep the storage from draining or flooding, a performance measure is introduced that penalizes a storage deviation from a predetermined reference value, which is taken as half the storage total volume. Furthermore, besides the hard constraint (7.12), the rate of change of the control input is also penalized in order to obtain a sufficiently smooth input. The overall performance measure is defined as a weighted sum of these two performance measures and is given by

$$J_{N_c}\left(V, u,\ \mathrm{u(k_0)}\right) = \sum_{k=1}^{N_c} \left(V(k) - \bar{V}\right)^2 + \alpha \| S \begin{pmatrix} u(k_0) \\ u \end{pmatrix} \|_2^2, \tag{7.15}$$

where α is a positive dimensionless parameter. Minimizing (7.15) implies that storage deviations and the rate of change of the input are penalized. Which one of the two is penalized more aggressively can be decided by attributing a value to α. Having the predictions, constraints and objectives defined, the controller can be designed.

As before, let k_0 denote the current time step. First the controller makes a prediction $\hat{d}$ of the disturbance over a finite control horizon N_c. This prediction is used to solve an optimization problem that results in a vector of inputs u of which only $u(k_1)$ is implemented. After the implementation the system evolves under the actual disturbance after which the time window is shifted such that current time step k_0 is set to k_1. These steps are then reiterated for all upcoming time steps. At each iteration step the following optimization problem is solved

$$\begin{aligned} \underset{u}{\text{minimize}} \quad & J_{N_c}\left(V, u,\ \mathrm{u(k_0)}\right) \\ \text{subject to} \quad & V^{min} \leq V(k) \leq V^{max} \\ & u^{min} \leq u \leq u^{max} \\ & \Delta u^{min} \leq S \begin{pmatrix} u(k_0) \\ u \end{pmatrix} \leq \Delta u^{max} \\ & 0 = S \begin{pmatrix} V(k_0) \\ V \end{pmatrix} + u + \hat{d}. \end{aligned} \tag{7.16}$$

In the case one wants to control not only the geothermal system but also the backup

system, the backup production costs and the possible constraints associated with such a backup system can be included in the objective function and constraints of (7.16), respectively. In this way the MPC controls both the geothermal system, as well as the backup facility by minimizing the production costs. However, as mentioned before, control of any backup system is considered out of the scope of this chapter and therefore neglected.

7.2 Modeling of the Groningen reservoir

In order to evaluate the impact on the reservoir using a varying production, a reservoir model was used. Since project level studies are needed to understand geothermal systems and gain insights, the model is based on data from the Groningen geothermal project (Daniilidis et al. 2016).

The model was built in the PetraSim pre-post processor (Rockware 2014), using the TOUGHREACT (Xu et al. 2006) code for chemically reactive, non-isothermal flow and utilizing the EOS1 (Equation of State) (Pruess et al. 2012). The TOUGHREACT code uses space discretization through Internal Finite Difference (IFD) (Narasimhan and Witherspoon 1976). The solver uses a sequential iteration approach for coupling between fluid and reactive flow (Yeh and Tripathi 1991).

The simulation includes a chemically reactive flow model which we briefly introduce. Overall characteristics and architecture are presented in Table 7.1 and Figure 7.2 respectively. The model is largely based on the model geometry and characteristics of the Groningen 3D reservoir model (Daniilidis et al. 2016). Simplifications were made to adapt the model from 3D to 2D. The contacts of the stratigraphic layers in the model are now horizontal, using the average depth of the respective 3D model layers; furthermore, the layers thickness is also averaged for each respective interval. The wells are vertical, maintaining at a distance of 1275m from each other at reservoir depth. The horizontal discretization of the mesh is symmetrical; it uses a finer mesh (5m) close to the wells that gradually coarsens (40m) towards the middle part of the reservoir (Figure 7.2). The Rotliegend Slochteren layers (upper and lower members) were used as the reservoir body for injection of cold and production of hot water. Vertical discretization ensures a constant thickness of the layers inside the producing interval. The results of this part of the simulation is considered outside of the scope of this thesis and are therefore not discussed but can be found in (Daniilidis et al. 2017).

Petrophysical data for porosity and permeability were obtained from Panterra (van Leeuwen et al. 2014) and were weighted to the most proximal well to the project area as presented in previous research (Daniilidis et al. 2016). Probability levels 90%, 50% and 10% are derived per reservoir layer and are denoted by P90, P50 and P10 (summarized

Overview	
Dimensions (X, Y, Z)	1275m x10m x 900m
Lithostratigraphic units	10
Vertical discretization	according to layer
Vertical layers	35
Horizontal discretization	5m, successively increasing
Horizontal cell increment factor	1.138
Reservoir layer height	≥10m and ≤12.5m
Total cell count	1,785
Average reservoir depth	3595m
Reservoir thickness	248m
Temperature gradient	31.3°C/km
Pressure gradient	hydrostatic[1]

Table 7.1: Characteristics of the reservoir model. A visual representation of the mesh can be found in Figure 7.2.

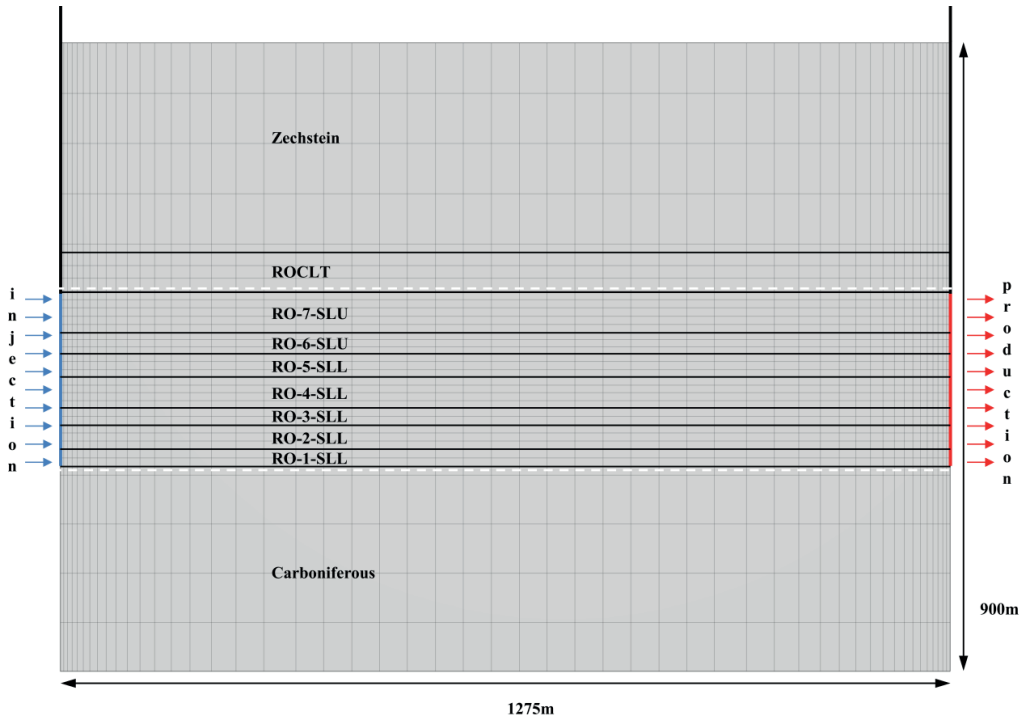

Figure 7.2: Reservoir model mesh. The productive layers consist of the SLU and SLL members, which are outlined by the white dashed lines.

	Permeability P90	Permeability P50	Permeability P10	Porosity	Density	Wet heat conductivity	Specific heat	Thickness
Unit	m^2 10^{-14}.	m^2 10^{-14}.	m^2 10^{-14}.	%	$\frac{kg}{m^3}$	$\frac{W}{Wm \cdot K}$	$\frac{J}{kg \cdot m}$	m
Zechstein	0.987	0.987	0.987	1.0	2170	3.5	1050	300
ROCLT	0.010	0.010	0.010	12.0	2625	3.0	840	56
Ro-7-SLU	0.098	0.222	0.913	17.4	2700	2.9	840	59
RO-6-SLU	1.474	4.700	14.946	18.5	2515	2.9	827	30
RO-5-SLL	1.357	4.336	13.829	17.7	2625	2.9	827	34
RO-4-SLL	1.413	4.565	15.100	19.5	2590	2.9	827	44
RO-3-SLL	1.049	3.411	11.239	17.5	2728	2.9	827	24
RO-2-SLL	0.265	1.073	4.133	18.3	2596	2.9	827	32
RO-1-SLL	0.426	1.437	4.743	14.9	2853	2.9	827	25
Carbo-niferous	9.87e-3	9.87e-3	9.87e-3	1.0	2900	2.7	840	400

Table 7.2: Model layer characteristics. Grouping the permeability values in P90-P50-P10 scenarios, the permeability range is taken into account as a worst-middle-best estimation, based on the petrophysical data presented. Vertical permeability is an order of magnitude lower than horizontal for all layers (Carlson 2003).

in Table 7.2).

The top and bottom cells were used as boundary conditions for the numerical simulation. The values for the temperature and pressure in the boundary cells were computed based on the respective pressure and temperature gradients (Table 7.1). Their distance to the productive reservoir ensures that they do not interfere with the reactive flow in the reservoir cells. Furthermore the boundaries remain valid in this geothermal setting that is dominated by conductive heat transfer (Moeck 2014).

The TOUGHREACT code includes mineral compositions and their reaction mechanisms. However, we consider the discussion of these mechanisms out of the scope of this thesis and we refer the reader to (Daniilidis et al. 2017) for more details.

Pressure depletion [bar]	Permeability [-]	Flow rate control strategy $\left[\frac{m^3}{h}\right]$	Re-injection temperature $[^\circ C]$	Injection pH [-]
0	P90	MPC output	40	4
100	P50	constant max	55	5.5
200	P10	constant min	70	7

Table 7.3: Uncertainty classes and respective discrete parameters considered. In total 243 unique reservoir simulation realizations are computed. The flow rate levels are unique for each re-injection temperature level as the heat content of the injected water changes. Therefore MPC, constant min and constant max flow rate levels are adjusted accordingly to reflect this (see also Figure 7.5).

7.3 Simulations of the controller in closed loop with the storage and demand

As mentioned in Section 7.1 a Groningen case study is considered. In this case study a simulation of the MPC is performed and presented under a suitable choice of parameters. In order to simulate the district heating network in closed loop with the MPC, the demand pattern for the Groningen case study is firstly introduced. This heat demand pattern is depicted in Figure 7.3a and is obtained from a statistical model representing 10,000 households.

Since the re-injection temperature of the geothermal system has a big influence on the energetic performance of the overall system, three different simulations are performed, each with a different return temperature. Along with the different temperatures, several other parameters are introduced in these simulations and are summarised in Table 7.4.

The parameters in Table 7.4 are physical constants or control parameters tuned for case specific conditions. In order to guarantee that the change in input stays small, $\Delta u^{\max}$ and $\Delta u^{\min}$ are chosen close to zero while α is large. It must be noted that the storage size is chosen larger than is desired in practice. However, depending on the demand pattern and requirements of the controller, the storage size can be taken smaller as is discussed in Section 7.3.1. Also the accuracy of the expected demand $\hat{d}$ plays a big role in the admissible storage sizing. The expected demand in the simulation is solely based on historical data and therefore does not rely on any predictions. As a consequence the performance of the controller can be improved if for example weather predictions are used.

Let k_0 be the current time step at which the demand is predicted. A heuristic demand

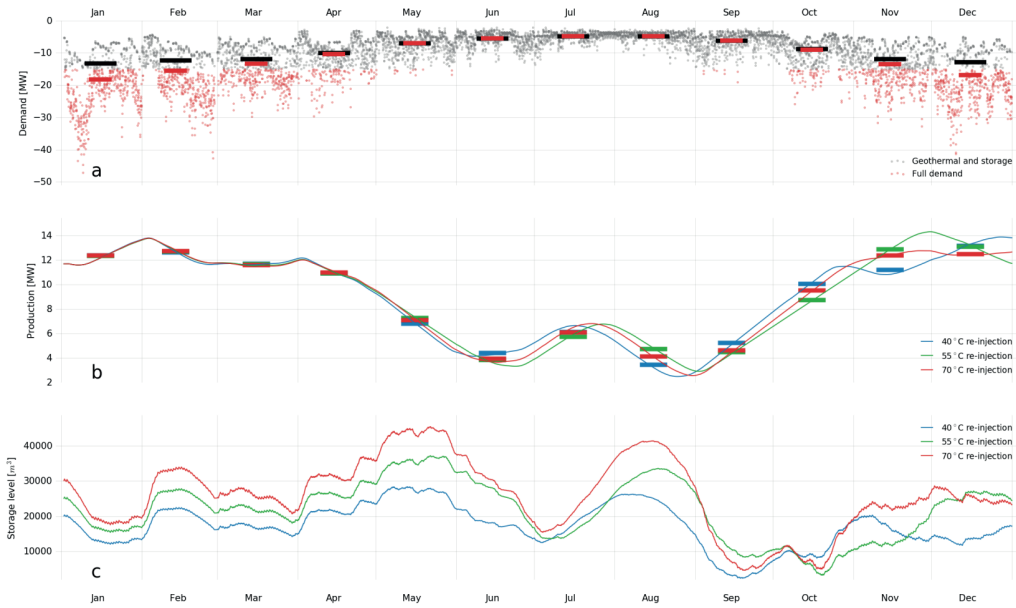

Figure 7.3: Model heating energy demand data per hour from the geothermal project of Groningen city (a). An upper limit of 15MW is used in the MPC for the geothermal system that is sufficient for 77% of the demand points; the demand in excess of this limit is expected to be delivered by other means, namely bio-gas burners. The markers represent the monthly averages of full and geothermal supplied demand. Production levels of the geothermal system resulting from the MPC (b). The markers represent resampled monthly averages of the data series and are used as flow rate levels in the reactive flow simulations. Storage levels for the respective scenarios (c).

prediction is made in which the average demand of the past three days is used, *i.e.*

$$\hat{d}(k) \;=\; \frac{1}{3}(d(k-24) \;+ d(k-2\cdot 24) \;+ d(k-3\cdot 24)), \tag{7.17}$$

for all $k \in \{t_1, \ \ldots, \ min\,(k_0 + N_c, \ \mathrm{k}_0 + 24)\}$ with k given in hours. For $k > k_0 + 24$ (since $N_c > 24$) let the prediction be equal to $\hat{d}(k_c)$ as in (7.16), where k_c is the corresponding hour on the first predicted day. Since on the first two days no historical data is available, it is for simplicity assumed that the average demand of these days are known and used.

The optimization problem that is solved in each iteration step is solved using CVX (Grant et al. 2008). The results of the simulations can be found in Figure 7.3b&c. It can be seen that the production is very low frequent in spite of the high frequent consumption. Furthermore, the volume capacity and production rate constraints are satisfied throughout the simulation.

Parameter	unit	sim 1	sim 2	sim 3
Re-Injection T (ΔT)	$°C$	40 (80)	55 (65)	70 (50)
c_p	$\frac{J}{g \cdot K}$	4077.2	4181.3	4190.0
ρ	$\frac{kg}{m^3}$	971.6	971.6	971.6
Δu^{min}	$\frac{m^3}{h}$	$-8 \cdot 10^{-2}$	$-8 \cdot 10^{-2}$	$-10 \cdot 10^{-2}$
Δu^{max}	$\frac{m^3}{h}$	$8 \cdot 10^{-2}$	$8 \cdot 10^{-2}$	$10 \cdot 10^{-2}$
V^{min}	m^3	0	0	0
V^{max}	m^3	$4 \cdot 10^4$	$5 \cdot 10^4$	$6 \cdot 10^4$
$\bar{V}$	m^3	$2 \cdot 10^4$	$2.5 \cdot 10^4$	$3 \cdot 10^4$
u^{min}	$\frac{m^3}{h}$	21.59	22.67	22.67
u^{max}	$\frac{m^3}{h}$	233.68	245.39	245.39
d^{max}	MW	15	15	15
α		10^4	10^4	10^4
Simulation time	h	24·364	24·364	24·364
N_c		2·24	2·24	2·24

Table 7.4: Parameters for the physical contacts obtained by controller tuning.

7.3.1 Tuning of the control parameters

In this section the influence of the parameters on the performance of the controller is discussed. As can be seen from (7.3) the demand d depends on the reciprocal of ΔT. For this reason the demand d increases for a decreasing ΔT given that d_g remains the same. A decrease in α results into a higher fluctuating production and lower deviation from the storage reference value. This has the consequence that a smaller storage device can be used without encountering a non-feasible solution in one of the iterations. An adjustment of the rate constraints Δu^{min} and $\Delta u^{\max}$ towards zero has a similar effect as the decrease of α. However, Δu^{min} and $\Delta u^{\max}$ only constrain the extreme rate changes and therefore do not affect small variations of the input. An increase on the control horizon N_c can, but does not necessarily, result in a better performance. To illustrate the influence of α, Δu^{min}, $\Delta u^{\max}$ and N_c the same simulation as in Figure 7.3 is performed but with values $\alpha = 10$, $\Delta u^{\min} = -0.3$, $\Delta u^{\max} = 0.3$ and $N_c = 20 \cdot 24$. The result can be found in Figure 7.4 in which a significantly smaller storage size suffices to meet the total demand. The drawback of taking $\Delta u^{\max}$ larger and $\Delta u^{\min}$ smaller is that resulting input has a higher fluctuation which could lead to undesired behaviour in the geothermal reservoir. Furthermore, increasing N_c leads to an increased simulation time caused by the increase in number of states in the optimization. If such a controller is implemented in practice, a necessary condition for the controller to work is that the time to solve optimization problem (7.16) is strictly smaller than the time step. Since the time step is taken as one

Figure 7.4: Geothermal system flow rate (a) and corresponding storage level (b) for a re-injection temperature of 40°C.

hour, only large values of N_c (*e.g.* $> 10^3$ hours) can result into non-feasible computation times. The minimal and maximal production levels u^{min} and $u^{\max}$ are determined by the physical constraints of the pipes, pumps and the characteristics of the well. If the demand pattern exceeds this upper or lower limit for large periods of time, the demand needs to rely on the storage device for the excess demand. Depending on the storage size and state at that time a non-feasible solution might appear and should therefore be treated with caution. Lastly, more accurate predictions result in smaller storage reference value deviations and therefore smaller storages can be used.

7.4 Simulations of the the reservoir

To account for the inherent uncertainty regarding geological data, but also to evaluate operational possibilities, a discrete parameter analysis is used. Uncertainty is taken into account regarding the initial reservoir pressure, the reservoir permeability, flow rate control strategy, re-injection temperature and injection pH (Table 7.3). The uncertainty classes cover the initial reservoir state (pressure depletion) and geological uncertainty (mainly permeability related), which are determined by the field conditions. Additionally the operational parameters of the flow rate control strategy, the re-injection tempe-

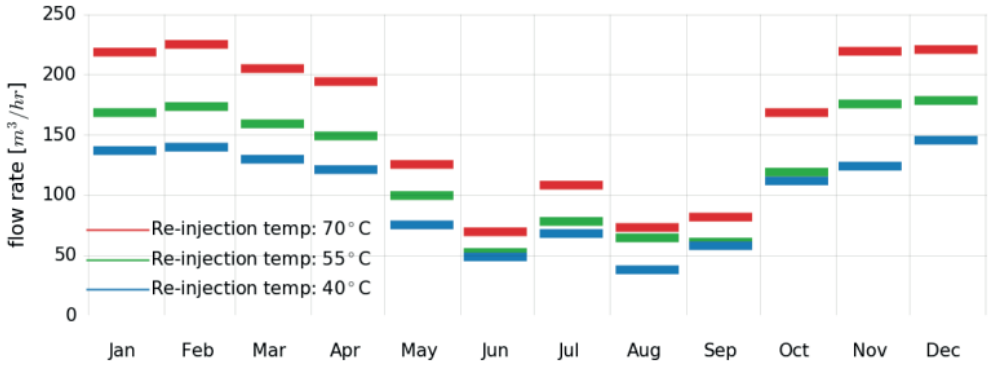

Figure 7.5: Flow rate levels for the different re-injection temperatures. Since the demand curve is expressed in MW (and it is unique for each re-injection temperature, see Figure 7.4b), the flow rates have to be adjusted accordingly when using different re-injection temperatures. Consequently, min and max flow rate control strategy levels for different re-injection temperatures are different for each scenario.

rature and the injection pH provide some degree of freedom in designing the geothermal system (Daniilidis et al. 2016). All these uncertainties result in 243 scenarios in which the effects on reservoir pressure, permeability change, power output at the injector and 2D property changes are analyzed.

Changes in pressure, temperature, permeability and chemical composition could affect the output of the geothermal system. It is therefore important to investigate what the consequences of time varying production are for the reservoir. For these reasons 2D reservoir simulations are carried out comparing constant and time varying production. In order to take the uncertainty of the reservoir parameters into account the simulations are performed for several scenarios, as discussed in the methods section. The results shown hereafter include data from all the performed simulations with the exception of the two dimensional plots.

The production rates that result from the MPC simulation are used as input for the reservoir simulation. However, due to the large timespan of the simulation (50 years) and total number of simulations (243) a lower resolution is used by taking the monthly averages (Figure 7.5). One needs to keep in mind that the resampling might affect the simulation results. That is, due to low frequent resampling, the high frequent behaviour of the production flow rate is neglected in the analysis of the reservoir. However, due to the conservative choices of α Δu^{max} and $\Delta u^{\min}$, the production flow rate is already low frequent which implies that the resampling is a good approximation of the original one. The obtained yearly pattern is then used as input for each of the 50 years of the reservoir simulations.

In these simulations the changes in the pressure difference between the producer and injector, the permeability around the injector ad the power production in the reservoir are investigated. After this investigation a comparison between the different flow rate control strategies (MPC, constant max and constant min) is made for the temperatures in the reservoir.

First the influence of the re-injection temperature, permeability and flow rate control strategy on the pressure is investigated. The pressure difference between the wells is mainly determined by reservoir permeability as seen by the distinct grouping of the results (Figure 7.6). A high permeability value (P10) results in a small Δp while for a low permeability (P90) we observe higher levels of pressure difference between the wells. The MPC controlled flow rate levels appear to fall between their respective max and min flow rate intervals. Moreover the range of Δp is broader for the P90 permeability scenarios; this range is attributed to the other parameters (injection pH and depletion).

A low re-injection temperature (40°C) results in a lower pressure difference compared to a high re-injection temperature. This effect is not very pronounced as the differences are in the order of a few bars. Causally the re-injection temperature effect on the pressure could be explained by the permeability changes in the reservoir.

All flow rate levels exhibit a slight increase of pressure over time, but this increase is more prominent for the P90 scenarios. When present, the pressure increase is gradual and never exceeds 50% of the initial pressure. The highest pressure increase is observed in the case of a constant max flow rate and less so for the MPC flow rate levels. The pressure increase for the min flow rate levels is only marginal. These results are consistent with the permeability results presented hereafter.

7.4.1 Power production, energy reserve and permeability of the reservoir

As discussed in Section 7.1.2, the power production P (in Watt) of the geothermal is derived from equation (7.5). However, the temperature and pressure are not necessarily constant which can result in a deviation from the desired power output; this deviation can be attributed to enthalpy changes, according to:

$$\Delta H = c_{pw}\Delta T + V(1 - \beta T)\Delta p, \tag{7.18}$$

where ΔH is the enthalpy change, ΔT the temperature change, V the volume, β the coefficient of thermal expansion, T the temperature and Δp the pressure change in the system. The simulations show that the deviations from the desired power output can be attributed to changing pressure levels inside the reservoir (Figure 7.7b). This is because these changes ultimately affect the producer T_p causing small temperature variations resulting in these minor changes in produced power.

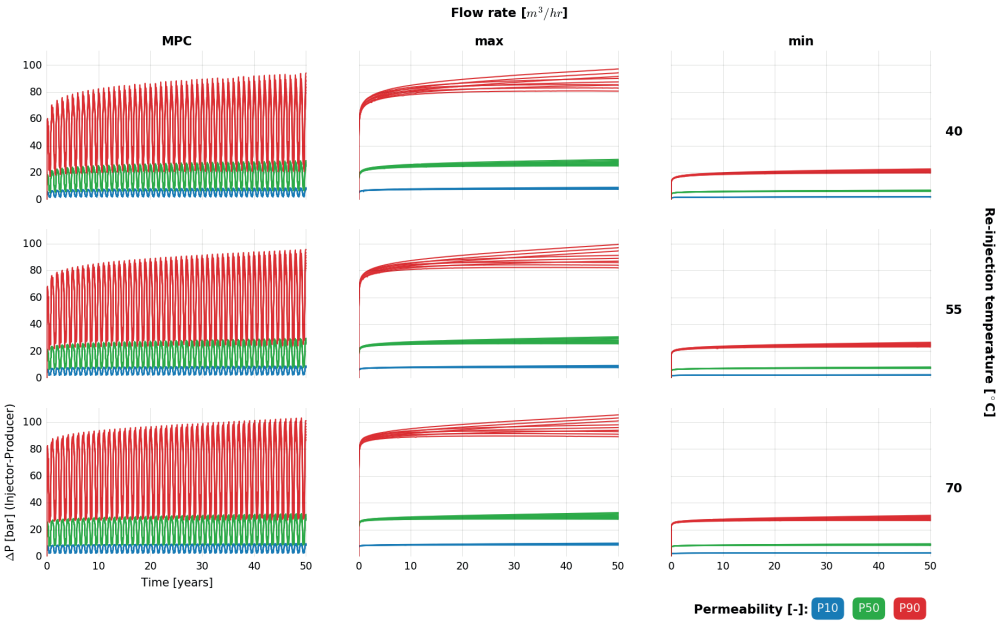

Figure 7.6: Pressure difference between the wells for all simulations. The data series are colored based on their permeability specifications. The subplot horizontal axis differentiates the flow rate levels, while the subplot vertical axis differentiates the re-injection temperature. All subplots use the same scale and are therefore cross-comparable.

The simulation results illustrate the dependency between the flow rate, temperature and power output (Figure 7.7). A first observation is that the power output in all simulations that use the MPC flow rate control strategy, is contained within power production levels corresponding to minimal and maximal flow rate (see also Figure 7.5). Secondly, we observe a small decrease in the power output, when moving from no depletion to 200 bar of depletion in the initial reservoir conditions (Figure 7.7b). Although small (between 1 MW and 1.7 MW), this decrease needs to be considered in designing and sizing the installation in case of pressure depletion. Lastly, the re-injection temperature levels cause minor changes (~0.5MW) in the power output (Figure 7.7c).

The permeability in the reservoir is not necessarily constant; changes in permeability are related to changes in mineral volume fraction, which are in turn affected by the simulation input parameters like the initial mineral compositions and their reaction mechanisms. These mineral compositions and their reaction mechanisms are studied in detailed in (Daniilidis et al. 2017) but are considered outside of the scope of this thesis and therefore not discussed here.

In order to compare the differences between the flow rate levels of the MPC and

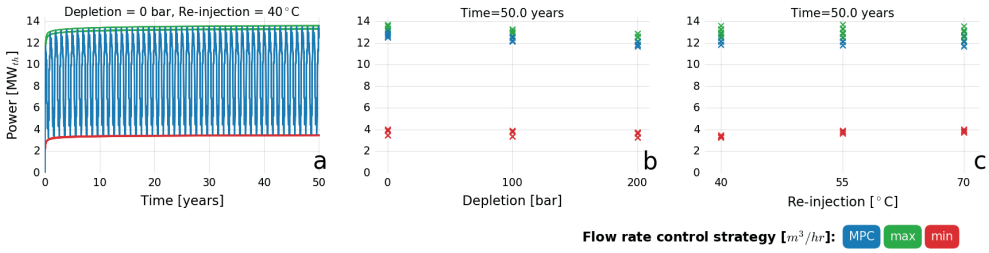

Figure 7.7: Doublet power production. The data series are coloured based on their flow rate levels. The time series data reveal no drop of power over time (a). Depletion level at year 50 reveal some difference between the power outputs (b), while re-injection temperature shows only marginal differentiation (c) for all simulations.

the max scenarios in terms of life expectancy of the geothermal system, the 2D heat distribution in the reservoir is analyzed. Under the MPC control strategy and after 50 years of production the cold front propagates to about a quarter of the distance between the injector and producer wells (Figure 7.8a). Using the max flow rate levels for the same re-injection temperature the cold front propagates further to about a third of the well distance (Figure 7.8b). The difference between the two scenarios (Figure 7.8c) highlights the benefits in terms of a more sustainable use of the geothermal resource when utilizing the MPC flow rate levels.

7.5 Discussion

The coupling of the controller with the reservoir model provides new insights regarding the energy network that they are both part of. These insights can facilitate a stronger integration between the system parts if they are analyzed and developed in tandem, while possible incompatibilities can be mapped out. As a result, the production of heat is constrained by the geothermal system specifications, while the geothermal system itself is more efficiently utilized by responding to demand changes.

The designed controller is able to generate a real time production level using demand predictions and storage level measurements as input. It is guaranteed that these productions levels satisfy several hard constraints. These include storage capacity constraints, minimal and maximal production levels and production rate constraints. There is insufficient research available to determine the values of the latter constraint. Moreover, if such bounds would be available, it is most likely that they depend on the characteristics of the geothermal system and are therefore case specific. Fortunately, the controller is designed such that updated values can be included once they are available. It implies that the methods and design presented in this chapter should be considered as a proof of

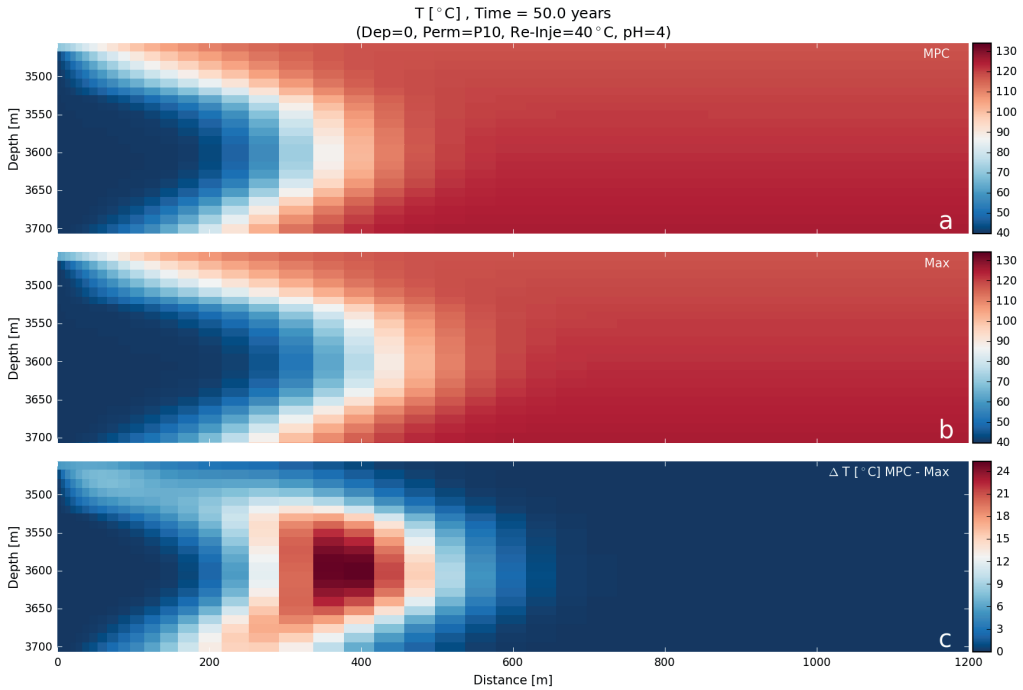

Figure 7.8: Reservoir temperature for (a) MPC flow rate, (b) Max flow rate and (c) the difference between the two scenarios. Other simulations parameters are the same for both flow rates.

concept.

It is well known that the stability of a MPC is hard to guarantee (Mayne et al. 2000). The stability depends on the constraints, demand pattern, objective function, control horizon and demand prediction. A sufficiently large storage device results in a set of constraints that is easier to satisfy and therefore in a stable system. However, due to the high costs this is undesirable in practice. For this reason, additional tuning (see for example (Lee and Yu 1994)), better predictions (see for example (Dotzauer 2002)) and the integrated control of additional heat sources should be addressed in future work.

With regard to the geothermal system, the relative changes in pressure levels can be explained by the geochemical changes in the reservoir. The changes in pressure over time appear to be minor (Daniilidis et al. 2017); this is in line with the mostly increasing permeability around the injector well. Notably the variable production rates of the geothermal system (as presented with the MPC control strategy) alter only the rate and not the nature of the changes in the chemical reservoir properties (Daniilidis et al. 2017). Initial pressure depletion in the Groningen case history does not appear to have a significant effect in any of the results. Especially the geochemical behavior and the precipi-

tation or dissolution of minerals is unaffected by possible pressure depletion (Daniilidis et al. 2017).

Chapter 8

Conclusions

We discus the results of this thesis and provide an outlook for open problems left as future work. In Chapter 3 we presented a model of a district heating system with a storage device, single producer and multiple consumers. The proposed controller is able to regulate the energy level in the storage device to a desired setpoint in spite of unmeasured, possibly time varying, heat demand. The inputs for the controllers that regulate the flows are set by a constant. An interesting extension is to let this constant depend on temperature measurements in the heat exchanger. In that way a feedback loop is created between the controllers and system dynamics of the temperatures and the flows, which require a modification of the analysis. Another extension is to consider a topology with multiple producers and storage tanks as in Chapters 4 and 5 that include the temperature dynamics. In such a setup an interesting generalization is to consider heterogenous setpoints for the temperatures. For example one could consider an optimization problem which provides these setpoints such that temperature cascading, in which the leftover heat coming from a consumer is re-used by other consumers, is optimally controlled with respect to the total costs. Lastly, an interesting extension is to study the controller under the presence of heat dissipation and time delays.

In Chapter 4 we proposed feedback controllers that dynamically adjusts the inputs and flows in a flow network to regulate the measured output at the nodes towards a desired setpoint. This is done using distributed controllers and in the presence of an unknown disturbance. The controllers are composed of two parts: the first part regulates the flows on the edges, which results in load balancing, while the second part provides an optimal input on the nodes at steady state. To achieve the economic optimal input a communication network was introduced. When the inputs are required to be bounded for all time, a similar result is obtained with the difference that the closed loop system converges to a point that can be made arbitrary close to the optimal steady state by tuning the gains. The cost functions are assumed to be quadratic and using Lyapunov methods stability is proven in case not all quadratic cost coefficients are identical.

In Chapter 5 these results were extended by considering second-order controllers. Based on Lyapunov arguments and an invariance principle, we have proven that the de-

sired optimal steady state is globally asymptotically stable. A case study on district heating systems and a case study on multi-terminal HVDC networks showed the effectiveness of the proposed solution. Although not included in this thesis, we aim to extend the presented results to include nodes that are modelled as

$$0 = -\sum_{k\in\mathcal{N}_i} B_{ik}u_{fk}(t) + u_{pi}(t) - d_i$$
$$y_i(t) = h_i(x_i(t)),$$

resulting in a differential-algebraic system. Due to the coupling between the dynamics on the different nodes more communication is required, but we are able to prove similar results as in Chapter 5. There are various other extensions that could be made, of which we list a few. An open problem is to consider general convex cost functions instead of the linear-quadratic cost functions we use. Another interesting problem is to extend this setup to time-varying disturbances as considered in (Bürger et al. 2015), or extend it to a tracking problem of more general time varying signals. Furthermore, the required communication in the distributed control structure is continuous in the current setting. An interesting extension is to consider the case where communication happens at discrete times, leading to a hybrid system. Since the results are obtained without the common requirement of strict output passivity of the nodes, it is worth exploring whether the proposed control structure can be applied to a wider class of systems than the considered flow networks, such as for example power networks with capacity constraints (Li et al. 2011).

In Chapter 6 the design of a distributed nonlinear controller for hydraulic networks with a multi-pump architecture is investigated. To guarantee that the desired heat demand at each end-user can be fulfilled, the pressure drop at each end-user valve is regulated towards a desired reference value. Since most pumps are not able to generate negative pressures we impose an additional positivity constraint on the output of the controller, which is enforced by the use of nonlinear functions and a state dependent integral gain. We provide sufficient conditions under which local asymptotic stability of the desired steady state can be proven. Finally, we investigated the performance of the controllers on a case study by simulation. An underlying assumption in this work is that there is only one producer. An interesting extension is to consider a network topology with multiple producers and end-users. This additionally opens the research direction towards the optimal allocation of the required generation among the producers such as in Chapters 4 and 5. Furthermore, the proposed control structure could be generalized such that it can be applied to classes of port-Hamiltonian or Euler-Lagrange systems.

In Chapter 7 we combined the use of an MPC controller and a geothermal model to

investigate a more efficient integration of a geothermal sources in a heating or energy network. An MPC is well suited to control the production of a geothermal system due to its ability to take several hard constraints into account. The performance of the controller depends highly on the demand pattern, the tuning of the controller and the quality of the prediction. Furthermore, the performance is also affected by the lower and upper bound of the rate of change of a geothermal reservoir. Since these bounds are usually unknown, obtaining a method to find these bounds is an interesting open problem. The controller is designed such that it can be easily adapted to include different or additional constraints. Since a better performance leads to a smaller storage size it is desirable to investigate how this performance can be optimized. The findings suggest that for the case study of the Groningen geothermal project in Rotliegend sandstone the use of a variable production rate has no adverse geochemical effects on the reservoir. Moreover, it enables a more efficient use of the geothermal resource by limiting the heat extraction to levels dictated by existing demand. To improve the performance of the controller, additional tuning (see for example (Lee and Yu 1994)), better predictions (see for example (Dotzauer 2002)) and the integrated control of additional heat sources should be addressed in future work.

Concluding, we have investigated control strategies for the next generation of district heating networks. That is, a network that has smaller pipes and includes multiple producers, consumers and storages. Also, the possibilities and consequences of a time varying production for a specific kind of producer, namely a geothermal well, have been investigated.

Each chapters contributes a control design that solves a specific problem for a specific model. Ideally these various models and control problems should be integrated in one single system with corresponding model, controller design and stability analysis. More specific, the topology with multiple produces, storages and consumers along with the communication network that guarantees economic optimality as in Chapters 4 and 5, the models of the components as in Chapter 6 and the optimal storage setpoints generated by a model predictive controller should be combined. Moreover, the temperature dynamics as in Chapter 3 along with a model (or prediction) of the heat demand could be included to capture these additional dynamics and avoid undesirable temperature fluctuations. It is most likely that the controllers require some adjustments to guarantee stability and optimality, as the resulting nonlinear model would be different to the ones considered in this thesis.

Appendix A

Model derivation

In this appendix we derive a preliminary result that is used to model a heat exchanger and storage device. Furthermore we derive a relation between temperature, volume and energy in order to motivate Problem 3.1.

A.1 Temperature dynamics

In order to provide a relation between temperature, volume and energy we first introduce the notion of enthalpy. Consider therefore a control volume of an open system where the change in energy ΔE is given by

$$\Delta E = E^{in} - E^{out} + W + \Phi, \tag{A.1}$$

with E^{in} and E^{out} the total in and outflow of energy by mass streams. The total work supplied by the surroundings is given by W and Φ is the heat exchanged with the environment. The total amount of energy in a control volume can be expressed in terms of *enthalpy* and is defined as

$$H = E + pV, \tag{A.2}$$

with E the energy, p the pressure and V the volume. Since we deal with temperatures between 0°C and 100°C at atmospheric pressure, water only exists in liquid form and no phase changes or chemical reactions occur. Under the additional assumption of a constant heat capacity c_p, enthalpy is only a function of the temperature (see *e.g.* (Skogestad 2009)). This implies that

$$H - H|_{T=T^{\text{ref}}} = mc_p(T - T^{\text{ref}}), \tag{A.3}$$

where m is the mass of the control volume, T its temperature, T^{ref} an arbitrary fixed reference temperature and $H|_{T=T^{\text{ref}}}$ is the enthalpy associated with this reference temperature. The mass satisfies $m = \rho V$ with ρ being the density.

We assume perfect mixing within the control volume from which it follows that

the inside temperature T is equal to the outflow temperature. After straightforward but lengthy derivation (see also (Skogestad 2009)), the temperature dynamics of this control volume are

$$V\dot{T} = q^{in}(T^{in} - T) + P, \tag{A.4}$$

where q^{in} and T^{in} are the inflow rate and temperature, respectively. Moreover $P := \frac{1}{\rho c_p}\dot{\Phi}$ is the heat injection or extraction rate with ρ the density, c_p the specific heat and $\dot{\Phi}$ the heat exchange rate.

A.2 Motivation for Problem 3.1

Next we provide a relation between a volume with a certain temperature and the corresponding stored energy. This relations provides the main motivation for the formulation of Problem 3.1. In order to provide such a relation we consider a volume of heated water. Since such a body of water can only be used for heating if its temperature is higher that the outside temperature we compare the heat of the water to a reference temperature T^{ref}. Let us define a relative energy as

$$\hat{E} := E - E|_{T=T^{ref}}, \tag{A.5}$$

where $E|_{T=T^{ref}}$ is the energy of a control volume V at temperature T^{ref}, then from (A.2) and (A.3) we obtain

$$\begin{aligned}\hat{E} =& H - pV - (H - pV)|_{T=T^{ex}} \\ =& mc_p(T - T^{ref}) + H|_{T=T^{ref}} - pV - (H|_{T=T^{ref}} - pV) \\ =& c_p\rho V(T - T^{ref}).\end{aligned} \tag{A.6}$$

Observe now that solving Problem 3.1 guarantees

$$\lim_{t\to\infty} |\hat{E} - \hat{\overline{E}}| = 0, \tag{A.7}$$

where $\hat{\overline{E}} = c_p\rho\overline{V}(\overline{T} - T^{ref})$. For this reason we are able to split an energy setpoint tracking problem into a volume and temperature setpoint tracking problem. For example $\overline{T}$ can be chosen such that a minimal operating temperatures will be guaranteed and $\overline{V}$ can be changed over time to store energy for later use.

Appendix B

Useful lemma's

In this Appendix we provide several lemmas and their proofs which are presented in two sections. The lemmas that support the proof of Theorem 3.9 are presented in the first section and second section is dedicated to lemmas that support the proof of Theorem 4.20.

B.1 Supporting lemma's of Theorem 3.9

In order to prove Theorem 3.9 we introduce the following lemmas.

Lemma B.1 (Exponential stability of a linear time varying system)**.** *Suppose* $\dot{x}(t) = A(t)x(t)$ *with* $x(t_0) = x_0$ *is uniformly exponentially stable*[10]*. Also suppose there exists a finite constant* β *such that for all* τ *we have that*

$$\int_{\tau}^{\infty} \|F(\sigma)\| d\sigma \leq \beta, \tag{B.1}$$

holds for all $\tau > t_0$*. This implies that*

$$\dot{z}(t) = [A(t) + F(t)]\, z(t), \tag{B.2}$$

is also uniformly exponentially stable.

Proof. The proof can be found in (Rugh 1996, Theorem 8.5). ■

[10] A linear time varying system is *uniformly exponentially stable* if there exist finite positive constants γ and λ such that its solution satisfies

$$\|x(t)\| \leq \gamma e^{-\lambda(t-t_0)} \|x_0\| \qquad t \geq t_0, \tag{B.3}$$

for any initial condition x_0 and any $t_0 > 0$.

Lemma B.2 (Bounds for x_s and ν_p)**.** *Consider system (3.9b) with ν_p as in (3.11), then there exist $\beta_1, \beta_2, \beta_3 \in \mathbb{R}_{>0}$ such that*

$$\int_\tau^\infty \left| \frac{1}{x_s(\sigma)} - \frac{1}{\overline{x}_s} \right| d\sigma \leq \beta_1, \tag{B.4}$$

$$\int_\tau^\infty \left| \frac{1}{x_s(\sigma)} \left(\nu_p(\sigma) - \overline{\nu}_p \right) \right| d\sigma \leq \beta_2, \tag{B.5}$$

and

$$\int_\tau^\infty |x_s(\sigma) - \overline{x}_s| \, d\sigma \leq \beta_3, \tag{B.6}$$

for any $\tau \geq 0$.

Proof. Observe that (B.6) is equivalent to finding β_3 such that

$$|(x_s(0) - \overline{x}_s)| \int_\tau^\infty e^{-\alpha\sigma} d\sigma \leq \beta_3. \tag{B.7}$$

Due to Assumption 2.2 we have that

$$|(x_s(0) - \overline{x}_s)| \leq V^{\max} - 2V^{\min}, \tag{B.8}$$

and moreover

$$\int_\tau^\infty e^{-\alpha t} d\sigma \leq \frac{1}{\alpha}, \tag{B.9}$$

for all $\tau \geq 0$. Using (B.8) and (B.9) it follows that (B.6) is satisfied if we take

$$\beta_3 = \frac{V^{\max} - 2V^{\min}}{\alpha}. \tag{B.10}$$

In order to prove (B.4) we use the following inequality:

$$\int_\tau^\infty \left| \frac{1}{x_s(\sigma)} - \frac{1}{\overline{x}_s} \right| d\sigma \leq \int_0^\infty \left| \frac{\overline{x}_s - x_s(\sigma)}{\overline{x}_s x_s(\sigma)} \right| d\sigma. \tag{B.11}$$

From Lemma 3.6 we obtain the bound

$$\frac{1}{\overline{x}_s x_s(\sigma)} \leq \frac{1}{(V^{\min})^2} \quad \text{for all } \sigma \geq 0, \tag{B.12}$$

which, in light of (B.8), (B.11) and (3.12), gives

$$\int_\tau^\infty \left| \frac{1}{x_s(\sigma)} - \frac{1}{\overline{x}_s} \right| d\sigma \leq \frac{1}{(V^{\min})^2} \int_0^\infty e^{-\alpha\sigma} \, |\overline{x}_s - x_s(0)| \, d\sigma.$$

Therefore (B.4) is satisfied if we take

$$\beta_1 = \frac{V^{\max} - 2V^{\min}}{\alpha(V^{\min})^2}. \tag{B.13}$$

Lastly, we prove that (B.5) is satisfied. By definition of (3.11) we have that

$$\frac{1}{\alpha\overline{x}_s}\int_\tau^\infty \left|\frac{1}{x_s(\sigma)}\left(v_p(\sigma) - \overline{v}_p\right)\right| d\sigma = \int_\tau^\infty \left|\frac{1}{x_s(\sigma)} - \frac{1}{\overline{x}_s}\right| d\sigma.$$

From this and (B.13) it follows therefore that (B.4) is satisfied if we take

$$\beta_2 := \frac{V^{\max} - 2V^{\min}}{\alpha^2(V^{\min})^3}, \tag{B.14}$$

which concludes the proof. ∎

Lemma B.3 (Exponential stability of (3.28) with $B'w = 0$)**.** *The origin of*

$$\dot{\zeta} = (A' + F'(t))\zeta, \tag{B.15}$$

is uniformly exponentially stable with A' and F' given in (3.29) and (3.30).

Proof. We use Lemma B.1 in order to prove that the origin of (B.15) is uniformly exponentially stable. By design A' is a Hurwitz matrix and therefore

$$\dot{x}(t) = A'x(t), \tag{B.16}$$

is uniformly exponentially stable. Next we show that there exists a β such that

$$\int_\tau^\infty \|F'(\sigma)\| d\sigma \leq \beta, \tag{B.17}$$

for any $\tau \geq 0$. Using $\|AB\| \leq \|A\|\|B\|$ we observe that

$$\int_\tau^\infty \|F'(\sigma)\| d\sigma \leq \int_\tau^\infty \|A_e(\sigma)\| d\sigma + \|\overline{G}\| \int_\tau^\infty \|B_e(\sigma)\| d\sigma. \tag{B.18}$$

where $A_e(t)$ and $B_e(t)$ are as in (3.26) and

$$\overline{G} = \begin{pmatrix} KC & H \\ 0 & 0 \end{pmatrix}.$$

Moreover

$$\|A_e\| \leq \|M(x)^{-1}[\nu^e] - M(\overline{x})^{-1}\| \cdot \|A(\overline{\nu})\| \tag{B.19}$$

$$\|B_e\| \leq \|M(x)^{-1} - M(\overline{x})^{-1}\| \cdot \|U\|, \tag{B.20}$$

with $A(\overline{\nu})$ and U as in (2.20a) and

$$\nu^e = \begin{pmatrix} \frac{\nu_p}{\overline{\nu}_p} & \frac{\nu_p}{\overline{\nu}_p} & 1 & \mathbf{1}_n^T \end{pmatrix}^T. \tag{B.21}$$

Since all time varying entries on the right hand side of both (B.19) and (B.20) enter in diagonal form, (B.17) is satisfied if there exists $\beta_{1,i}$ and $\beta_{2,i}$ such that

$$\begin{aligned} \int_\tau^\infty \left| \frac{\nu_i^e(\sigma)}{[M(x(\sigma))]_{ii}} - \frac{1}{[M(\overline{x})]_{ii}} \right| d\sigma \leq \beta_{1,i} \\ \int_\tau^\infty \left| \frac{1}{[M(x(\sigma))]_{ii}} - \frac{1}{[M(\overline{x})]_{ii}} \right| d\sigma \leq \beta_{2,i}, \end{aligned} \tag{B.22}$$

are satisfied for all i, where $[M(x(\sigma))]_{ii}$ is the i-th diagonal component of $M(x(\sigma))$. Notice that

$$\frac{\nu_i^e(\sigma)}{[M(x(\sigma))]_{ii}} - \frac{1}{[M(\overline{x})]_{ii}} = \begin{cases} \frac{1}{\overline{\nu}_p V^P}\left(\nu_p - \overline{\nu}_p\right) & \text{for } i = 1 \\ \frac{1}{\overline{\nu}_p}\left(\frac{\nu_p}{x_s} - \frac{\overline{\nu}_p}{\overline{x}_s}\right) & \text{for } i = 2 \\ \frac{1}{x_{\bar{s}}} - \frac{1}{\overline{x}_{\bar{s}}} & \text{for } i = 3 \\ 0 & \text{for } i \geq 4, \end{cases} \tag{B.23}$$

and

$$\frac{1}{[M(x(\sigma))]_{ii}} - \frac{1}{[M(\overline{x})]_{ii}} = \begin{cases} 0 & \text{for } i = 1 \\ \frac{1}{x_s} - \frac{1}{\overline{x}_s} & \text{for } i = 2 \\ \frac{1}{x_{\bar{s}}} - \frac{1}{\overline{x}_{\bar{s}}} & \text{for } i = 3 \\ 0 & \text{for } i \geq 4. \end{cases} \tag{B.24}$$

By definition of (3.11) we have $\nu_p - \overline{\nu}_p = \overline{\nu}_p\,(\overline{x}_s - x_s)$ implying that

$$\frac{1}{\overline{\nu}_p V^P}\left(\nu_p - \overline{\nu}_p\right) = \frac{\upsilon}{\overline{\nu}_p V^P}\,(\overline{x}_s - x_s) \tag{B.25}$$

$$\frac{1}{\overline{\nu}_p}\left(\frac{\nu_p}{x_s} - \frac{\overline{\nu}_p}{\overline{x}_s}\right) = \frac{\upsilon}{\overline{\nu}_p}\frac{\overline{x}_s - x_s}{x_s} + \overline{\nu}_p\left(\frac{1}{x_s} - \frac{1}{\overline{x}_s}\right). \tag{B.26}$$

From Lemma B.2 it follows that there exists a $\tilde{\beta}_1, \tilde{\beta}_2, \tilde{\beta}_3$ and $\tilde{\beta}_4$ such that

$$\int_\tau^\infty \left| \frac{\overline{x}_s - x_s}{x_s} \right| d\sigma \leq \tilde{\beta}_1 \tag{B.27}$$

$$\int_\tau^\infty |x_s - \overline{x}_s| \, d\sigma \leq \tilde{\beta}_2 \tag{B.28}$$

$$\int_\tau^\infty \left| \frac{1}{x_s} - \frac{1}{\overline{x}_s} \right| d\sigma \leq \tilde{\beta}_3 \tag{B.29}$$

$$\int_\tau^\infty \left| \frac{1}{x_{\tilde{s}}} - \frac{1}{\overline{x}_{\tilde{s}}} \right| d\sigma \leq \tilde{\beta}_4, \tag{B.30}$$

an therefore there exists $\beta_{1,i}$ and $\beta_{2,i}$ such that (B.22) is satisfied for all i. Consequently, there exists a β such that (B.17) is satisfied and due to Lemma B.1 it follows that origin of (B.15) is uniformly exponentially stable. ■

B.2 Supporting lemma's of Theorem 4.20

In order to prove Theorem 4.20 we introduce the following lemmas.

Lemma B.4 (Multiple full rank conditions)**.** *Let Q be a diagonal matrix with positive entries, let $\overline{Q}$ and $\tilde{Q}$ be as in (4.36c) and (4.46), respectively and let Assumption 5.12 be satisfied, then $(\gamma\overline{Q} - L^{com}Q + \mathbb{1}\mathbb{1}^T)$, $(\gamma\overline{Q} - L^{com}Q + \frac{1}{n}\mathbb{1}\mathbb{1}^T)$ and $\tilde{Q}^T\tilde{Q}$ are full rank for all $\gamma \in \mathbb{R}_{\geq 0}$.*

Proof. We will first proof that all the columns of $\tilde{Q}$ are linearly independent for all $\gamma \in \mathbb{R}_{\geq 0}$. From this we will then conclude that $\tilde{Q}^T\tilde{Q}$, $(\gamma\overline{Q} - L^{com}Q + \mathbb{1}\mathbb{1}^T)$ and $(\gamma\overline{Q} - L^{com}Q + \frac{1}{n}\mathbb{1}\mathbb{1}^T)$ are full rank. Let

$$A_n := L^{com}Q - \gamma\overline{Q}, \tag{B.31}$$

now, since $\overline{Q}_{ij} \geq 0$ and $[L^{com}Q]_{ij} \leq 0$ for all $i \neq j$ we know that the off-diagonal elements of A_n are non-positive. Furthermore, since the graph associated to L^{com} is connected due to Assumption 5.12, we have that $L^{com}_{ii} > 0$ and since $\mathbb{1}^T(L^{com}Q - \gamma\overline{Q}) = 0$, all the diagonal elements of A_n are strictly positive. Therefore we can write

$$A_n = \begin{pmatrix} a_{11} & -a_{12} & \dots & -a_{1n} \\ -a_{21} & a_{22} & \dots & -a_{2n} \\ \vdots & \vdots & \ddots & \vdots \\ -a_{n1} & -a_{n2} & \dots & a_{nn} \end{pmatrix}, \tag{B.32}$$

with $a_{ii} > 0$ for all i and $a_{ij} \geq 0$ for all $i \neq j$. Moreover, since

$$\mathbb{1}^T(\gamma\overline{Q} - L^{com}Q) = 0, \tag{B.33}$$

we can conclude that the diagonal elements are equal to the negative column sum of the off diagonal elements, *i.e.* $a_{ii} = \sum_{k=1,k\neq i}^{n} a_{ki}$. We will now prove that $\tilde{Q}$ is full column rank. To this end we consider a square sub-matrix of $\tilde{Q}$ which we define as

$$\tilde{Q}_{sub} = \begin{pmatrix} A_{n-1} & -a_{[n]} \\ \mathbb{1}_{n-1}^T & 1 \end{pmatrix}, \tag{B.34}$$

where $a_{[n]} := \begin{pmatrix} a_{1n} & a_{2n} & \dots & a_{(n-1)n} \end{pmatrix}^T$. By the Schur complement we know that

$$\det(\overline{Q}_{sub}) = \det(A_{n-1} + a_{[n]}\mathbb{1}_{n-1}^T) = (1 + \mathbb{1}_{n-1}^T A_{n-1}^{-1} a_{[n]}) \det(A_{n-1}). \tag{B.35}$$

Since A_{n-1} is a diagonal column-dominant matrix we obtain from the Gershgorin circle theorem that all the eigenvalues of A_{n-1}^T are strictly positive. This implies that

$\det(A_{n-1}^T) \neq 0$ and since A_{n-1} is square we obtain $\det(A_{n-1}) \neq 0$. Furthermore, again due to the diagonal dominance property of A_{n-1}, we have that every principal minor (see *e.g.* (Fiedler and Ptak 1962) for a definition) of A_{n-1} is positive. This implies that A_{n-1} is inverse-positive, as is proven in (Fiedler and Ptak 1962). From this it follows that $\mathbb{1}_{n-1}^T A_{n-1}^{-1} a_{[n]} > 0$ which results in $\det(\tilde{Q}_{sub}) \neq 0$, implying that all the columns of $\tilde{Q}_{sub}$ are linearly independent. Since the number of columns of $\tilde{Q}$ and $\tilde{Q}_{sub}$ are equal, we can conclude that all the columns of $\tilde{Q}$ are linearly independent for all $\gamma \in \mathbb{R}_{\geq 0}$. This, and since $\tilde{Q}^T\tilde{Q}$ is a square matrix, immediately implies that $\tilde{Q}^T\tilde{Q}$ is full rank. Since $\tilde{Q}^T\tilde{Q}$ is full rank, it follows directly that also $(\gamma\overline{Q} - L^{com}Q + \frac{1}{n}\mathbb{1}\mathbb{1}^T)$ is full rank. In fact, suppose it is not full rank, then there exists a $x \neq 0$ such that $(\gamma\overline{Q} - L^{com}Q + \frac{1}{n}\mathbb{1}\mathbb{1}^T)x = 0$. Now observe that

$$\tilde{Q}^T\tilde{Q} = A_n^T A_n + \mathbb{1}\mathbb{1}^T = \left(\mathbb{1}\mathbb{1}^T - A_n\right)^T \left(\frac{1}{n}\mathbb{1}\mathbb{1}^T - A_n\right), \tag{B.36}$$

where A_n is as in (B.31). It therefore follows that $\tilde{Q}^T\tilde{Q}x = 0$, which is a contradiction with $\tilde{Q}^T\tilde{Q}$ being full rank. Using the same argumentation it follows directly from (B.36) that also $(\gamma\overline{Q} - L^{com}Q + \mathbb{1}\mathbb{1}^T)$ is full rank. ■

Lemma B.5 (Dynamics in incremental form)**.** *Let $\overline{\mu}$ be any solution to (4.20), $\overline{\theta}$ be as in (4.19) and $\hat{\theta}$, $\hat{\mu}$, $\hat{x}$ as defined as in (4.35), then the solution to (4.1) in closed loop with (4.32) and (4.33), satisfies*

$$\begin{aligned}
\dot{\tilde{x}} =& B\mathrm{sat}_\mu(\tilde{x}, \tilde{\mu}) + \gamma_\theta Q^{-1}\mathrm{sat}_\theta(\tilde{\theta}) \\
\dot{\tilde{\mu}} =& -\gamma_l L^{com}\mathrm{sat}_\theta(\tilde{\theta}) + \gamma_\theta\gamma_c Q^{-1}B\mathrm{sat}_\mu(\tilde{x}, \tilde{\mu}) - \gamma_\theta Q^{-1}\tilde{x} \\
\dot{\tilde{\theta}} =& \gamma_\mu B^T\tilde{x},
\end{aligned} \tag{B.37}$$

with $\tilde{x}$, $\tilde{\mu}$ and $\tilde{\theta}$ as in (4.34), $sat_\mu(\tilde{x}, \tilde{\mu})$ defined in (4.65) and $sat_\theta(\tilde{\theta})$ as in (4.66).

Proof. We first write system (4.1) in closed loop with (4.32) and (4.33) and obtain

$$\begin{aligned}
\dot{x} =& \gamma_\theta Q^{-1}\mathrm{sat}\left(\mu; \frac{1}{\gamma_\theta}Q(u^- + r), \frac{1}{\gamma_\theta}Q(u^+ + r)\right) \\
&+ B\mathrm{sat}\left(-\gamma_c B^T(x - \overline{x}) - \gamma_\mu\mu; 0, \lambda^+\right) + \overline{d} - Q^{-1}r \\
\dot{\mu} =& -\gamma_l L^{com}\mathrm{sat}\left(\mu; \frac{1}{\gamma_\theta}Q(u^- + r), \frac{1}{\gamma_\theta}Q(u^+ + r)\right) \\
&- \gamma_\theta Q^{-1}(x - \overline{x}) + \gamma_\theta\gamma_c Q^{-1}B\mathrm{sat}\left(-\gamma_c B^T(x - \overline{x}) - \gamma_\mu\mu; 0, \lambda^+\right) \\
\dot{\theta} =& \gamma_\mu B^T(x - \overline{x}),
\end{aligned} \tag{B.38}$$

where we used the identities $\mathrm{sat}(x + a; x^-, x^+) = \mathrm{sat}(x; x^- - a, x^+ - a) + a$ and $\mathrm{sat}(A^{-1}x; x^-, x^+) = A^{-1}\mathrm{sat}(x; Ax^-, Ax^+)$ for any vector a and diagonal matrix A. Using

(4.19), (4.20), (4.34) and (4.35) we can see that (B.38) gives the desired result. ■

Lemma B.6 (Error bounds)**.** *Let $\overline{Q}$ and Φ as in (4.36c) and (4.36d), then Φ^{-1} exists. Furthermore, let*

$$0 < \gamma \leq \frac{\zeta}{\|\Phi^{-1}\overline{Q}\|}, \tag{B.39}$$

for some $0 < \zeta < 1$, and let $\hat{u}$, $\hat{\lambda}$ and $\hat{x}$ be as in (4.57), (4.58) and (4.44), then

$$\|\hat{u}\| \leq \gamma \frac{1}{1-\zeta} \|\Phi^{-1}\overline{Q}^2 Q\tilde{d}\| \tag{B.40}$$

$$\|\hat{\lambda}\| \leq \gamma \frac{1}{1-\zeta} \|B^{\dagger}\| \cdot \|\Phi^{-1}\overline{Q}^2 Q\tilde{d}\| \tag{B.41}$$

$$\|\hat{x}\| \leq \frac{\gamma_c}{\mathbb{1}^T Q^{-1}\mathbb{1}} \left(\|\mathbb{1}\mathbb{1}^T Q^{-1}\overline{Q}Q\tilde{d}\| + \frac{\gamma}{1-\zeta} \|\mathbb{1}\mathbb{1}^T Q^{-1}\| \cdot \|\Phi^{-1}\overline{Q}^2 Q\tilde{d}\| \right). \tag{B.42}$$

Proof. First we prove that Φ^{-1} exists. From Lemma B.4 it follows directly that $(\gamma\overline{Q} + \Phi)$ is invertible for any $\gamma \geq 0$. By taking $\gamma = 0$ it follows that Φ^{-1} exists. Next we prove that (B.40)-(B.42) holds. To do this we make use of the following identity

$$\sum_{k=0}^{N} (-\gamma\Phi^{-1}\overline{Q})^k (I + \gamma\Phi^{-1}\overline{Q}) = I + (-1)^N (\gamma\Phi^{-1}\overline{Q})^{N+1}. \tag{B.43}$$

Due to (B.39) we have

$$\|\gamma\Phi^{-1}\overline{Q}\| < 1, \tag{B.44}$$

which implies that $I + \gamma\Phi^{-1}\overline{Q}$ is invertible. That is, suppose that $I + \gamma\Phi^{-1}\overline{Q}$ is not invertible, then there exists a non-zero x such that $(I + \gamma\Phi^{-1}\overline{Q})x = 0$. In such a case $0 \leq \|x\|(1 - \|\gamma\Phi^{-1}\overline{Q}\|)$, which contradicts (B.44). Then, after lengthy but standard arguments, (B.43) and (B.44) imply that

$$\sum_{k=0}^{\infty} (-\gamma\Phi^{-1}\overline{Q})^k = (I + \gamma\Phi^{-1}\overline{Q})^{-1}, \tag{B.45}$$

from which we obtain, together with (B.39), that

$$\|(I + \gamma\Phi^{-1}\overline{Q})^{-1}\| \leq \sum_{k=0}^{\infty} \|(-\gamma\Phi^{-1}\overline{Q})\|^k \leq \sum_{k=0}^{\infty} \zeta^k. \tag{B.46}$$

Notice that the right hand side of (B.46) is a standard geometric series and this implies

that

$$\| \left(\gamma \Phi^{-1} \overline{Q} + I \right)^{-1} \| \leq \frac{1}{1-\zeta}. \tag{B.47}$$

Combining (B.47) with (4.57) and (4.37) gives us that

$$\begin{aligned} \|\hat{u}\| =& \| - \gamma \left(\gamma \overline{Q} + \Phi \right)^{-1} \overline{Q}^2 Q \tilde{d} \| && \text{(B.48)} \\ \leq & \gamma \| \left(\gamma \Phi^{-1} \overline{Q} + I \right)^{-1} \| \cdot \| \Phi^{-1} \overline{Q}^2 Q \tilde{d} \| && \text{(B.49)} \\ \leq & \gamma \frac{1}{1-\zeta} \| \Phi^{-1} \overline{Q}^2 Q \tilde{d} \|, && \text{(B.50)} \end{aligned}$$

which proves (B.40). Similarly, combining (B.47) with (4.58) and (4.38) give us (B.41). Finally, again using (B.47) and combining this with (4.39), we obtain

$$\begin{aligned} \|\hat{x}\| =& \| - \gamma_c \frac{\mathbb{1}\mathbb{1}^T Q^{-1}}{\mathbb{1}^T Q^{-1} \mathbb{1}} \cdot \left(I - \gamma \left(\gamma \overline{Q} + \Phi \right)^{-1} \overline{Q} \right) \overline{Q} Q \tilde{d} \| \\ \leq & \frac{\gamma \gamma_c}{\mathbb{1}^T Q^{-1} \mathbb{1}} \| \mathbb{1}\mathbb{1}^T Q^{-1} \left(\gamma \overline{Q} + \Phi \right)^{-1} \overline{Q}^2 Q \tilde{d} \| + \frac{\gamma_c}{\mathbb{1}^T Q^{-1} \mathbb{1}} \| \mathbb{1}\mathbb{1}^T Q^{-1} \overline{Q} Q \tilde{d} \| \\ \leq & \frac{\gamma \gamma_c}{\mathbb{1}^T Q^{-1} \mathbb{1}} \frac{1}{1-\zeta} \| \mathbb{1}\mathbb{1}^T Q^{-1} \| \cdot \| \Phi^{-1} \overline{Q}^2 Q \tilde{d} \| + \frac{\gamma_c}{\mathbb{1}^T Q^{-1} \mathbb{1}} \| \mathbb{1}\mathbb{1}^T Q^{-1} \overline{Q} Q \tilde{d} \|, \end{aligned} \tag{B.51}$$

which implies (B.42) and concludes the proof. ■

Lemma B.7 (Conditions on the gains)**.** *Let $\hat{u}$, $\hat{\lambda}$ be as in (4.57), (4.58) and let $\hat{x}$ be as in (4.40) and (4.44). If γ_c, γ_θ and γ_l are such that for $0 < \zeta < 1$,*

$$\gamma_c < \frac{\mathbb{1}^T Q^{-1} \mathbb{1} \epsilon_x}{\| \mathbb{1}\mathbb{1}^T Q^{-1} \overline{Q} Q \tilde{d} \| + \| \mathbb{1}\mathbb{1}^T Q^{-1} \| \epsilon_u} \tag{B.52a}$$

$$\| \Phi^{-1} \overline{Q}^2 Q \tilde{d} \| \frac{{\gamma_\theta}^2}{\gamma_l} < \frac{1-\zeta}{\gamma_c} \min \left\{ \delta_\theta, \delta_\mu, \delta_\zeta, \epsilon_u \right\}, \tag{B.52b}$$

with $\tilde{d}$, $\overline{Q}$ and Φ as in (4.36b)-(4.36d) and

$$\delta_\theta = \min \{ \min_i \{ u_i^+ - \overline{u}_i \}, \min_j \{ \overline{u}_j - u_j^- \} \} \tag{B.53}$$

$$\delta_\mu = \frac{1}{\left\| B^\dagger \right\|} \min \{ \min_i \{ \lambda_i^+ - \overline{\lambda}_i \}, \min_j \{ \overline{\lambda}_j \} \} \tag{B.54}$$

$$\delta_\zeta = \begin{cases} \frac{\| \Phi^{-1} \overline{Q}^2 Q \tilde{d} \|}{\| \Phi^{-1} \overline{Q} \|} \frac{\zeta}{(1-\zeta)} & \text{if } \| \Phi^{-1} \overline{Q} \| \neq 0 \\ +\infty & \text{if } \| \Phi^{-1} \overline{Q} \| = 0 \end{cases}. \tag{B.55}$$

then

$$\|\hat{u}\| < \min\{\min_i\{u_i^+ - \overline{u}_i\}, \min_j\{\overline{u}_j - u_j^-\}, \epsilon_u\} \tag{B.56}$$

$$\|\hat{x}\| < \epsilon_x \tag{B.57}$$

$$\|\hat{\lambda}\| < \min\{\min_i\{\lambda_i^+ - \overline{\lambda}_i\}, \min_j\{\overline{\lambda}_j\}\}. \tag{B.58}$$

Proof. In order to prove this, we make use of Lemma B.6, where we note that (B.39) is satisfied due to (B.52b). To prove (B.56) we combine (B.40) and (B.52b) such that

$$\|\hat{u}\| \leq \gamma \frac{1}{1-\zeta} \left\| \Phi^{-1} \overline{Q}^2 Q \tilde{d} \right\| < \min\{\min_i\{u_i^+ - \overline{u}_i\}, \min_j\{(\overline{u}_j - u_j^-\}, \epsilon_u\}. \tag{B.59}$$

From this, together with (B.52a) and (B.42) we obtain

$$\|\hat{x}\| \leq \frac{\gamma_c}{\mathbb{1}^T Q^{-1} \mathbb{1}} \left(\|\mathbb{1}\mathbb{1}^T Q^{-1} \overline{Q} Q \tilde{d}\| + \|\mathbb{1}\mathbb{1}^T Q^{-1}\| \epsilon_u \right) < \epsilon_x, \tag{B.60}$$

which implies (B.57). Lastly, from (B.52b) and (B.41) we have that

$$\|\hat{\lambda}\| < \left\| B^\dagger \right\| \delta_\mu \leq \min\{\min_i\{\lambda_i^+ - \overline{\lambda}_i\}, \min_j\{\overline{\lambda}_j\}\}, \tag{B.61}$$

with δ_μ as in (B.54). This implies (B.58) and concludes the proof. ∎

Remark B.8 (Feasibility of (B.52))**.** *To guarantee that Theorem 4.20 solves Problem 4.8, a sufficient condition for $\gamma_c > 0$, $\gamma_\theta > 0$ and $\gamma_l > 0$ is that they satisfy (B.52). Note that these gains can always be found since δ_μ, δ_θ and δ_ζ are all strictly positive due to the feasibility condition. Moreover, in the special case that all nodes supply their own demand (i.e., if $\overline{Q}Q\tilde{d} = 0$), (B.52b) is satisfied for any γ_θ and γ_l. Since γ_c acts as the proportional feedback in (4.32) and has to be chosen sufficiently small due to (B.52a), a smaller steady state error comes at the cost of a lower convergence rate. Although the controller is fully distributed, global information of the topology, cost functions, disturbance bounds and saturation bounds are required to guarantee bounds on the deviation from the optimal steady state. It is easy to show that a $\gamma_c > 0$, $\gamma_\theta > 0$ and $\gamma_l > 0$ can be found such that (B.52) is satisfied for all the disturbances whose magnitude belongs to a compact interval of values.*

Lemma B.9 (Incremental saturation bounds bounded away from the origin)**.** *Let $\overline{\theta}$ be as in (4.19) and let $\overline{\mu}$, $\hat{\theta}$ and $\hat{\mu}$ be the solutions to (4.20) and (4.35). If all the conditions of Lemma B.7 are satisfied, then*

$$\mu^- < 0, \qquad \mu^+ > 0, \qquad \theta^- < 0, \qquad \theta^+ > 0, \tag{B.62}$$

with μ^-, μ^+, θ^- and θ^+ as defined in (4.67a)-(4.67d).

Proof. From Lemma B.7 we get that

$$\|\hat{u}\| < \min\{\min_i\{(u^+ - \overline{u})_i\}, \min_j\{(\overline{u} - u^-)_j\} \tag{B.63}$$

$$\|\hat{\lambda}\| < \min\{\min_i\{(\lambda^+ - \overline{\lambda})_i\}, \min_j\{(\overline{\lambda})_j\}\}. \tag{B.64}$$

This, together with (4.54) and (4.56), implies that

$$u^- < \hat{u} + \overline{u} < u^+ \tag{B.65}$$

$$0 < \hat{\lambda} + \overline{\lambda} < \lambda^+, \tag{B.66}$$

and due to (4.50) and (4.51) we get

$$u^- < \gamma_\theta Q^{-1}(\overline{\theta} + \hat{\theta}) - r < u^+ \tag{B.67}$$

$$0 < -\gamma_\mu(\overline{\mu} + \hat{\mu}) < \lambda^+. \tag{B.68}$$

In light of (4.67a)-(4.67d) we can conclude that (B.62) is satisfied, which concludes the proof. ■

Appendix C

Additional case study

Additionally to the case study presented in Section 3.4, we present a second case study where we consider a real demand pattern.

We investigate the performance of the controller in the presence of a real demand pattern. We simulate a complete day with a storage device of $V^{\max} = 2000m^3$ where heat is stored during low demand and drained during high demand. To this end we let $0s \leq t \leq 86400s$ and use a demand pattern that is provided in (Verda and Colella 2011), to which we applied a discretization with a resolution of one hour. This demand pattern can be found in Figure C.1. The flowrate of the consumers is set such that $\mathbb{1}^T \nu_c$ is proportional to the demand at all time.

Again we let $\rho = 975kg/m^3$ and $C_p = 4190J/Kg°C$ and the volumes of the heat exchangers are given by $x_p = x_c = 0.02m^3$. The initialization of the temperature of the heat exchangers is given by $z_p(0) = z_c(0) = 50°C$. The initial temperature of the storage and setpoint throughout the day is given by $\bar{z}_s = z_s(0) = 85°C$. The initial temperature for the cold layer is $z_{\bar{s}}(0) = 30°C$ and the volume of the hot layer is initialized at $x_s(0) = 600m^3$. The gain for the controller of the flowrate is set to $\upsilon = 0.005$. Similar as in Section 3.4 we saturate the flows such that $0.05m^3/s \leq \nu_p \leq 0.5m^3/s$ in order to avoid

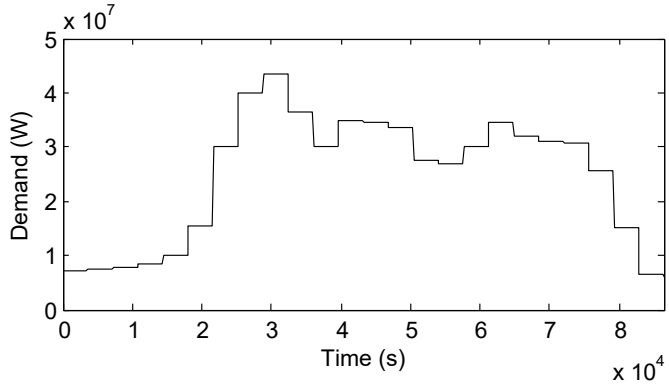

Figure C.1: Heat demand pattern of a whole day.

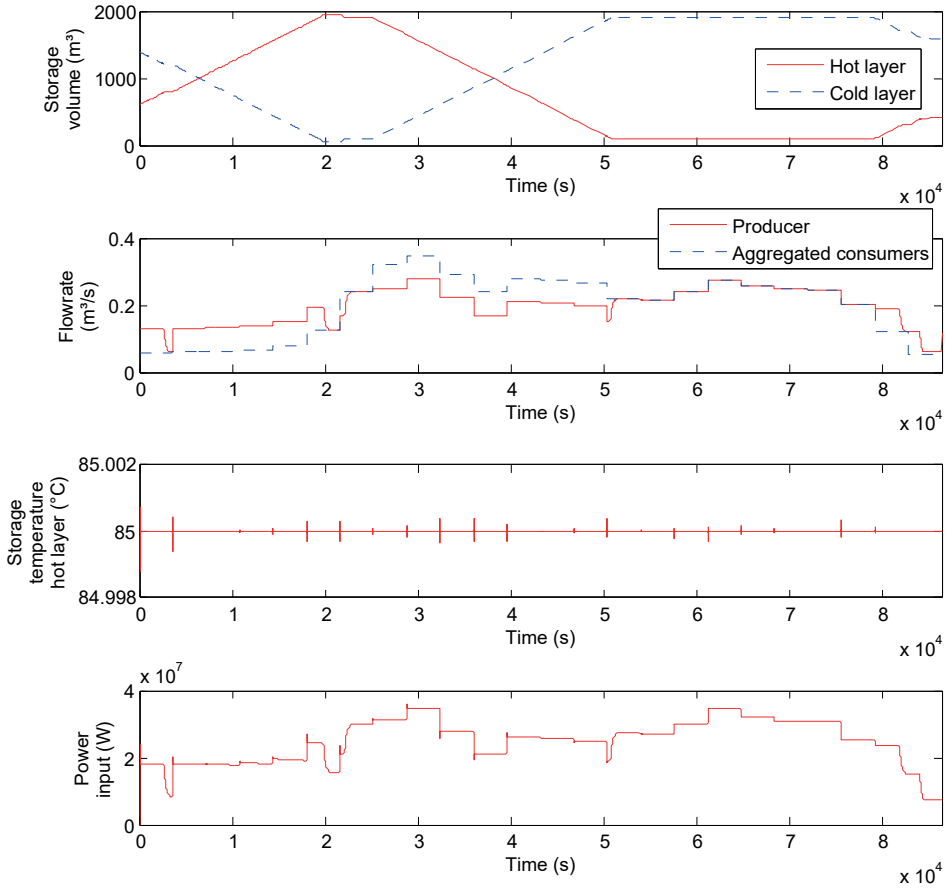

Figure C.2: Simulation results under a real demand pattern.

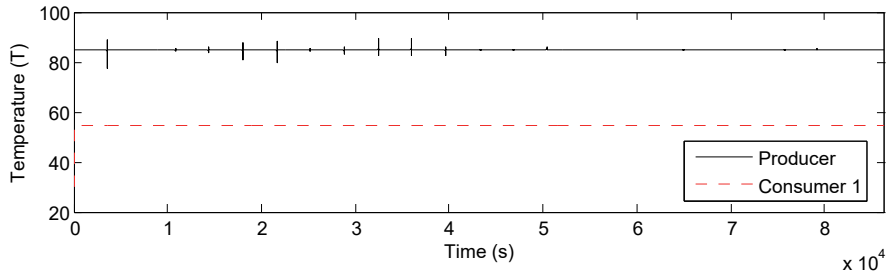

Figure C.3: Temperatures in the heat exchangers under real demand.

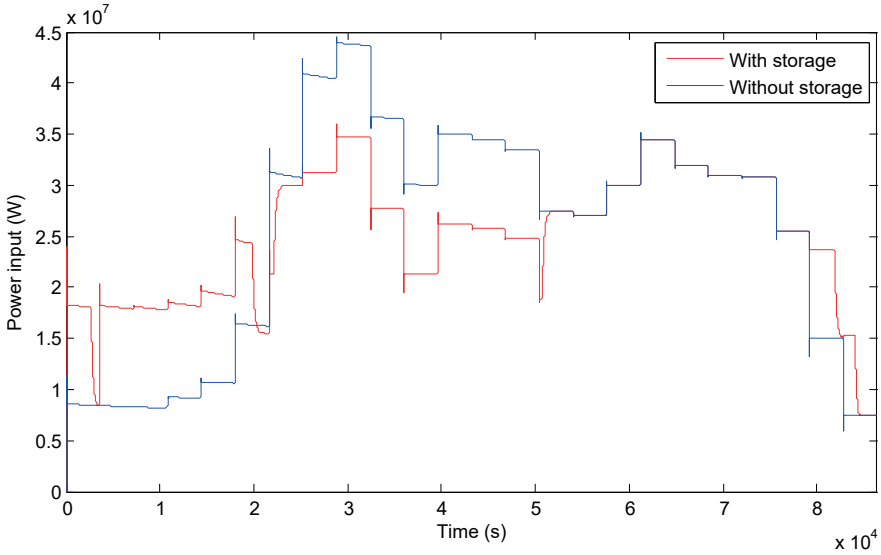

Figure C.4: Comparison of the power injection between two setups, one with and one without storage.

Time	1	2	3	4	5	6	7
Setpoint	7.25	7.5	7.75	8.5	10	15.5	30
8	9	10	11	12	13	14	15	16
40	43.5	36.5	30	35	34	33.5	27.5	27
17	18	19	20	21	22	23	24	25
30	34.5	32	31	30.75	25.5	15	6.5	6

Table C.1: Volume setpoints with the time in hours.

negative and too large flowrates that are too large. The controller (3.16) that is used remains identical throughout the whole simulations and given by

$$
\begin{aligned}
F &= \begin{pmatrix} 2 & -3 & 1 & -80 & -800 \\ 1 & -1 & 0 & 0 & 0 \\ 0 & 1 & -1 & 0 & 0 \\ 0 & 0 & 0 & -1800 & 1 \\ 0 & 0 & 0 & -810000 & 0 \end{pmatrix} \\
G &= \begin{pmatrix} 0 & 0 & 0 & 1800 & 810000 \end{pmatrix}^T \\
H &= \begin{pmatrix} 3 & -3 & 1 & -80 & -800 \end{pmatrix},
\end{aligned}
\tag{C.1}
$$

and $K = 0$.

The setpoints for the volume of the hot layer are given in Table C.1. In contrast to the case study in Section 3.4, we chose these setpoints such that most time intervals are too short to achieve steady state. As a consequence the storage will continuously fill or drain over multiple time-intervals. Moreover, the setpoints are also chosen such that peaks are shaved (*i.e.* the maximal power input is lowered) while the storage is filled during low demand. The result of the simulation is given in Figure C.2 and the heat exchanger temperatures are given in Figure C.3. In Figure C.2 it can be seen that the temperature in the hot storage layer converges to the desired $\bar{z}_s = 85°C$. The controller is able to maintain this temperature throughout the whole day despite the changing demand. Also in the time-intervals where the volume is not able to achieve steady state the temperature of the hot storage layer is kept close to the desired $\bar{z}_s = 85°C$. It can be seen that the storage is almost continuously filled until $20000s$ after which it is continuously drained until $53000s$. After $53000s$ the level of the storage is kept constant since it is almost fully drained and after $79200s$ the storage is filled again to the same level as the initial condition to prepare for the next day. As a consequence loads are shifted resulting in lower peaks compared to a setup without a storage tank which can be seen in Figure C.4.

Note that the demand is a piecewise constant signal due to the discretization. Since the flowrate of the consumers is set proportional to this demand the flowrate has the same behaviour. A transient behaviour (which look like spikes with the used resolution) can be seen in Figure C.3 at the time that the demand and flowrate is discontinuous.

Bibliography

Alessandri, A., Gaggero, M. and Tonelli, F.: 2011, Min-max and predictive control for the management of distribution in supply chains, *Transactions on Control Systems Technology* **19**(5), 1075–1089.

Allgower, F., Badgwell, T. A., Qin, J. S., Rawlings, J. B. and Wright, S. J.: 1999, *Nonlinear Predictive Control and Moving Horizon Estimation — An Introductory Overview*, Springer London, pp. 391–449.

Andreasson, M., Dimarogonas, D. V., Sandberg, H. and Johansson, K. H.: 2016, Distributed controllers for multi-terminal hvdc transmission systems, *Transactions on Control of Network Systems* **PP**(99), 1–1.

Arcak, M.: 2007, Passivity as a design tool for group coordination, *Transactions on Automatic Control* **52**(8), 1380–1390.

Aringhieri, R. and Malucelli, F.: 2003, Optimal operations management and network planning of a district heating system with a combined heat and power plant, *Annals of Operations Research* **120**(1-4), 173–199.

Astolfi, A., Karagiannis, D. and Ortega, R.: 2007, *Nonlinear and adaptive control with applications*, Springer Science & Business Media.

Axelsson, G.: 2010, Sustainable geothermal utilization case histories; definitions; research issues and modelling, *Geothermics* **39**(4), 283–291.

Bapat, R. B.: 2010, *Graphs and matrices*, Springer-Verlag London.

Bardi, S. and Astolfi, A.: 2010, Modeling and control of a waste-to-energy plant [applications of control], *Control Systems* **30**(6), 27–37.

Bauso, D., Blanchini, F., Giarré, L. and Pesenti, R.: 2013, The linear saturated decentralized strategy for constrained flow control is asymptotically optimal, *Automatica* **49**(7), 2206 – 2212.

Benvenuti, L. and Farina, L.: 2002, Positive and compartmental systems, *Transactions on Automatic Control* **47**(2), 370–373.

Bertsekas, D. P.: 1998, *Network Optimization: continuous and discrete methods*, Vol. 8, Athena Scientific, Belmont, Massachusetts.

Blanchini, F., Franco, E., Giordano, G., Mardanlou, V. and Montessoro, P. L.: 2016, Compartmental flow control: Decentralization, robustness and optimality, *Automatica* **64**, 18–28.

Borghesan, F., Vignali, R., Piroddi, L., Prandini, M. and Strelec, M.: 2013, Approximate dynamic programming-based control of a building cooling system with thermal storage, *Proc. of the Conference on Innovative Smart Grid Technologies Europe*, pp. 1–5.

Boyd, S. and Vandenberghe, L.: 2004, *Convex optimization*, Cambridge University Press.

Burbano, D. and Di Bernardo, M.: 2014, Distributed pid control for consensus of homogeneous and heterogeneous networks, *arXiv preprint arXiv:1409.2324* .

Bürger, M. and De Persis, C.: 2015, Dynamic coupling design for nonlinear output agreement and time-varying flow control, *Automatica* **51**, 210–222.

Bürger, M., De Persis, C. and Allgöwer, F.: 2015, Dynamic pricing control for constrained distribution networks with storage, *Transactions on Control of Network Systems* **2**(1), 88–97.

Bürger, M., Zelazo, D. and Allgöwer, F.: 2013, Hierarchical clustering of dynamical networks using a saddle-point analysis, *Transactions on Automatic Control* **58**(1), 113–124.

Bürger, M., Zelazo, D. and Allgöwer, F.: 2014, Duality and network theory in passivity-based cooperative control, *Automatica* **50**(8), 2051–2061.

Campo, P. J. and Morari, M.: 1989, Model predictive optimal averaging level control, *AIChE Journal* **35**(4), 579–591.

Cantoni, M., Weyer, E., Li, Y., Ooi, S. K., Mareels, I. and Ryan, M.: 2007, Control of large-scale irrigation networks, *Proc. of the IEEE* **95**(1), 75–91.

Carlson, M. R.: 2003, *Practical reservoir simulation: using, assessing, and developing results*, PennWell Books.

Como, G.: 2017, On resilient control of dynamical flow networks, *Annual Reviews in Control* .

Como, G., Savla, K., Acemoglu, D., Dahleh, M. A. and Frazzoli, E.: 2013, Robust distributed routing in dynamical flow networks-part i: Locally responsive policies and weak resilience, *Transactions on Automatic Control* **58**(2), 317–332.

Danielson, C., Borrelli, F., Oliver, D., Anderson, D. and Phillips, T.: 2013, Constrained flow control in storage networks: Capacity maximization and balancing, *Automatica* **49**(9), 2612–2621.

Daniilidis, A., Doddema, L. and Herber, R.: 2016, Risk assessment of the groningen geothermal potential: From seismic to reservoir uncertainty using a discrete parameter analysis, *Geothermics* **64**, 271–288.

Daniilidis, A., Scholten, T., Hoogheim, J., De Persis, C. and Herber, R.: 2017, Geochemical implications of production and storage control by coupling a direct use geothermal system with heat networks, *Applied Energy* p. submitted.

Darup, M. S. and Renner, J.: 2016, Predictive pressure control in deep geothermal systems, *Proc. of the European Control Conference (ECC)*, pp. 605–610.

De Persis, C.: 2013, Balancing time-varying demand-supply in distribution networks: an internal model approach, *Proc. of the European Control Conference (ECC)*, IEEE, pp. 748–753.

De Persis, C., Jensen, T. N., Ortega, R. and Wisniewski, R.: 2014, Output regulation of large-scale hydraulic networks, *Transactions on Control Systems Technology* **22**(1), 238–245.

De Persis, C. and Kallesoe, C. S.: 2011, Pressure regulation in nonlinear hydraulic networks by positive and quantized controls, *Transactions on Control Systems Technology* **19**(6), 1371–1383.

Dincer, I. and Rosen, M.: 2002, *Thermal energy storage: systems and applications*, John Wiley & Sons.

Dotzauer, E.: 2002, Simple model for prediction of loads in district-heating systems, *Applied Energy* **73**(34), 277–284.

Fiedler, M. and Ptak, V.: 1962, On matrices with non-positive off-diagonal elements and positive principal minors, *Czechoslovak Mathematical Journal* **12**(3), 382–400.

Gambino, G., Verrilli, F., Canelli, M., Russo, A., Himanka, M., Sasso, M., Srinivasan, S., Del Vecchio, C. and Glielmo, L.: 2016, Optimal operation of a district heating power plant with thermal energy storage, *Proc. of the American Control Conference (ACC)*, pp. 2334–2339.

Gelegenis, J. J.: 2009, Use of a probabilistic model to design energy transmission and distribution networks for low enthalpy geothermal multiple use schemes, *Applied Energy* **86**(3), 284–289.

Gharesifard, B. and Cortés, J.: 2014, Distributed continuous-time convex optimization on weight-balanced digraphs, *Transactions on Automatic Control* **59**(3), 781–786.

Glemmestad, B., Skogestad, S. and Gundersen, T.: 1999, Optimal operation of heat exchanger networks, *Computers & Chemical Engineering* **23**(45), 509 – 522.

Grant, M., Boyd, S., Blondel, V., Boyd, S. and Kimura, H.: 2008, Cvx: Matlab software for disciplined convex programming, *Recent Advances in Learning and Control* pp. 95–110.

Gupta, S. K., Kar, K., Mishra, S. and Wen, J. T.: 2015, Distributed consensus algorithms for collaborative temperature control in smart buildings, *Proc. of the American Control Conference (ACC)*, IEEE, pp. 5758–5763.

Haddad, W. M. and Chellaboina, V.: 2008, *Nonlinear dynamical systems and control: a Lyapunov-based approach*, Princeton University Press.

Hangos, K. M., Bokor, J. and Szederkényi, G.: 2004, *Analysis and control of nonlinear process systems*, Springer, London.

Hao, H., Lin, Y., Kowli, A. S., Barooah, P. and Meyn, S.: 2014, Ancillary service to the grid through control of fans in commercial building hvac systems, *Transactions on Smart Grid* **5**(4), 2066–2074.

Hogben, L.: 2010, Minimum rank problems, *Linear Algebra and its Applications* **432**(8), 1961 – 1974.

Hoy, M., Livernois, J., McKenna, C., Rees, R. and Stengos, T.: 2011, *Mathematics for Economics*, MIT Press.

Hu, Y., Koroleva, O. I. and Krstić, M.: 2003, Nonlinear control of mine ventilation networks, *Systems & Control Letters* **49**(4), 239–254.

Iftar, A.: 1999, A linear programming based decentralized routing controller for congested highways, *Automatica* **35**(2), 279 – 292.

Isidori, A., Marconi, L. and Serrani, A.: 2003, *Robust autonomous guidance: an internal model approach*, Springer.

Jäschke, J. and Skogestad, S.: 2014, Optimal operation of heat exchanger networks with stream split: Only temperature measurements are required, *Computers & Chemical Engineering* **70**(0), 35 – 49. Manfred Morari Special Issue.

Jayawardhana, B., Ortega, R., García-Canseco, E. and Castanos, F.: 2007, Passivity of nonlinear incremental systems: Application to PI stabilization of nonlinear RLC circuits, *Systems & Control Letters* **56**(9), 618–622.

Kallesøe, C. S., Jensen, T. N. and Wisniewski, R.: 2015, Adaptive reference control for pressure management in water networks, *Proc. of the European Control Conference (ECC)*, pp. 3268–3273.

Khalil, H. K.: 2002, *Nonlinear systems*, Vol. 2, Prentice hall, Upper Saddle River.

Kim, H. and De Persis, C.: 2015, Adaptation and disturbance rejection for output synchronization of incrementally output-feedback passive systems, *arXiv preprint arXiv:1509.03840* .

Koroleva, O. I. and Krstic, M.: 2005, Averaging analysis of periodically forced fluid networks, *Automatica* **41**(1), 129–135.

Koroleva, O. I., Krstić, M. and Schmid-Schönbein, G. W.: 2006, Decentralized and adaptive control of nonlinear fluid flow networks, *International Journal of Control* **79**(12), 1495–1504.

Kyriakis, S. A. and Younger, P. L.: 2016, Towards the increased utilisation of geothermal energy in a district heating network through the use of a heat storage, *Applied Thermal Engineering* **94**, 99–110.

Lee, J. H. and Yu, Z. H.: 1994, Tuning of model predictive controllers for robust performance, *Computers & Chemical Engineering* **18**(1), 15–37. ID: 271414271414.

Lee, S.-J., Park, D. J., Kim, J. H. and Ahn, H.-S.: 2017, Distributed coordination of asymmetric compartmental systems under time-varying inputs and its applications, *Transactions on Control Systems Technology* .

Lemale, J. and Jaudin, F.: 1999, La geothermie, une energie davenir, une realite en ile de france [geothermal heating, an energy of the future, a reality in ile-de-france], *Report, IAURIF, Paris* .

Li, H., Sun, Q., Zhang, Q. and Wallin, F.: 2015, A review of the pricing mechanisms for district heating systems, *Renewable and Sustainable Energy Reviews* **42**, 56–65.

Li, N., Chen, L. and Low, S.: 2011, Optimal demand response based on utility maximization in power networks, *Proc. of the Power and Energy Society General Meeting*, pp. 1–8.

Linnhoff, B. and Hindmarsh, E.: 1983, The pinch design method for heat exchanger networks, *Chemical Engineering Science* **38**(5), 745 – 763.

Liu, G. and Daley, S.: 2001, Optimal-tuning pid control for industrial systems, *Control Engineering Practice* **9**(11), 1185 – 1194.

Lovisari, E., Como, G. and Savla, K.: 2014, Stability of monotone dynamical flow networks, *Proc. of the Conference on Decision and Control (CDC)*, IEEE, pp. 2384–2389.

Lund, H., Werner, S., Wiltshire, R., Svendsen, S., Thorsen, J. E., Hvelplund, F. and Mathiesen, B. V.: 2014, 4th generation district heating (4gdh): Integrating smart thermal grids into future sustainable energy systems, *Energy* **68**, 1–11.

Lund, J. W. and Boyd, T. L.: 2016, Direct utilization of geothermal energy 2015 worldwide review, *Geothermics* **60**, 66–93.

Ma, Y., Borrelli, F., Hencey, B., Packard, A. and Bortoff, S.: 2009, Model predictive control of thermal energy storage in building cooling systems, *Proc. of the Conference on Decision and Control (CDC)*, pp. 392–397.

Ma, Y., Kelman, A., Daly, A. and Borrelli, F.: 2012, Predictive control for energy efficient buildings with thermal storage, *Control system magazine* **32**(1), 44–64.

Marinaki, M.: 1999, A non-linear optimal control approach to central sewer network flow control, *International Journal of Control* **72**(5), 418–429.

Mayne, D. Q., Rawlings, J. B., Rao, C. V. and Scokaert, P. O. M.: 2000, Constrained model predictive control: Stability and optimality, *Automatica* **36**(6), 789–814.

Moeck, I. S.: 2014, Catalog of geothermal play types based on geologic controls, *Renewable and Sustainable Energy Reviews* **37**, 867–882.

Monshizadeh, N., Zhang, S. and Camlibel, M. K.: 2014, Zero forcing sets and controllability of dynamical systems defined on graphs, *Transactions on Automatic Control* **59**(9), 2562–2567.

Moss, F. and Segall, A.: 1982, An optimal control approach to dynamic routing in networks, *Transactions on Automatic Control* **27**(2), 329–339.

Narasimhan, T. N. and Witherspoon, P. A.: 1976, An integrated finite difference method for analyzing fluid flow in porous media, *Water Resources Research* **12**(1), 57–64.

Olfati-Saber, R., Fax, J. A. and Murray, R. M.: 2007, Consensus and cooperation in networked multi-agent systems, *Proceedings of the IEEE* **95**(1), 215–233.

Olfati-Saber, R. and Murray, R. M.: 2004, Consensus problems in networks of agents with switching topology and time-delays, *Transactions on Automatic Control* **49**(9), 1520–1533.

Ortega, R., van der Schaft, A., Castanos, F. and Astolfi, A.: 2008, Control by interconnection and standard passivity-based control of port-Hamiltonian systems, *Transactions on Automatic Control* **53**(11), 2527–2542.

Pavlov, A. and Marconi, L.: 2008, Incremental passivity and output regulation, *Systems and Control Letters* **57**, 400 – 409.

Pruess, K., Oldenburg, C. and Moridis, G.: 2012, Tough2 user's guide, version 2.1, *Technical Report LBNL-43134*, Earth Sciences Division.

Rami, M. A. and Tadeo, F.: 2007, Controller synthesis for positive linear systems with bounded controls, *Transactions on Circuits and Systems II: Express Briefs* **54**(2), 151–155.

Rantzer, A.: 2011, Distributed control of positive systems, *Proc. of the Conference on Decision and Control and European Control Conference (CDC-ECC)*, pp. 6608–6611.

Rezaie, B. and Rosen, M. A.: 2012, District heating and cooling: Review of technology and potential enhancements, *Applied Energy* **93**, 2–10.

Rockafellar, R. T.: 1984, *Network flows and monotropic optimization*, Wiley-Interscience.

Rockware: 2014, Petrasim.
URL: *https://www.rockware.com/product/overview.php?id=148*

Romero, J. G., Donaire, A. and Ortega, R.: 2013, Robust energy shaping control of mechanical systems, *Systems & Control Letters* **62**(9), 770–780.

Rosander, P.: 2012, Averaging level control in the presence of frequent inlet flow upsets.

Rugh, W. J.: 1996, *Linear system theory*, Prentice-Hall, Inc.

Sandou, G., Font, S., Tebbani, S., Hiret, A., Mondon, C., Tebbani, S., Hiret, A. and Mondon, C.: 2005, Predictive control of a complex district heating network, *Proc. of the Conference on Decision and Control (CDC)*, pp. 7372–7377.

Sayegh, M. A., Danielewicz, J., Nannou, T., Miniewicz, M., Jadwiszczak, P., Piekarska, K. and Jouhara, H.: 2016, Trends of european research and development in district heating technologies, *Renewable and Sustainable Energy Reviews* .

Scholten, T. W., De Persis, C. and Tesi, P.: 2015, Modeling and control of heat networks with storage: the single-producer multiple-consumer case, *Proc. of the European Control Conference (ECC)*, pp. 2247–2252.

Scholten, T. W., De Persis, C. and Tesi, P.: 2016a, Modeling and control of heat networks with storage: The single-producer multiple-consumer case, *Transactions on Control Systems Technology* pp. 414–428.

Scholten, T. W., De Persis, C. and Tesi, P.: 2016b, Optimal steady state regulation of distribution networks with input and flow constraints, *Proc. of the American Control Conference (ACC)*, pp. 6953–6958.

Scholten, T. W., De Persis, C. and Tesi, P.: 2016c, Optimal steady state regulation of distribution networks with input and flow constraints, *Proc. of the American Control Conference (ACC)*, pp. 6953–6958.

Scholten, T. W., Trip, S. and De Persis, C.: 2017, Pressure regulation in large scale hydraulic networks with input constraints, *Proc. of the IFAC World Congress*, pp. 5534–5539.

Scholten, T. W., Trip, S. and De Persis, C.: In preparation, Pressure regulation in large scale hydraulic networks with positivity constraints.

Shortall, R., Davidsdottir, B. and Axelsson, G.: 2015, Geothermal energy for sustainable development: A review of sustainability impacts and assessment frameworks, *Renewable and Sustainable Energy Reviews* **44**, 391–406.

Siroky, J., Oldewurtel, F., Cigler, J. and Privara, S.: 2011, Experimental analysis of model predictive control for an energy efficient building heating system, *Applied Energy* **88**(9), 3079–3087.

Skogestad, S.: 2009, *Chemical and energy process engineering*, CRC press Boca Raton.

Sloth, C. and Wisniewski, R.: 2015, Stability verification for energy-aware hydraulic pressure control via simplicial subdivision, *Proc. of the European Control Conference (ECC)*, pp. 2694–2699.

Tahavori, M., Leth, J., Kallesøe, C. and Wisniewski, R.: 2014, Optimal control of nonlinear hydraulic networks in the presence of disturbance, *Nonlinear Dynamics* **75**(3), 539–548.

Thulukkanam, K.: 2013, *Heat exchanger design handbook*, CRC Press.

Trip, S., Bürger, M. and De Persis, C.: 2016, An internal model approach to (optimal) frequency regulation in power grids with time-varying voltages, *Automatica* **64**, 240–253.

Trip, S. and De Persis, C.: 2017, Distributed optimal load frequency control with non-passive dynamics, *Transactions on Control of Network Systems* **PP**(99), 1–1.

Trip, S., Scholten, T. W. and De Persis, C.: 2017, Optimal regulation of flow networks with input and flow constraints, *Proc. of the IFAC World Congress*, IEEE, pp. 9854–9859.

Trip, S., Scholten, T. W. and De Persis, C.: submitted, Optimal regulation of flow networks with transient constraints.

van der Schaft, A.: 2012, *L2-gain and passivity techniques in nonlinear control*, Springer, Berlin Heidelberg.

van der Schaft, A. J. and Jeltsema, D.: 2014, Port-hamiltonian systems theory: An introductory overview, *Foundations and Trends in Systems and Control* **1**(2-3), 173–378.

van der Schaft, A. J. and Maschke, B.: 2013, Port-Hamiltonian systems on graphs, *SIAM Journal on Control and Optimization* **51**(2), 906–937.

van der Schaft, A. J. and Wei, J.: 2012, A Hamiltonian perspective on the control of dynamical distribution networks, *Proc. of the IFAC Workshop on Lagrangian and Hamiltonian Methods for Non Linear Control*, pp. 24–29.

van Leeuwen, L., Boker, U. and van de Weerd, A.: 2014, Geothermal energy in groningen geological investigation (groot geologisch onderzoek groningen), *Technical Report G1111*, Panterra Geoconsultants.

Verda, V. and Colella, F.: 2011, Primary energy savings through thermal storage in district heating networks, *Energy* **36**(7), 4278 – 4286.

Wan, P. and Lemmon, M. D.: 2007, Distributed flow control using embedded sensor-actuator networks for the reduction of combined sewer overflow (cso) events, *Proc. of the Conference on Decision and Control (CDC)*, pp. 1529–1534.

Wang, Z., Polycarpou, M. M., Uber, J. G. and Shang, F.: 2006, Adaptive control of water quality in water distribution networks, *Transactions on Control Systems Technology* **14**(1), 149–156.

Wei, J. and van der Schaft, A. J.: 2013, Load balancing of dynamical distribution networks with flow constraints and unknown in/outflows, *Systems & Control Letters* **62**(11), 1001–1008.

Wei, J. and van der Schaft, A. J.: 2014, Constrained proportional integral control of dynamical distribution networks with state constraints, *Proc. of the Conference on Decision and Control (CDC)*, pp. 6056–6061.

Xu, T., Sonnenthal, E., Spycher, N. and Pruess, K.: 2006, Toughreacta simulation program for non-isothermal multiphase reactive geochemical transport in variably saturated geologic media: Applications to geothermal injectivity and co2 geological sequestration, *Computers & Geosciences* **32**(2), 145–165.

Yeh, G.-T. and Tripathi, V. S.: 1991, A model for simulating transport of reactive multispecies components: Model development and demonstration, *Water Resources Research* **27**(12), 3075–3094.

Yoo, H. and Pak, E.-T.: 1993, Theoretical model of the charging process for stratified thermal storage tanks, *Solar Energy* **51**(6), 513 – 519.

Zhao, J. and Dörfler, F.: 2015, Distributed control and optimization in dc microgrids, *Automatica* **61**, 18–26.

Zheng, Y., Zhu, Y. and Wang, L.: 2011, Consensus of heterogeneous multi-agent systems, *IET Control Theory & Applications* **5**(16), 1881–1888.

Summary

Recently, district heating networks gained a lot of renewed interest since they can contribute to lowering CO_2 emissions. However, to achieve this changes are required in the way we operate and design these systems. For example, smaller pipes could be used and multiple producers, consumers and storages should be integrated in these systems. As a consequence new control strategies are required and their design and stability analysis are the focus of this thesis. Before designing various controllers, three models are introduced that describe the dynamics of a district heating network by considering the relations between volume, temperature, flowrate and pressure. Since the considered dynamics in some of these models represent a broader class of systems the results of the modeling (and subsequent controller design) have many other applications such as supply chains, power grids, data networks, traffic networks and compartmental systems. The presented models are used in the design and analysis of several controllers, each having its own control goal.

The first goal is to solve a volume and temperature regulation problem for a conventional setup with a single heat source and thermal storage. As the aggregated demand of such a network is highly periodic, we propose an internal model based controller that regulates the heat injection. Together with a proportional controller for the flowrates, asymptotic stability is proven towards desired setpoints of the storage volume and temperature despite the time varying demand.

The second goal is to design controllers that coordinate production, regulate the storage and control transportation of the water in large scale (heat) networks such that the demand (which acts as a disturbance) is met. This coordination allows multiple producers owned by different entities to produce in a single network, which is called third party access. A graph is used to model the network in which nodes represent producers, consumers and/or storage and a link the pipes interconnecting them. Controllers at the nodes use a communication network to guarantee optimal economic inputs at steady state. Moreover, controllers at the links control the flows between the nodes. With these choices the controllers are completely distributed, meaning that only local measurements are required. In order to guarantee that production capacities, flow directions and flow capacities are never violated, we also require that inputs and flows set to remain within pre-set bounds at all times. The first controller we design uses saturation functions to guarantee the input and flow constraints. Using Lyapunov arguments we show global convergence to an arbitrarily small neighborhood of the desired optimal steady state. The second controller uses nonlinear functions instead of the standard saturation functions and an additional state is introduced that increases the performance. Exploiting an incremental passivity property, the desired

steady state is proven to be globally asymptotically stable under the closed loop dynamics. Besides a district heating system we present a case study of a multi-terminal high voltage direct current network that shows the effectiveness of the proposed solution.

The third goal is to design controllers that regulate the pressures in hydraulic networks. More specifically, we assure that the inputs are non-negative, as many (centrifugal) pumps commonly used in these networks can only generate positive pressures. The networks we consider are equipped with a multi-pump architecture such that higher frictions in the pipes can be tolerated. As a result smaller pipes can be used such that the heat dispersion is decreased. We propose a controller that has similarities with a PI controller but the output is mapped through a nonlinear function and an additional state-dependent gain is introduced, guaranteeing the positivity constraint of the input. These controllers regulate the pressure drop at each end-user asymptotically towards desired setpoints and the obtained closed-loop nonlinear system is proven to be locally asymptotically stable.

Lastly, the final goal is to investigate the implications of a time varying production to a geothermal reservoir in a similar setup as considered for the first goal. We propose and design a model predictive controller as it can easily include constraints such as flow rate, storage and production capacities, but also uses predictions of the heat demand to generate the most optimal input signal. The controller uses volume measurements in the storage tank and predictions of the demand in order to regulate the production of the geothermal system. The numerical data generated by the controller in closed loop with a modelled district heating network are used as input for the reservoir simulations that uses a 2D reactive transport reservoir model. These make use of discrete parameter analysis to evaluate the effect of pressure depletion, reservoir permeability, flow rate, re-injection temperature and injection pH on the geothermal reservoir. We show that such a time varying production does not create adverse geochemical effects in the reservoir, but instead improves the efficiency of the geothermal heat extraction. The findings pave the way towards a stronger integration between heat networks and a more sustainable development of geothermal resources.

Samenvatting

Recent hebben warmtenetten veel herniewde interesse ontvangen omdat ze kunnen bijdragen aan het verlagen van de CO_2 uitstoot. Echter, om dit te berijken zijn wijzigingen nodig in de manier hoe we deze systemen aansturen en ontwerpen. Voorbeelden van deze wijzigingen zijn het gebruik van kleinere pijpen en het integreren van meerdere producenten, consumenten en opslagtanks in deze systemen. Als consequentie zijn er nieuwe regeltechnische strategieën nodig en het ontwerp samen met de stabiliteitsanalyse hiervan is de focus van deze these. Voordat we de verschillende regelaars gaan ontwerpen, introduceren we drie modellen die de dynamica van een dergelijk systeem beschrijven waarbij relaties tussen volume, temperatuur, stroomsnelheid en druk gerelateerd worden. Omdat de beschouwde dynamica in sommige van de modellen een bredere klasse van systemen beschrijft hebben de resultaten van de modellering (en het daarop volgende ontwerp van de regelaars) veel verschillende andere applicaties zoals 'supply chains', elektriciteitsnetwerken, data netwerken, verkeersnetwerken, en systemen van compartimenten. Deze modellen worden vervolgens gebruikt in het ontwerp en de stabiliteitsanalyse van verschillende regelaars die elk hun eigen doel hebben.

Het eerst doel is om een regelprobleem op te lossen waarbij het volume en de temperatuur in een conventioneel warmtenetwerk met één enkele warmte bron en een warmteopslag worden gereguleerd naar referentiepunten. Omdat de totale vraag in een dergelijk netwerk vaak een sterk periodiek karakter heeft stellen we een regelaar voor met inwendig model dat de warmte injectie regelt. Samen met een proportionele regelaar voor de stroomsnelheid bewijzen we asymptotische stabiliteit naar een gewenst referentiepunt voor zowel het volume als de temperatuur ondanks een tijdvarierend vraagpatroon.

Het tweede doel is om een regelaar te ontwerpen dat productie coordineerd, opslag niveaus reguleert en het transport van water regelt in grootschalige warmtenetten zodanig dat de vraag (die zich manifesteert als een verstoring) wordt voorzien. Deze coordinatie geeft meerdere producenten van verschillende eigenaars de mogelijkheid om zich gezamelijk aan te sluiten op n netwerk, ook wel 'third party access' genoemd.

A graph is used to model the network in which nodes represent producers, consumers and/or storage and a link the pipes interconnecting them. Een graaf wordt gebruikt om het netwerk te modelleren waarbij de knooppunten producenten, consumenten en/of opslag voorstellen terwijl de linkjes de pijpen modelleren die de knooppunten verbindt.

Regelaars op de knooppunten van een netwerk gebruiken een communicatienetwerk om economische optimaliteit te garanderen in evenwichtstoestand. Daarnaast zorgen de regelaars op

de linkjes voor de gewenste stroomsnelheden tussen de knooppunten. Met deze keuzes zijn de regelaars compleet gedecentraliceert wat betekend dat alleen lokale metingen nodig zijn. Om te garanderen dat produciecapaciteiten, stroomrichtingen en stroomcapaciteiten altijd binnen voorgegeven grenzen blijven, eisen we dat de inputs en stromingen aan corresponderende voorwaarden voldoen voor alle tijd. De eerste controller die we ontwerpen gebruikt saturatiefuncties om de voorwaarden voor de input en de stroomsnelheden te garanderen. Doormiddel van Lyapunov argumenten tonen we aan dat globale convergentie gegarandeerd is naar een omgeving die willekeurig dicht bij de gewenste optimale evenwichtstoestand ligt. De tweede controller gebruikt niet-lineare funties inplaats van de standaard saturatiefunties en de dynamica is aangepast met een extra toestandsvariabele waardoor de prestaties verbeteren. Door een incrementele passiviteitseigenschap te gebruiken zijn we in staat te bewijzen dat de gewenste evenwichtstoestand globaal asymptotisch stabiel is onder de dynamica in gesloten kring. Naast een warmtenetwerk presenteren we ook een casestudy van een multi-terminal hoog voltage netwerk met gelijkspanning die de effectiviteit van de voorgestelde oplossing illustreerd.

Het derde doel is om een regelaar te ontwerpen dat de druk reguleert in hydraulische netwerken. Specifieker, we garanderen dat de inputs niet negatief worden omdat veel centrifugale pompen die normaalgesproken worden gebruikt in deze netwerken alleen positieve inputs kunnen leveren. Het netwerk dat we beschouwen is uitgerust met een architectuur waarin meerdere pompen gebruikt worden, zodat hogere weerstand in de pijpen getollereerd kan worden. Dit heeft tot gevolg dat er dunnere pijpen gebruikt kunnen worden wat lagere warmteverliezen tot gevolg heeft. We stellen een regelaar voor die overeenkomsten heeft met een PI-regelaar, maar de output wordt door niet-lineare functies gemapt en een extra toestandsvariable afhankelijke gain is geïntroduceerd die garandeerd dat de input altijd positief blijft. De regelaar stuurd de drukval bij elke eindgebruiker asymptotisch naar de gewenste referentiepunten en we bewijzen dat de gesloten feedbackloop lokaal asymptotisch stabiel is.

Tot slot onderzoeken we de implicaties van een tijdsvariërende productie op een geothermie reservoir in een vergelijkbare setup als in het eerstbeschreven doel. We kiezen voor een model-voorspellende regelaar omdat deze eenvoudig randvoorwaarden mee kan nemen zoals capaciteiten van de buizen, opslag en productie, maar ook voorspellingen van de warmte vraag gebruikt om het meest optimale signaal te genereren. De regelaar die we ontwerpen gebruikt volume metingen in de opslagtank en voorspellingen van de totale warmtevraag om de productie van de geothermiebron te regelen. De numerieke data gegenereerd door een simulatie van de regelaar in gesloten loop met een model van het warmtenetwerk is gebruikt als input voor een 2D reactief transport model van het reservoir. We tonen aan dat een tijdsvariërende productie geen nadelige geologische effecten heeft in het reservoir, terwijl deze de efficientie verhoogt van de geothermische warmte extractie. Deze resultaten maken de weg vrij voor een sterkere integratie tussen warmtenetwerken en een meer duurzame ontwikkeling en exploitatie van geothermische energie.